Study of Power Transformer Abnormalities and IT Applications in Power Systems

Xuzhu Dong

Dissertation submitted to the Faculty of the
Virginia Polytechnic Institute and State University
In partial fulfillment of the requirements for the degree of

Doctor of Philosophy

In

Electrical Engineering

Dr. Yilu Liu, Chair
Dr. Arun G. Phadke
Dr. Robert Broadwater
Dr. Alex Huang
Dr. Tao Lin

January 3, 2002

Blacksburg, Virginia

Keywords:

Power Transformer, Electrical Transients, Geomagnetically Induced Current (GIC), Information Model, Virtual Hospital

Study of Power Transformer Abnormalities and IT Applications in Power Systems

Xuzhu Dong

(ABSTRACT)

With deregulation, diagnosis and maintenance of power equipment, especially power transformers, become increasingly important to keep power systems in reliable operation. This dissertation systematically studied two kinds of transformer failure and abnormality cases, and then developed a new Internet based Virtual Hospital (VH) for power equipment to help power equipment diagnosis and maintenance.

A practical case of generator-step-up (GSU) transformer failures in a pumped storage plant was extensively studied. Abnormal electrical phenomena associated with GSU transformers, including switching transients and very fast transients (VFT), and lightning, were analyzed. Simulation showed that circuit breaker restriking could be a major cause of transformer successive failures, and current surge arrester configuration did not provide enough lightning protection to GSU transformers. Mitigation of abnormal electrical phenomena effects on GSU transformers was proposed and discussed. The study can be a complete reference of troubleshooting of other similar transformer failures.

Geomagnetically induced current (GIC) is another possible cause of transformer abnormality. A simplified method based on the equivalent magnetizing curve for transformers with different core design was developed and validated to estimate harmonic currents and MVar drawn by power transformers with a given GIC. An effective indicator was proposed using partial harmonic distortion, *PHD*, to show when the transformer begins saturating with the input GIC. The developed method has been applied to a real time GIC monitoring system last year for a large power network with thousands of transformers.

A new Internet based Virtual Hospital (VH) for Power Equipment was conceptually developed to share experience of power equipment diagnosis and maintenance, and update the existing diagnostic techniques and maintenance strategies, and a comprehensive information model was developed for data organization, access, and archiving related to

equipment diagnosis and maintenance. An Internet based interactive fault diagnostic tool has been launched for power transformers based on dissolved gas analysis (DGA).

The above results and findings can help improving power equipment diagnosis and utility maintenance strategies.

ACKNOWLEDGEMENT

I would like to express my deepest gratitude to my advisor, Dr. Yilu Liu for her guidance, encouragement, and her friendship throughout this study. She is always there when I need help, not only in academics, but also in all aspects of my student life at Virginia Tech.

I also would like to thank my Ph.D. committee members Dr. Arun G. Phadke, Dr. Robert Broadwater, Dr. Alex Huang, and Dr. Tao Lin for their valuable comments on this work and serving on my dissertation committee.

I also would like to thank Dr. Nien-chung Wang of Taiwan Power Company, Dr. John G. Kappenman of Metatech Company, and Dr. Steven D. Sheetz of Department of Accounting and Information Systems at Virginia Tech for their technical help.

A special note of recognition and appreciation goes to Dr. Zhenyuan Wang, Mr. Sebastian P. Rosado, Mr. Frank A. LoPinto, and Kevin P. Scheibe for their involvement and corporation.

Finally, the most sincere appreciation goes to my wife, Haili Xue, and my family for their companionship, great understanding and continuous encouragement in my study.

DEDICATED To

My lovely family

and my two-year-old daughter, Wendy Dong

TABLE OF CONTENTS

LIST OF FIGURES

LIST OF TABLES

CHAPTER 1
INTRODUCTION

1.1. Overview

With deregulation, diagnosis and maintenance of power equipment, especially power transformers, become increasingly important to keep power systems in reliable operation. Power transformer failure could result in huge economic loss and unplanned outage of the power system, which may affect a large number of industries and commercial customers. In order to keep power transformers in health condition and reduce probability of transformer failures or abnormalities while simultaneously cutting the maintenance cost, a variety of factors that affect transformer performance should be analyzed carefully, including electrical, mechanical, and chemical properties. Some new techniques can play a key role to reach this objective, such as condition monitoring, predictive maintenance, and artificial intelligence (AI) based diagnostic techniques.

1.1.1. Transformer Failure and Abnormality

Transformer failure means that the transformer cannot remain in service, and remedial actions are required before it can be returned to service, including dielectric, mechanical, or thermal failure [Harl00]. Transformer abnormality means that transformer operation is beyond the normal status, and this may adversely affect the performance or asset life of the transformer itself or other apparatus, or system reliability and operation.

Power transformers can fail or be abnormal in a variety of ways and for a variety of reasons. Important factors are: 1) design and manufacturing weaknesses, 2) abnormal system conditions, 3) aged condition / service loading, 4) pre-existing faults, and 5) timescales for fault development [Lapw98]. There are various abnormal system conditions which may affect transformer performance, including [Alla95]:

- Switching transients or very fast transients can cause partial winding resonance or lead to strongly non-linear voltage distribution in the transformer windings. Partial winding resonance normally occurs when a system voltage transient, perhaps of relatively low amplitude, recurs at a frequency resonant with part of the transformer winding. The magnitude of the resonant voltage can be up to 20 times the operating voltage.

- High overloads, even if temporary, can accelerate aging of transformer insulation due to high temperature.

- Static electrification is caused when transformer oil is pumped at high speed through an insulating system, e.g. insulated directional oil channels or the winding ducts in a transformer. Charge separation takes place and the winding system acts as an electrostatic generator building up sufficient voltage to cause local surface tracking or a major electrical flashover. Over 20 large transformers have failed in this manner between 1989 and 1991 [Alla91].

- Geomagnetic disturbances are another possible cause of transformer failure or abnormality, but are limited to the northern hemisphere. Geomagnetic activity will produce abnormal currents of very low frequency in long transmission lines over terrain of certain geological formation. These currents are of high amplitude and when flowing through the windings will provide sufficient magnetic flux to saturate the core and actuate the protection systems to disconnect the transformer. The operation of protection systems can cascade disconnections and result in blackouts of entire power systems. Saturation of transformer cores cause the magnetising flux to flow outside the core, resulting in local overheating of structural parts and inducing circulating currents in winding connections, leading to overheating and possible failure. Geomagnetic disturbances have been so severe and so widespread that they caused all power supplies in the entire Province of Quebec to fail on March 13, 1989 [Alla91].

Other factors include short circuit forces, moisture in the paper and oil, partial discharge, and etc. These abnormal phenomena must be understood and then maintenance or design

philosophies should be developed to encompass the potential transformer failure or abnormality.

1.1.2. IT Applications in Power Equipment Diagnosis and Maintenance

In order to diagnose and maintain power transformers and other equipment, the engineers rely upon: 1) operation experience, 2) design knowledge, 3) knowledge of aging processes, 4) condition assessment test, 5) evidence from failure or abnormality, and 6) engineering judgment [Lapw98]. Technologies of diagnosis and maintenance have been developed from individual parameter monitoring of the equipment, expert based diagnostics, and preventive maintenance into integrated equipment condition monitoring, artificial intelligence (AI) based diagnostics combining with expert experiences, and strategic predictive maintenance with expert system as its framework [Phoh96].

From 1990s, IT and Internet has found many applications in power equipment condition monitoring, remote diagnosis and networked maintenance of substations and power plants, largely due to its low cost, remote access capability, standard communication protocol and thin client man-machine interface [Dong00]. Chapter 6 will discuss the detailed IT/Internet applications in power equipment diagnosis and maintenance.

1.2. The Objective and Scope of This Dissertation

1.2.1. Area of Interest

This dissertation includes three areas:

1). Investigation of effects on internal insulation of main transformers in the operation environment of a pumped storage plant.

Three large generator-step-up (GSU) transformers failed successively since 1992 in a pumped storage power plant. On July 10, 1992, Tr.#1 failed during generation mode after

one month in service. Inspection showed that insulation breakdown occurred between high-voltage (HV) winding, low-voltage (LV) winding, and ground at Phase C. On August 28, 1995, Tr.#1, made for replacing the first one, failed again during generation mode after about twenty months in service. Insulation failure also happened at Phase C. On April 10, 1999, Tr.#4 failed during pump mode after four years in service. Insulation failure between HV winding and ground was suspected at Phase C.

The plant houses six 300 MVA reversible turbine generator-motors (G/M) with a total installed capacity of 1800 MW, and six 300 MVA, 16.5 kV/345 kV GSU transformers. The GSU transformers are all of the special three-phase type, namely, multi-tank units equipped with separate core and coil assemblies for each phase, and connected with a common tank top cover. The cooling system for each transformer is oil-immersed, forced-oil cooled and forced-water-cooled. An on-load tap-changer (OLTC) is also provided with each transformer to regulate the voltage taps according to the system voltage variations [Liu91 and Chia97].

Since abnormal transformer failures resulted in considerable economic loss, an extensive investigation of electrical environment of the GSU transformer operation is done in order to search for the possible causes of the transformer failures and most importantly avoid such failures in the future. The study is attempting to investigate the possible abnormal electrical phenomena associated with the GSU transformers, with particular consideration given by the unique operation environment at the plant. Special attention is paid to the following aspects:

- Possible overvoltages seen at the terminals of GSU transformers resulting from frequent CB and DS switching operations in the GIS;

- Lightning overvoltages seen at the transformers and protection performance of arresters in the GIS to the transformers;

- Effects of spikes and harmonics at the transformer terminals originated from the static frequency converter (SFC) operations.

2). Comparative analysis of exciting current harmonics and reactive power consumption from GIC saturated transformers.

3). Internet based Virtual Hospital (VH) for Power Equipment and Internet based diagnostic tool for power transformers.

1.2.2. Contributions Through the Research

The major contributions of this dissertation include:

1) A practical case of GSU transformer failures in a pumped storage plant was extensively studied. Abnormal electrical phenomena associated with GSU transformers, including switching transients and VFT, and lightning were modeled and simulated. Suggestions were given for troubleshooting of the GSU transformer failures.

2) A simplified method for transformers with different core design was developed and validated to estimate harmonic currents and MVar drawn by power transformers with a given GIC. The developed method has been applied to a real time GIC monitoring system in the United Kingdom last year for a large power network with thousands of transformers.

3). A new Internet based Virtual Hospital (VH) for Power Equipment was conceptually developed, and an Internet based interactive fault diagnostic tool was launched for power transformers based on the dissolved gas analysis information. From anywhere in the world one can access the diagnosis tool via Internet for their transformer diagnosis.

1.2.3. Outline of This Dissertation

This dissertation has seven chapters. Chapter 1 is an introduction of the problem. Chapter 2 reviews GSU transformer failures. Chapter 3 presents effects of switching transients and very fast transients on GSU transformers. Chapter 4 studies lightning effects on GSU transformers. Chapter 5 extensively discusses GIC effects on power transformers. Chapter 6

introduces the Virtual Hospital for power equipment, information model, and Internet based diagnostic tool for power transformers. As a conclusion, Chapter 7 summarizes the study and major achievements of this dissertation.

CHAPTER 2
OVERVIEW OF GSU TRANSFORMER FAILURES

Chapter 2 extensively reviewed the historical GSU transformer failures, and discussed possible effects of switching transients, very fast transients (VFT), lightning, and harmonics, on the transformers, some suggestions are given for the troubleshooting of the GSU transformer failures in the pumped storage plant.

2.1. Statistical Analysis of GSU Transformer Failures

A GSU transformer failure or outage usually results in huge costs due to the loss of generation and resulting unavailability of a generation station during long repair times. Review of past performance and various problems associated with the GSU transformer failure or outage is helpful to its future design, operation, maintenance, and extending its service life [Kroo90].

In 1998, IEEE Power Engineering Society published a survey of GSU transformer failures, for transformers larger than 100 MVA, which failed from 1980 to the beginning of 1995 [PES98a]. The survey included the transformer manufacturer and installation information, the transformer status when the failure happened, presumed failure causes, failure locations, the phenomena resulted from the failure, etc. The survey feedbacks were received from 96 companies in North America. Some statistical results are shown in Table 2.1 to 2.4. Though detailed statistical analysis is not possible due to the limited nature of the information obtained, some basic conclusions are helpful to understanding the common characteristics of the transformer failures.

Most transformer failures happened when they were in service or found during maintenance [Kass96, Flee94, and Baty94]. It seems that most failures need a long time to develop until they are detected or resulted in the transformer trip. Immediate failure directly resulting from the energization and re-energization are few, and only one failure happened during the installation in Table 2.1. It shows that routing test and maintenance are very

important to prevent transformer failures or detect abnormal phenomena when the GSU transformer is still in service.

As shown in Table 2.2, GSU transformer failures can be grouped into four main categories [Alla95 and Lapw98]:

(1) Failures due to inadequate specifications, design deficiencies, manufacturing weaknesses, material defects, or inadequate short circuit strength. More than half of failures have their origin in this category. Such deficiencies may develop and result in the transformer failure in the normal operation conditions. In order to increase the statistical reliability of the GSU transformer, more attentions should be paid to the design, manufacturing, and materials.

(2) Failures due to system disturbances, operational environment, or interactions between the transformers and other equipment on the system. Excessive short circuit duty, operational error, and lightning resulted in about 14% failures.

(3) Failures which result from maintenance operations, repairs or refurbishment that have or have not been undertaken. About 11% failures happened due to improper storage, installation, application, maintenance, and protection.

(4) Failures due to unknown reasons or other reasons, such as overload, transportation, earthquake, animals, etc. Such failures are difficult to avoid since the reasons are various, and some failures are very difficult to identify their origins.

Due to various fault causes, failures could happen in any parts of the transformer. However, frequent failures always happen in some components, statistics of fault locations are beneficial for design, maintenance, and trouble-shooting. GSU transformers tend to fail at the high voltage side, such as HV winding, HV bushing, and leads-terminal boards, about 41% such failures are reported in Table 2.3. Windings are more prone to fail, 41% failures are associated with HV or LV windings [Hend88]. Only 10% failures are related to the

magnetic circuit and the core. Considerable failures happened with the tap changers and other ancillary equipments, such as tank, fluid circulation system, current transformers, etc. Many transformer failures involve several transformer components.

Those conclusions are verified again in Table 2.4. Insulation breakdown is the main failure mode since about 30% transformer failures resulted in the dielectric breakdown. Whatever mechanical, thermal, or electrical faults, they will result in the electrical failure when they develop to some extent. Dissolved gas-in-oil analysis (DGA) is proven to be one of the most valuable tools in identifying problems slowly developing inside transformers or bushings since 24.5% failures generate high combustible gas. Several phenomena may result at the same time from the transformer failures. Fire, fluid expulsion, tank rupture, may happen in some cases.

2.2. Effects of Electrical Transients and Lightning on Transformers

Many possible factors could be involved in transformer failures in the Plant, such as oil quality, partial discharge, moisture, ambient temperature, static electrification, oxidation, thermal degradation, and over or under excitation, etc [Kroo90, Baty94, Saha99, and Eber00]. Since little information can be obtained with the limitation of operation conditions and other reasons, comprehensive investigation of transformer failures are impractical. However, based on the preliminary analysis of the transformer failures and characteristics of the specific plant, electrical transient overvoltages and harmonics were suspected that might contribute to the failures besides defects within the transformers themselves. Hence, effects of electrical transients and harmonics on transformers are extensively reviewed [EPRI82 and Bick86] and some former experiences are expected to be helpful for the transformer operation and maintenance in this plant.

Table 2.1. Transformer status when the failure happened

Status	During installation	During energization	In service	During maintenance, inspection or test	During renergization after maintenance	Others
Number	1	13	97	28	3	5
Percent (%)	0.7	8.8	66.0	19.1	2.0	3.4

Table 2.2. Presumed causes of transformer failures

Cause	Design, Manufacturing and material	Inadequate short circuit strength	Improper storage, installation, application, maintenance, and protection	Excessive short circuit duty	Operational error	Lightning	Others	Unknown
Number	74	15	18	4	9	10	15	19
Percent (%)	45.1	9.1	11.0	2.4	5.5	6.1	9.1	11.6

Table 2.3. Locations of transformer failures

Location	HV Bushing	LV Bushing	Leads-terminal boards	HV winding	LV winding	Magnetic circuit	Shielding insulation
Number	23	2	10	44	33	8	7
Percent (%)	12.3	1.1	5.3	23.5	17.6	4.3	3.7
Location	Core Insulation	Core clamping	Coil clamping	Others	Unknown		
Number	10	3	11	29	7		
Percent (%)	5.3	1.6	5.9	15.5	3.7		

Table 2.4. The phenomena resulted from transformer failures

Phenomena	Fluid contamination	Over-heating	Dielectric breakdown	Impedance change	High combustible gas	Mechanical breakdown	Others
Number	41	17	75	5	61	10	40
Percent (%)	16.5	6.8	30.1	2.0	24.5	4.0	16.1

2.2.1. Effects of Temporary Overvoltages on Transformers

A temporary overvoltage is an oscillatory phase-to-ground or phase-to-phase overvoltage that is of relatively long duration and is undamped or only weakly damped. Temporary overvoltages that may contribute to the transformer failure usually originate from:

- Ferroresonance
- Linear resonance or induced resonance from coupled circuits
- Faults

Ferroresonance is a series resonance involving nonlinear inductance and capacitance [Gree91 and Irav00]. The general requirements for ferroresonance are an applied (or induced) voltage source, a saturable magnetizing inductance of a transformer, a capacitance, and very little damping. The capacitance can be in the form of capacitance of underground cables or long transmission lines, capacitor banks, coupling capacitances between double circuit lines or in a temporarily-undergrounded system, and voltage grading capacitors in HV circuit breakers. System events that may initiate ferroresonance include single phase switching or fusing, or loss of system grounding. Ferroresonance can lead to transformer overheating due to high peak currents and high core flux density. High temperatures inside the transformer may weaken the insulation and cause a failure under electrical stresses. In EHV systems, ferroresonance may result in high overvoltages during the first few cycles, resulting in an insulation coordination problem involving frequencies higher than the operating frequency of the system.

Resonance at a particular frequency occurs when the capacitive reactance and the inductive reactance are roughly equal. If a transformer nearby experiences saturation, the resultant harmonics can further amplify the resonant voltage, leading to an even higher temporary overvoltage. Temporary overvoltages resulted from resonance, fault, Ferranti effect, load rejection, etc., can lead to transformer saturation or ferroresonant condition. Overheating may occur inside the transformer because of temporary overvoltages [Past88 and Sybi85].

2.2.2. Effects of Switching Transients on Transformers

Switching overvoltages result from switching operations or faults, which are usually highly damped and of short duration. The magnitude and duration of switching overvoltages may vary over a wide range depending on system parameters, system configuration, and switching conditions. Switching overvoltages may occur whenever the initial voltage at the time of switching is not equal to the final voltage, which is usually described in statistical terms. Details of switching overvoltages can be found in a variety of references [Male88, Balt69, Duba74, Balt70, and Gert78]. Current chopping, pre-strike, and re-strike may contribute to the overvoltage occurrences in many switching operations [Elki93, Popo99, Kosm95, and Mura77]. Switching overvoltages may be classified according to their origin as follows:

- Line energization and reclosing
- Fault occurrence and clearing
- Switching of capacitive current:
  - Line dropping
  - Capacitive bank switching
- Switching of inductive currents:
  - Transformer magnetizing currents
  - Reactor switching
- Special switching operations:
  - Series capacitors
  - Resonant and ferroresonant circuits
  - Secondary switching

Typically, the risetime of switching overvoltages ranges from a few hundred microseconds to one or two milliseconds [Lee90]. Durations range from a fraction of a millisecond to a few milliseconds. The magnitude can be up to 3.0 or 4.0 p.u. Very fast transients in GIS will be discussed later.

The effects of switching overvoltages on transformer insulation are substantially different from those of the temporary overvoltages described above. Transformers behave in a complex manner when impressed by a switching overvoltage. The dielectric components of a transformer coil can be electrically stressed in two ways if a transient voltage is impressed across its terminals. First, the voltage distribution along the coil will be highly nonuniform if the transient voltage has a steep front. This will concentrate the electrical stresses at the end turns, causing possible dielectric failure between adjacent turns at these locations. Second, the coil may resonate at some nature frequencies of the entire or part of the winding if the applied transient voltage contains such a frequency component. Under this condition, some internal points of the coil may attain a voltage peak much higher than the applied voltage [Prei84, Nasr99, and Vaki95]. It may cause dielectric failure between parts of the coil, even when the peak amplitude of the applied voltage is below the BIL of the coil [Pret84].

Sometimes, switching transients can excite the resonance between the transformer and adjacent power equipment and impress a high overvoltage on the transformer, such a case may occur when an unloaded transformer is switched via a relatively long cable [Sche84]. When a transformer-terminated line or cable is energized, harmonics generated by the magnetizing characteristics of the transformers may interact with the line or cable capacitance and cause nonlinear oscillations. In some instances, these oscillations or resonance may be sustained for a relatively long time, and consequently, they may lead to transformer saturation or impose overly severe thermal duty on the transformer.

2.2.3. Effects of Very Fast Transients (VFT) on Transformers

Very fast transients (VFT) are generated during switching operations performed within GIS (disconnectors, circuit breakers or load switches) or system faults in GIS. VFT is basically a capacitive load switching transient but has different phenomenon from transients originated in air due to special physical properties of GIS [Sabo88, Mepe89, and Fuji88]:

- Collapse time is very short, about 5 ~ 10 ns, regarding conductor-earth-breakdown as well as disconnector (DS) or circuit breaker (CB) re-ignition.

- Smaller dimension of GIS as compared to conventional substations may cause less traveling time for wave refractions and reflections. This may result in high transient frequencies in the MHz range.

- Less damping of the traveling waves or standing waves respectively due to coaxial design and only slightly inhomogeneous field without corona losses enables sustained oscillations in the MHz range.

VFT generated during DS operations are consequence of the propagation of step voltages created by the voltage collapse across the inter-contact gap at multiple pre- or re-strikes due to the relatively slow movement of the disconnector contacts. However, the specific VFT wave shape is formed by the multiple refractions and reflections of these steps at all points where they encounter impedance changes inside the GIS. The highest frequency component and the peak transient voltage will be limited by the finite voltage collapse time which depends on gas pressure and can be estimated to be 15 ns for 0.1 Mpa but only 3 ns for 0.5 Mpa. The VFT peak can be up to 2.5 p.u. A typical VFT wave consists of a steep voltage with a rise time in the range of a few nanoseconds, superimposed by three major frequency clusters, one in the frequency range up to about 5 MHz, one in the range between 5 MHz and 30 MHz, and one up to the frequency of 100 MHz. In addition to the fast risetime, VFT is also characterized by high frequency of occurrence and the relatively short duration (typically from a few microseconds to tens of microseconds). Due to the traveling wave nature and the short risetime, VFT wave shape can be significantly different at points separated by only a few meters within the GIS, and the ~100 MHz high frequency oscillations exist only in the vicinity of the DS [Okab91, Bogg84, Ogaw86, Lui94, Miri95, and Yana90]. The oscillation frequencies of the VFT are determined by electrical lengths of GIS bus in which VFT travels.

CBs and load break switches may also generate transients in GIS but due to their very rapid operation only a few strikes may occur. However, a larger number of strikes may occur

for the special case of switching small inductive currents, e.g. switching of shunt reactors and no-load or lightly loaded transformers.

As DS and CB are operated routinely in many substations, GIS components and connected equipment may be exposed to a large number of transients. However, the magnitude of VFT tends to be relatively low (typically 1.5 to 2.0 pu), although values in the range of about 2.5 pu can occur in some instances.

Transformers are either directly connected to GIS through oil-SF_6-bushing or indirectly by SF_6-air-bushing, overhead lines and air-oil-bushing, or by SF_6-oil-bushing, cables and oil bushing. VFT arriving at transformer windings are difficult to qualify because they depend not only on the type and length of the transformer connection to the GIS, but also on the transformer parameters and winding design. However, in the worst case it might be expected that the wave front will be slightly extended and the amplitude slightly larger. Traveling wave theory can be used to analyze the VFT propagation in the windings. Transformer windings may be affected by VFT in the following two modes [Shib99, Kres93, and Corn93].

- Steep front wave impulses create an extremely nonlinear voltage distribution along the high voltage winding connected to the oil-SF_6-bushing for the directly connected transformers. The nonlinear voltage distribution creates considerable potential differences appearing some portion of the transformer winding, which may result in inter-turn or inter-disc winding failures. Several such failures have been observed in the windings connected to GIS [Gock98, Henr98, Mart96, Mart91, Dire82, and Dire84]. For the indirectly connected transformers, the path through the bushings and an overhead line or cable smoothes the steep front to values comparable to chopped waves, which are well established and covered by impulse testing, and the effect of steep front is expected to be smaller than on directly connected transformers.

- VFT can excite extremely high partial winding resonance voltages in the transformer windings. For directly connected transformers, frequencies up to several MHz can be

transmitted through the bushings. For indirectly connected transformers, the highest frequency transmitted is about 1 MHz. In both cases partial winding resonance could occur near the connection points, e.g. the entrance coils and the selected tap of a step winding connected to the neutral point on the on-load tap changer (here neutral point is referred to the tap changer's neutral point, not the transformer winding's neutral point). The smaller the proportion of two subsequent amplitudes of same polarity, the smaller the developed resonant amplitudes and the higher insulation strength.

Investigation on a 500 kV transformer shows that partial winding resonance resulting from VFT can generate high interturn (turn to turn) voltage, which could reach 0.25 times of the applied voltage. In the tested transformers the estimated interturn voltage developed under an incoming VFT can be up to 3 times higher than in the lightning impulse voltage test. Another measurement on a layer winding without shield reported this maximum interturn voltage at 48% of the incoming voltage with a waveform of 10/20 ns and the traveling wave propagates along the winding with reduced peak value [Naka97, Fuji98, and Mull83].

The extremely nonlinear voltage distribution related to a steep front and high partial winding resonance voltage may result in direct dielectric breakdown, or deterioration of winding insulation and the occurrence of partial discharges. If frequent VFT are imposed on a normal transformer, such as frequent CB or DS switching in GIS, the aging process will degrade the insulation in general, and the transformer will be prone to problems sooner or later.

In 1994, CIGRE conducted a survey about transformer failures with respect to VFT in GIS, which involved 22 utilities/manufacturers in 9 countries [Gock98 and Henr98]. About 537 direct connected transformers and 596 indirect connected transformers were included with all voltage levels. Details are shown in Table 2.5. About 6 winding failures were reported at 500 kV level, in which 3 failures were initiated by flashover in the connected GIS system and 3 failures during normal operation associated with VFT. About 9 bushings failed at 500 kV level, and some of failures were related to inadequate design.

Based on the reported numbers of GIS systems in operation it cannot be concluded that switching operations in GIS represent a general problem for the connected transformers. However in special configurations and particular operation conditions there might be a problem. To be able to analyze these cases, specific information about the GIS system and connected transformers is needed.

2.2.4. Effects of Lightning Overvoltages on Transformers

Lightning overvoltage is a phase-to-ground or phase-to-phase overvoltage produced by one specific lightning discharge. Types of lightning overvoltages include those due to shielding failures, caused by a direct stroke to one conductor, back-flashovers, caused by strokes to the tower or ground wires, and induced voltages, caused by strokes to nearby grounded objects [EPRI82 and Chow96].

Measurements show that the initial lightning stroke is most commonly of negative

Table 2.5. Statistics of transformer failures with respect to VFT in GIS

Failures	Voltage level kV	Number of transformers		Chopped wave tested	Arrester protection	Busbar length m
		Direct connected	Indirect connected			
None	50	0	5	No	Yes	-
None	63	3	43	No	Yes	8-30
None	75	0	2	No	No	12
None	110-154	127	135	87% Yes	90% Yes	6-30
None	187-275	131	289	75% Yes	93% Yes	5-120
None	300	8	7	No	Yes	5-55
None	380-420	104	54	15% Yes	81% Yes	5-200
3 + (3)	500-550	139	61	Yes	Yes	10-100
None	800	15	0	Yes	Yes	50
Sum winding failures 3 + (3)						
Bushing failures 9	550-550					
OFFLTC failures 1	550-550					
Total 13 + (3)		537	596			

polarity and unidirectional. Lightning current magnitude can be approximated quite well by the Anderson expression [Chow96 and IEEEw93]:

$$P_I = \frac{1}{1+(\frac{I}{31})^{2.6}} \tag{2.1}$$

where P_I is the probability of exceeding the stroke current I in kA.

The lightning overvoltages have duration between 1 and 100 microseconds and a wave front between 1 and 5 microseconds. The standard wave shape for testing the ability of insulation to withstand overvoltages due to lightning is a unidirectional impulse with a front time of 1.2 us and a tail time of 50 us. The wave shape of the lightning current is different from the voltage produced at the point of contact of the lightning stroke. The rate of rise of a lightning current is approximately given by:

$$P_{dl} = \frac{1}{1+(\frac{dI/dt}{24})^{4}} \tag{2.2}$$

where P_{dl} is the probability that a specified value of dI/dt is exceeded, and dI/dt is the specified maximum rise time in kA per microsecond.

Frequency of lightning occurrence is another concern. The ground-flash density could be estimated by the equation [Elah90]:

$$n_g = 0.04T^{1.25} \tag{2.3}$$

where n_g is the ground-flash density (flashes/km^2/year) and T is the number of thunderstorm days per year or Keraunic level.

Though lightning surges have been reduced to an acceptable level in modern substation insulation coordination, still transformer failures related to lightning are often reported [Wech88]. Two possible transformer failure modes may happen if a lightning surge appears at the transformer terminals. The transformer main insulation (the insulation between HV winding and LV winding, HV winding and core, or HV windings) will be threatened because of the large magnitude of the lightning surge. On the other hand, the insulation between turns at the beginning of the HV winding is often disproportionally more stressed because of the large potential gradient appearing in the initial voltage distribution. Similar to switching overvoltages and VFT, it is possible that lightning overvoltage may excite partial winding resonance in the transformer windings. The distance between the arrester and the transformer will determine the overvoltage magnitude at the transformer HV terminals [Gree91 and Chow96].

2.3. Effects of Harmonics and Transients Resulting from Power Conversion Equipment on Transformers

With the application of FACTs, HVDC, static frequency converter (SFC), and other power electronics devices in power systems, harmonics and transients resulting from switching of power conversion devices are becoming more concern. The major effects of power electronics on power transformers are: 1) insulation failures related to the commutation transients; 2) resonance excited by harmonics; 3) transformer overheating by harmonic currents, which can lead to transformer derate or reduce its lifetime.

Commutation of converters or inverters causes the ac current to switch suddenly from one circuit to another, thus, a voltage spike is produced due to the leakage inductance and capacitance. Such transients are occurring continually when in normal operation. High voltage spikes not only contribute to the power electronics device failures, but also affect the insulation of directly connected transformers or motors. Though snubber circuits are always used to limit the peak transient voltage across the device and connected equipment, failures of induction motors are occasionally reported when fed by the inverters due to high voltage spikes [Lani98]. Few insulation failures happened due to commutation transients in converter

transformers or other converter and inverter connected transformers in recent times, but it is still a concern in some special conditions [Tana99 and Work96].

Either series or parallel resonance can occur in the transformer and load circuit if the resonant frequency coincides with one of the characteristic harmonic frequencies of the converter or inverter, then a amplification of currents and voltages at that frequency can result. The magnitude of the amplification encountered will depend on the amount of resistance in the circuit, which acts to damp the current. The possibility of harmonic resonance is illustrated in several references. Saturation and overheating of transformers may result if such cases happened. Sometimes due to asymmetrical six-pulse converter firing, earth return and other effects, a DC current component may appear on the transformer windings. This, in turn, results in asymmetrical saturation of the transformer and great modification of the corresponding magnetizing current [Rick86, Kell99, and Dela96].

Harmonics occurring in power systems result in additional losses in both transformer magnetic core and windings. Transformer losses are divided into three broad categories: no-load losses, load losses, and total losses (sum of no-load loss and load loss). The hysteresis and eddy current losses in the core make up the no-load loss component, which is due to the applied voltage. The harmonic distortion of the system voltage is usually below 5% unless there is excessive harmonic loading or a resonance condition, so the no-load loss should be close to the design value. Load current harmonics passing through the transformer do not significantly affect the no-load losses of the transformer.

The load losses, due to the current passing through the windings, are the main losses in a transformer. Load losses consist of I^2R winding losses and stray losses. It is the stray loss component that is of special importance when evaluating the added heating due to current harmonics. The stray loss is further divided into the eddy-current losses in the winding and those in core, clamps, and other structural parts. The winding stray loss includes winding conductor strand eddy-current loss and the loss due to circulating currents between strands or parallel winding circuits. This loss will rise in proportion to the square of the load current and the square of frequency, which plays a key role in transformer overheating. Transformer

overheating by the harmonic current may lead transformer to derate, reduce lifetime, or accelerate insulation aging [Bish96, Ram88, and Kras87]. Transformer oil and winding thermal time constant are usually more than 2 and 0.5 hours for large power transformers, so temporary current harmonics passing through the transformer are not expected to cause transformer overheating and other effects [Dela96].

2.4. Summary

Review of transformer failures is helpful to find out the possible root causes of several GSU transformer failures in a pumped storage plant. Based on the extensive review of historical GSU transformer failures, discussion of various abnormal electrical transient effects on the transformers, and special operation conditions in the pumped storage plant under study, three topics are focused, including: 1) possible effects of CB and DS switching transients in GIS on the transformer insulation; 2) possible effects of the lightning stroke on transformer insulation and the influence of arrester locations on overvoltage protection of the transformer; 3) possible effects of SFC commutation on transformers, including commutation voltage spikes and possible excited harmonic resonance.

CHAPTER 3
STUDY OF SWITCHING TRANSIENTS EFFECTS ON GSU TRANSFORMERS

Three 345 kV generator-step-up (GSU) transformers failed successively in a large pumped storage plant in recent years, resulting in a considerable economic loss due to loss of generation. In order to search for possible causes of transformer failures, and most importantly, avoid such failures in the future, the electrical environment of the GSU transformer was extensively investigated. Possible abnormal electrical phenomena associated with the GSU transformer were studied, with particular consideration given by the unique operation environment of the pumped storage plant. This chapter will focus on the switching transient effects on the transformers due to circuit break restriking and disconnector restriking.

3.1. Introduction

3.1.1. Overview of Operation in the Pumped Storage Plant

As shown in Fig.3.1, the transformers are connected to the 345 kV GIS via oil-filled 345 kV cables of 630 m in the pumped storage plant. Four transmission lines are connected to the Chung-Liao Switching Station, and one of transmission lines was put into operation only after Tr.#4 failed in 1999. The detailed technical data of power equipment and the system is included in Appendix A. The bus bars are the single phase configuration in the GIS. Circuit breaker (CB), disconnector (DS), earthing switch, and current transformer (CT), etc., are mounted in each enclosure filled with SF6 gas. ZnO arresters are installed at the end of the connecting buses in the GIS, which protect the switchgear from incoming surges and intend to protect the transformers from the surges coming from the GIS. The GIS operates as a double bus, simple line breaker scheme with two bus-tie breakers and two bus-sectionalizing breakers, and a starting bus used for back-to-back starting.

All transmission lines are energized all the time during normal condition unless fault related trip out. All buses normally are tied together except during maintenance.

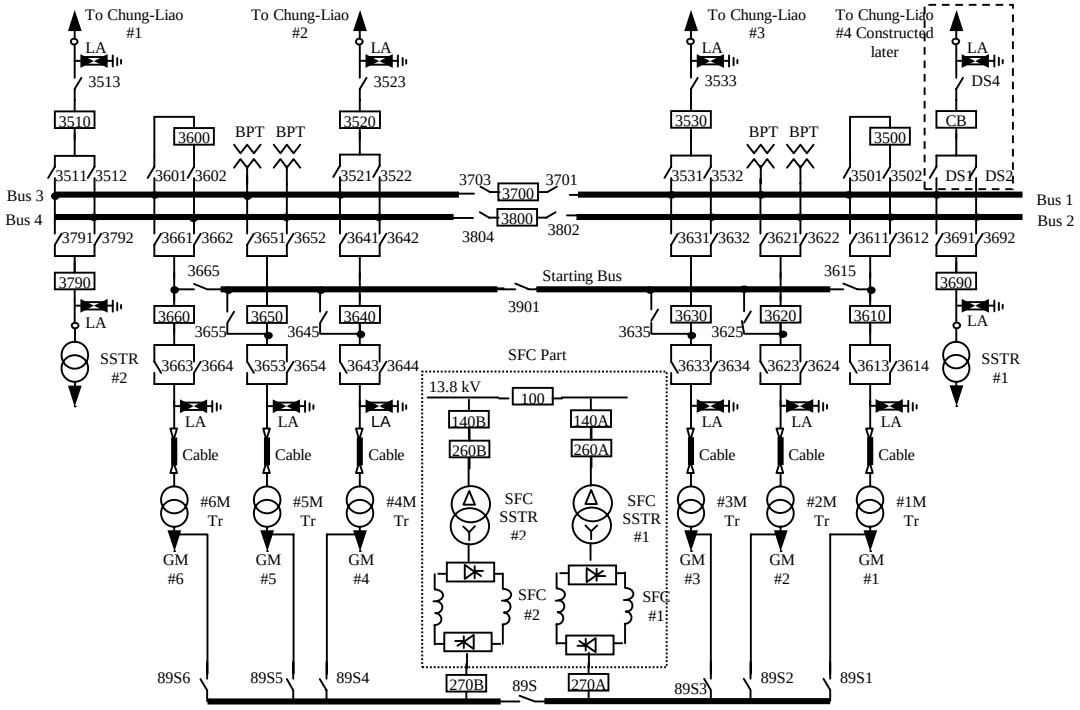

Fig.3.1. Main electrical schematic of the pumped storage plant

The number of operation changes of a reversible pumping units is high, frequently as many as four times a day. The G/M units are normally at generation mode three times and at pump mode once a day, and the total number of operation changes are about 1800 times annually.

Two kinds of starting methods are applied to start the generator/motor units to the pump mode of operation, back-to-back synchronous starting and static frequency converter (SFC). Back-to-back starting involves simultaneously two units, which are electrically connected [Osbu92 and Alle91]. The driving unit feed the driven unit at continually increasing frequency up to nominal frequency. Then the driven unit is connected to the grid at pump mode, the driving unit is disconnected and slowed down to standstill. The driving unit then has to stop before being able to start another unit. This method is therefore time consuming.

Unit 1 and 6 are usually used as the driving units to start other units in this plant. Before 1995, back-to-back starting is the main starting method.

SFC consists of two bridges, a three-phase thyristor rectifier and a variable frequency inverter connected together through a current smoothing inductor [Harl81 and Pete72]. It allows complete starting of a unit from standstill to rated speed in approximately 5 minutes. Starting and electrical braking can be carried out at rated speed without overcurrent. For starting from standstill, the forced commutation method is used up to 10% of rated speed, afterwards the inverter bridge commutation is directly controlled by the frequency of the induced alternative voltages of the synchronous machine above 10% of the rated speed. One static converter may be shared by several units. After several DS failures and Tr.#1 failure again in Mingtan plant, SFC starting strategy is used until now. However, SFC starting requires power from the system, back-to-back starting strategy is expected to be used again soon.

3.1.2. Operation Characteristics

Several switching strategies are used for starting the units at pump mode, as shown in Appendix B. The synchronizing requirements of CBs when switching to the system are that the speed is 400 rpm, the frequency is 60 Hz, and the output voltage of the unit is 16.5 kV. As described above, many CB and DS switching operations occur when the unit operation mode is changed. Some switching operations are expected to generate VFT in the GIS, and such VFT will propagate to the GSU transformers. The sequences of DS and CB operations are different when the G/M unit is started with different starting strategies, hence voltage responses resulting at GSU transformer terminals may also vary. It is of interest to find out what kinds of switching operations can generate large very fast transient (VFT) overvoltages at the transformer terminals that may affect transformer insulation, due to CB or DS restriking.

3.2. System Modeling

3.2.1. Overview

In general, accurate results in computer simulations require the use of detailed models. However, system studies on a large GIS, which incorporates many components, requires simple but accurate components models to achieve an overall GIS model of a manageable size. Specific applications determine the grade of details in the modeling. The inclusion of more details in the simulation, such as representation of each spacer, can result in more detailed agreement but with great complexity in the overall model. On the other hand, simplified models can generate acceptable results in a short computation time in most cases, at the expense of minor details, such as small spikes or deviations [Fuji88].

In order to simulate VFT in GIS and lightning phenomena, several factors are taken into account here to model the components in the GIS and other equipment.

1). Most of the components have their capacitances dominating over other parameters since VFT and lightning contain predominately high frequency components ranging from hundreds of kHz to tens of MHz.

2). As the transients seen at the terminal of the transformer is concerned and the transformer is connected to the GIS via a long cable of 630 m, very high frequency components of hundreds of MHz resulting from VFT can not be seen at the transformer terminals. Components with several pF or tens of pF and some short buses with the travel time less than 2 ns in GIS are ignored in simulation without much loss of accuracy, such as spacers, elbows, corona shields, et al.

3). Modeling and simulation of VFT using single-phase circuit can characterize the detailed VFT propagation in GIS and connected equipment since the bus bars are single phase enclosed in GIS.

3.2.2. Modeling of GIS Components and Connected Equipment

Modeling of GIS components and electrical equipment can be found in many references [Gran88, Esme88, Cars91, Lewi88, Vino99, Boec87, and Povh96]. Table 3.1 shows the detailed representation of GIS components and connected equipment in this plant.

Table 3.1. Component representation

GIS bus bar	z_0 = 80 ohm v = 0.9c, c – light velocity
CB, DS, and earthing switch	In the closed position: extension of the GIS bus bar. In the open position: open-circuit
Surge arrester	15 pF in series with a grounding resistance of 0.1 ohm.
Potential transformer (PT)	300 pF
Current transformer (CT)	300 pF
Capacitive voltage transformer (CCVT)	8 nF
Bushing	100 pF
GSU transformer	5 nF
Station service transformer (SSTR)	500 pF
Overhead transmission line	z_0 = 350 ohm v = c
345 kV oil-filled cable	$R_0 = 1.0679 \cdot 10^{-3}$ ohm/m z_0 = 37.769 ohm $v = 2.11 \cdot 10^8$ m/s

z_0: surge impedance
v: wave velocity
R_0: Resistance

GIS Bus Bar

As the GIS sections are a concentric cylinder type bus bar, they are usually modeled in distributed parameter form by its wave velocity and surge impedance, z_0, given by the formula:

$$z_0 = 60 \ln \frac{D_2}{D_1} \text{ ohm} \qquad (3.1)$$

where D_2 is the inner diameter of enclosure and D_1 the outer diameter of the conductor. The travel time is determined by the physical length of the bus and the wave velocity, which is assumed equal to $2.7*10^8$ m/s (0.9c, c – light velocity). Here surge impedance of the bus is assumed to be 80 ohm according to the literatures.

Disconnector and Earthing Switch

DS and earthing switch in the closed position are represented as an extension of the gas-insulated bus bar. In the open position the representation is an open-circuit and the length of DS and earthing switch is also considered as an extension of the bus bar.

Circuit Breaker

CB is a much more complicated piece of apparatus than other components as there are various diameters along its length due to shields and contact assemblies. Two separate detailed models were developed, one for a closed breaker and one for an open breaker [Froh99, Carv99, Work98, and Pail99]. Both of these models, however, are too complex to be used when modeling an entire GIS. Furthermore, it was found that, for most purposes, good results could be achieved with simpler models.

Due to the limited information about CB obtained from Mingtan plant, for a closed CB, the simpler model is used that considers the CB as a section of bus, with the same surge impedance and velocity. For an opened CB, the representation is an open-circuit and the length of CB is also considered an extension of the bus.

Surge Arrester

All of calculated and experimental data indicate that the voltages produced by DS switching will not cause the MOV to conduct due to the VFT duration and magnitudes. Additionally, unless the concern with the internal voltages in the arrester, this highly complicated model is not necessary [Amur88, Clay83, and Kim96]. Instead, only the arrester capacitance needs to be modeled. Here the arrester is represented by a capacitance of 15 pF in series with a resistance of 0.1 ohm when simulating VFT resulting from DS and CB switching.

In the lightning overvoltage study, the representation of the arrester was assumed by using a non-linear resistance taking into account different sparkover voltages and V-I characteristics according to the behavior of the time to crest of the incoming waves [Erik86, Jin93, Pinc99, and Work92a]. The rated voltage of the modeled arrester is 312 kV, MCOV

(Maximum Continuous Operating Voltage Rating) is 209 kV, and 8/20 μs maximum discharge voltage is below.

Reference voltage		624 kV
V-I characteristics	Current (kA)	Voltage (kV)
	1.5	522
	3.0	552
	10.0	604
	40.0	752

Potential Transformer (PT), Current Transformer, and Capacitive Voltage Transformer (CCVT)

Both PTs and CTs in GIS are represented simply as capacitances to ground of 300 pF. They have little effect on the overvoltages seen at the transformer terminals because of their small value and long cables connected in between.

CCVTs, which are installed only at Phase B of overhead lines, are represented by a lump capacitance of 8 nF.

Bushings

The bushings connecting GIS to transmission lines are represented by a section of GIS bus, plus an additional lumped capacitance of 100 pF. The bushings connecting GIS to oil-filled cables are only represented by an extension of GIS bus [Ardi92].

Power Transformers

The power transformers are simulated by their surge capacitances [Mart98, Qure93, and Papa94]. These capacitances range from 2 to 10 nF, depending on the transformer design. This representation, however, is not critical for lightning overvoltages and VFT developed inside the GIS and approximate values can be used. Usually for a 345 kV GSU transformer, 5 nF is used.

For the station service transformers (SSTR), a capacitance of 500 pF is used.

Transmission Lines

The lightning waves penetrate in the GIS through the transmission lines, so their representation must be very accurate. Usually a single-phase representation is applied and produces conservative results. When studying VFT generated in GIS and seen at the transformer terminals, the representation of transmission lines is not critical. Here the overhead lines are considered to be of infinite length and represented by a single-phase positive wave impedance of 350 ohm to ground with the light velocity, so that there is no reflection from the end.

When simulating VFT, the equivalent AC sources are connected to the transmission lines. The peak value of the voltage is 281.69 kV with a phase angle of zero. The source impedance is 8.4 mH with regard to the maximum short-circuit capacity of 37645 MVA based on the formula below.

$$L = \frac{U^2}{\omega S} = \frac{345000^2}{2\pi \times 60 \times 37645 \times 10^6} = 8.4\,\text{mH} \qquad (3.2)$$

Oil-filled Cables

Many of the cable models used in the EMTP have their roots in the modeling of overhead transmission lines, and they fall into one of the two categories [Mart93, Mart88, and Mere97]:

- Lumped-parameter models, and
- distributed-parameter, traveling wave models.

Here single-phase frequency-independent distributed-parameter model is used to represent the oil-filled cable. The line/cable subroutine in ATP-EMTP is used to calculate the distributed parameters of the cable based on the cable configuration. The frequency for calculation is fixed at 100 kHz and the length is 630 m. The obtained parameters are

Resistance	1.0679 * 10-3	ohm/m
Surge impedance	37.769	ohm
Wave velocity	2.11 *108	m/s

3.2.3. Arc Modeling

CB and DS restrikes are modeled as an exponentially decaying resistance and a small resistance in series to take care of the residual arc resistance. This is implemented using a Type 91, TACS time-varied resistance *R* in ATP-EMTP. The mathematical equation for the above is given by

$$R = R_0 e^{-\frac{t}{T}} + r \qquad (3.3)$$

where R_0 is 10^{10} ohm and the time constant, *T* is 1 ns. For DS restrikes, *r* is assumed 0.5 ohm; for CB restrikes, *r* is assumed 0.01 ohm because of smaller arc resistance.

3.2.4. System Network Reduction

Based on the individual models discussed above, the entire system modeling is done according to the electrical configuration of the plant. Furthermore, special simulation can be realized by combining them together with regards to the status of DS, CB and earthing switches. Then the network is reduced by combining some bus sections together, which are connected each other and of same characteristics.

3.3. Simulation Strategy

3.3.1. Possible Transients Causes

With analysis of the switching sequences in Appendix B, three kinds of phenomena may cause large transients related to GSU transformers in the plant.

3.3.1.1. Current Chopping

Current chopping, which means that the current is forced to zero at times other than the natural current zero crossing, generally can occur with all kinds of circuit breakers and is the result of an unstable interaction between the arc and the circuit. Sometimes current chopping may result in high chopping overvoltages especially when interrupting an inductive current. The large value of chopped current may happen in Vacuum CB and SF6 Puffer CB because of stronger arc-quenching mediums.

The chopped current can be up to 10.0 A or more in SF6 CB depending on the SF6 pressure, switching conditions, and power factors of the chopped current [Lee90]. Usually for SF6 CB, chopped currents of about 2 to 5 A can be expected.

3.3.1.2. CB Restrike

Switching of SF6 CBs is expected to generate few restrikes due to their very rapid operation and progressing design. However, SF6 CB restrikes do occur especially with the interruption of small inductive current or with contaminated contact surfaces. In this specific case, frequent CB switching also increases the possibility of CB restrikes. In April 2000, a cable box between the GSU Transformer #1 HV terminal and the oil-filled cable has failed due to CB 3610 restriking. Hence, SF6 CB restrikes are considered as a possible cause of high VFT at the transformer terminals. Though the overvoltages resulting from CB restrikes are statistical, the out-of-phase CB operation is used here to simulate CB restrikes as it generates the largest overvoltages giving the conservative estimation.

3.3.1.3. DS Prestrike and Restrike

Unlike CBs, a DS requires several seconds to reach its final position on account of its slow-moving contact. During this time the transient voltages generated by prestrikes or restrikes passes through several cycles of the power frequency voltage. The precise number and amplitude distribution of strikes during a typical switching depend on the specific DS design and operational speed, the behavior of the GIS after each restrike or prestrike spark extinction, and specific GIS functional procedures.

In this plant, more DS restrikes are related to opening a floating section of bus (a pure capacitive load) in the GIS, especially when using back-to-back starting. A trapped charge may be left on the floating section. Typically the measured trapped charge left gives remaining voltages ranging from 0.1 to 0.5 pu with the mean value of around 0.3-0.4 pu [Sabo88 and Fuji88]. Here only the worst case in each switching operation is simulated for security, this means that the trapped charge is assumed always at 1.0 pu. A 1.0 pu voltage source connected to the floating bus in series with a 1 H inductance is used to simulate the trapped charge, as shown in Fig.3.2. Before DS restrikes, this voltage source ensures that the potential of the floating bus is 1.0 pu (1 pu = 281.69 kV); when the DS restrike occurs, the voltage source is isolated with the floating bus by the 1 H inductance due to high frequency oscillation.

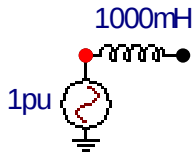

Fig.3.2. Simulation of the trapped charge

3.3.2. Simulation Setting

The alternative transients program (ATP), a widely used version of EMTP, is applied here to simulate switching transients and lightning overvoltages. The voltage waveforms at the transformer terminals will be analyzed.

In order to compare the overvoltages, the same setting is applied for all switching simulation strategies except current chopping simulations.

Time step: Δt = 2.5 ns
Maximum calculating time: T_{max} = 0.05 ms

3.3.3. Analysis Strategy

All DS and CB routine operations were reviewed, more than 100 switching operations of about 25 typical switching sequences were simulated. Each switching sequence might take DS restriking, CB restriking, and current chopping of the SF6 CB into account whenever necessary based on Appendix B. In terms of each switching operation, the detailed simulation is done to obtain the overvoltage at the transformer terminals. Each overvoltage trace obtained will be analyzed to determine the peak voltage, the maximum voltage change, the maximum rate of rise of the overvoltage, and predominant frequencies, defined in Fig.3.3.

3.3.4. Description of the Simulation Circuit

In order to simplify the simulation procedure and keep the common features, several assumptions are made with consideration of the practical operation environment:

1). Since three phases are separately enclosed in GIS and inter-phase mutual effects can be ignored, transients are expected to be similar for three phases. Therefore, only Phase A is simulated in all cases. Simulation of Phase B and Phase C are expected to have the similar results.

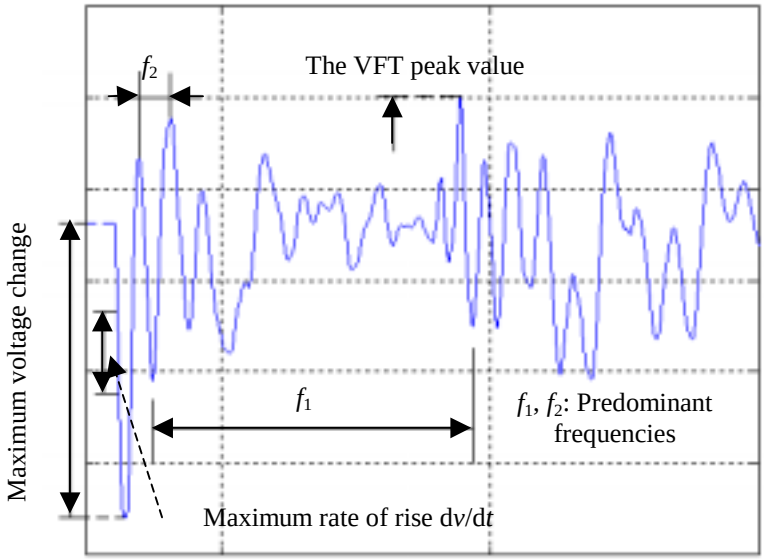

Fig.3.3. Typical VFT voltage measurement

2). Since all buses normally are tied together and the bus bay to Chung-Liao #4 Station was put into operation only after Tr. #4 failure, the status of CBs and DSs are assumed below referred to Fig.3.1:

- The transmission line to Chung-Liao #1 is connected to Bus 3;
  The transmission line to Chung-Liao #2 is connected to Bus 4;
  The transmission line to Chung-Liao #3 is connected to Bus 1;
  The transmission line to Chung-Liao #4 is not considered.

In three bus bays to transmission lines, CB 3510, 3520, and 3530 are closed, DS 3512, 3521, and 3532, DS 3513, 3523, and 3533 are closed, and DS 3511, 3522, and 3531 are opened.

- The bus tie CBs, CB 3700 (DS 3703, DS 3701), CB 3800 (DS 3804, DS 3802), and CB 3500 (DS3501, DS 3502) are closed, and only CB 3600 (DS 3601, DS 3602) is opened.

3). Station Service Transformer (SSTR) #1 is connected to Bus 2, and SSTR #2 to Bus 4. Therefore, CB 3690 and 3790 are closed, DS 3691 and 3791 are closed, and DS 3692 and 3792 are opened.

4). Only the driving unit and driven unit are considered when back-to back starting, other units are assumed not in operation and related CBs and DSs are opened. When the driven unit reaches the rated speed, it can only be connected to Bus 1 or Bus 3.

5). DS 89S1, 89S2, 89S3, 89S4, 89S5, and 89S6, are opened.

3.4. Simulation of Switching Transients Using the Back-to-back Starting Method

Two switching sequences are analyzed here to illustrate how to evaluate the possible generated switching transients at GSU transformer terminals using the back-to-back starting method. For other switching sequences in Appendix B, similar analysis procedures can also be applied.

3.4.1. Case 1 – Unit 2 Started by Unit 1

When Unit 2 is started by Unit 1 using the Back-to-Back starting method, the following switching sequence is used:

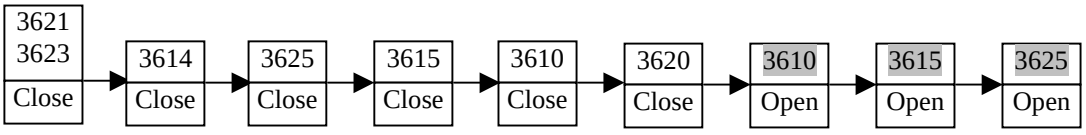

As seen from Fig.3.1, only switching operations shaded may generate high overvoltages, including:

- Chopping overvoltage resulting from CB 3610 opening;
- Switching transient resulting from CB 3610 restrikes;
- VFT resulting from DS 3615 and 3625 restrikes.

3.4.1.1. Current Chopping Due to CB 3610 Opening

Fig.3.4 shows part of the simulation circuit related to Tr.#1 when using Unit 1 to start Unit 2. AC source, Unit1, represents the equivalent voltage source of Unit 1 as a generator, which is connected to the oil-filled cable via the transformer short-circuit inductance X_t. The load of Unit 2 as a motor is assumed 3.0 MW and 0 Mvar. CB 3610 is opened at t =10.0 ns and the chopped current is 10.6 Amp.

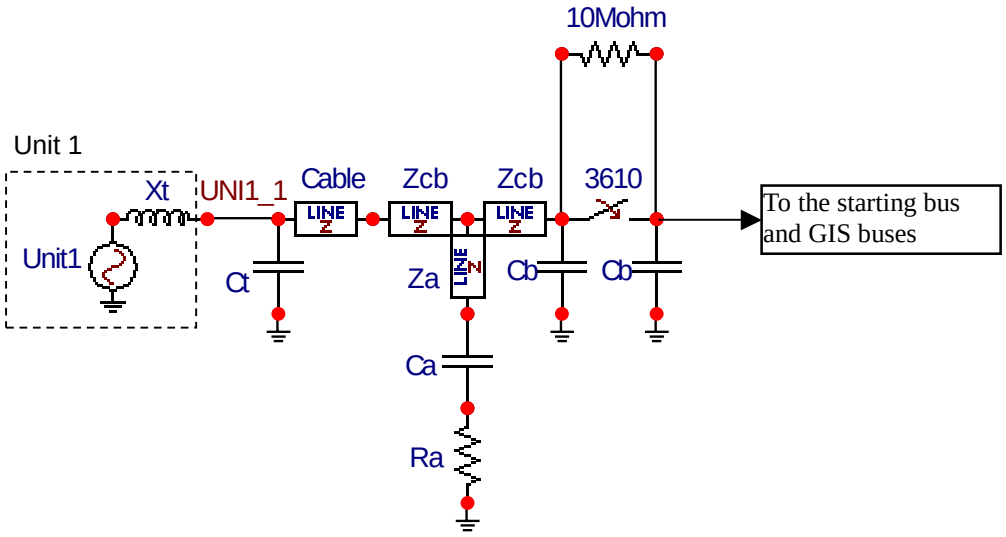

Fig.3.4. Part of the simulation circuit when Unit 2 is started by Unit 1

The voltage waveforms seen at the terminals of Tr.#1 and #2 are shown in Fig.3.5. The overvoltage at the terminal of Tr.#1 is 1.05 pu, and 1.0 pu at Tr.#2. The amplitudes are very small, and should have little effects on the transformer operation. When using Unit 1 or Unit 6 back-to-back to start other units, similar chopping overvoltages can be obtained.

As it is well known, in most cases, high overvoltages due to current chopping may occur when interrupting small inductive currents. However, in the studied case, the long cable can mitigate the overvoltage due to its large capacitance, current chopping should not be a big concern.

3.4.1.2. CB Restrike Due to CB 3610 Opening

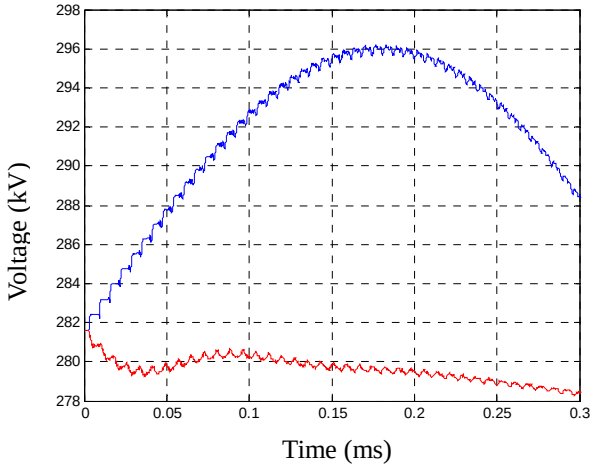

Fig.3.5. Chopping overvoltages seen at the terminals of Tr.#1 (Solid) and #2 (Dash) when Unit 2 is started by Unit 1

The detailed simulation circuit and ATP-EMTP data file are shown in Appendix C. CB restrike is discussed in Chapter 3.3.1.2. Here just the worst case is considered, assuming that CB 3610 is switched at 180° out-of–phase, and the potential difference between CB contacts is 2 pu. Though it is less possible to happen in practice, similar cases with same waveforms and smaller amplitudes do occur when φ is other than 180°.

Fig.3.6a and 3.6b shows the voltage waveform seen at the terminal of Tr.#1 and its frequency spectrum. The overvoltage is 2.7 pu, and the maximum rate of rise dv/dt is 1.2 MV/us.

The predominant resonant frequency is 87.0 kHz and 231.0 kHz. The resonant frequency is the natural frequency of the cable. As shown in Table 3.1, the surge velocity of the cable, v, is 2.1E8 m/s, and the length, l, is 630 m, and the natural frequency of the cable is $1/(4 \cdot l/v)$, 83.3 kHz. Resonance could generate high overvoltages at the transformer terminal and may afftect the transformer insulation coordination specially considering high rate of rise of the overvoltge. It is also possible that such resonant frequencies may excite part-winding

resonance or full winding rosonance in the transformer HV windings. This kind of CB restrike is very dongerous for the transformer insulation.

Similar to the voltage at Tr.#1, the voltage seen at the terminal of Tr.#2 is shown in Fig.3.6c, and the overvoltage is 2.2 pu. The overvoltage is a little smaller than at Tr.#1, but it is still severe for the insulation of Tr.#2.

Fig.3.6d shows the voltage at the GIS side of CB 3610, and the overvoltage is 1.5 pu. It can be seen that with the long cable filtering, the high frequency components in Fig.3.6c disappear at the transformer terminals.

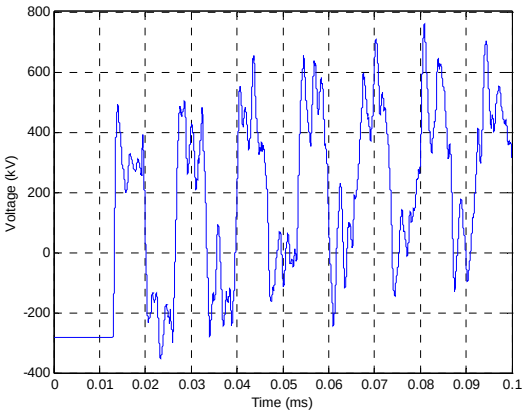

a. The voltage seen at the Tr. #1 terminal

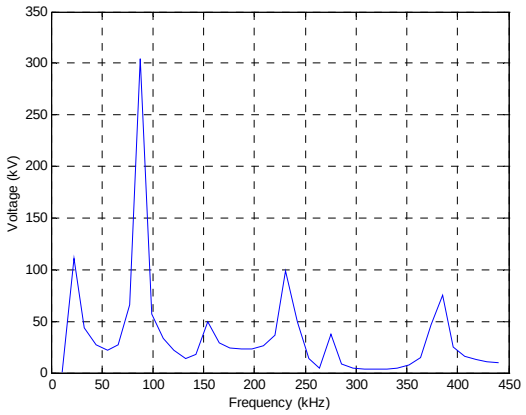

b. The frequency spectrum of Fig.3.6a

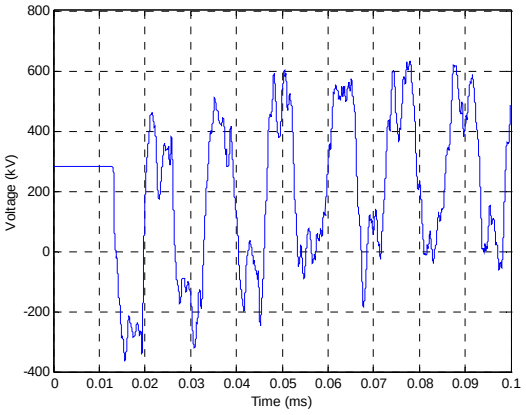

c. The voltage seen at the Tr. #2 terminal

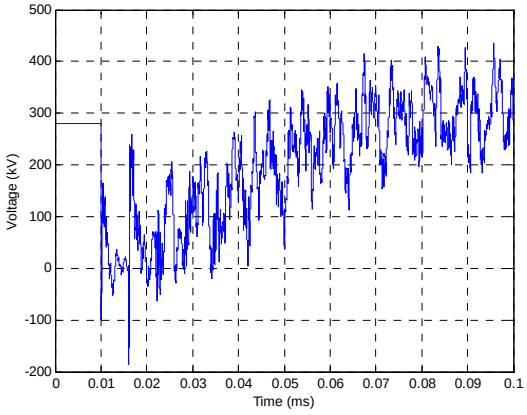

d. The voltage at the GIS side of CB 3610

Fig.3.6. The overvoltages due to CB 3610 restrike when Unit 2 is started by Unit 1

3.4.1.3. DS Restrike Due to DS 3615 Opening

Modeling of DS restrike is described in Chapter 3.3.1.3. The trapped charge in the floating bus between DS 3615 and CB 3610 is assumed 1.0 pu.

Fig.3.7a and 3.7b show the VFT seen at the terminal of Tr.#2 and its frequency spectrum. The maximum VFT is 1.08 pu due to the short floating bus. The maximum voltage change is 45.4 kV. The resonant frequency is around 140 kHz. VFT has been delayed and filtered when reaching the transformer. The VFT at Tr.#1 side of the DS 3615 is 1.76 pu and shown in Fig.3.7c. Results show that VFT resulting from DS 3615 restrikes has little effects on the insulation of Tr. #2.

3.4.1.4. DS Restrike Due to DS 3625 Opening

The trapped charge in the floating bus between DS 3615 and DS 3625 is assumed 1.0 pu. Fig.3.8a and 3.8b show the VFT seen at the terminal of Tr.#2 and its frequency spectrum. The maximum VFT is 1.18 pu. The maximum voltage change is 145.9 kV and the maximum rise of rate is 1.56 MV/us. VFT is larger than in Chapter 3.4.1.3 due to the longer floating bus. The resonant frequency is around 140 kHz.

It is possible that VFT may excite part-winding resonance in the transformer windings. Extremely non-linear voltage distribution along the winding may happen due to high rate of VFT rise. According to [Fuji98], it is assumed that the maximum interturn voltage is 0.015 times the applied impulse voltage for 345 kV transformers. Since the test impulse voltage for the studied transformers is 1050 kV, the interturn voltage can be estimated to be:

$$1050 * 0.015 = 15.75 \text{ kV} \quad (3.4)$$

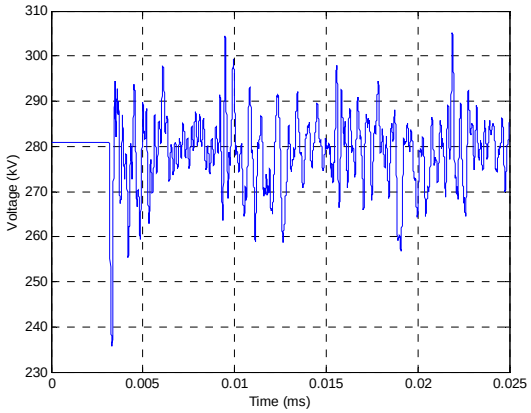

a. The voltage seen at the Tr. #2 terminal

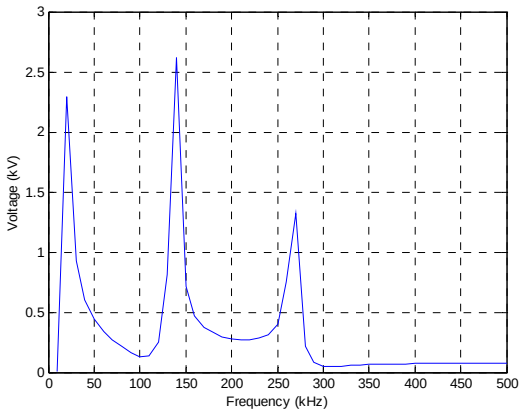

b. The frequency spectrum of Fig.3.7a

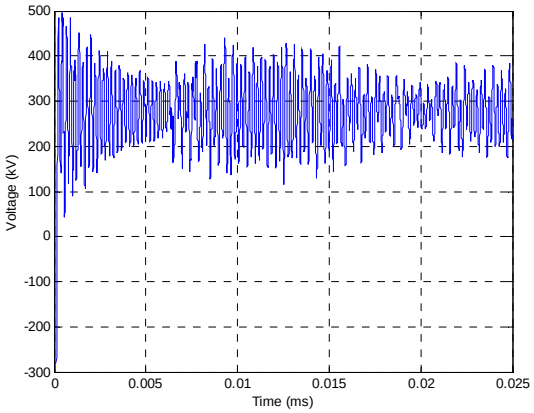

c. The voltage seen at Tr. #1 side of DS 3615

Fig.3.7. The voltages due to DS 3615 restrike when Unit 2 is started by Unit 1

Experiments show that the maximum interturn voltages at the entrance can reach approximately up to 0.25 of the applied VFT. In this case, the maximum interturn voltage is estimated to be

$$145.9 * 0.25 = 36.5 \text{ kV} \qquad (3.5)$$

This value is more than twice the estimated for the test impulse given earlier. It can make the transformer insulation vulnerable to breakdown.

The VFT at the starting bus side of the DS 3625 is 1.79 pu and shown in Fig.3.8c. It can be seen that VFT has been delayed and filtered when reaching the transformer.

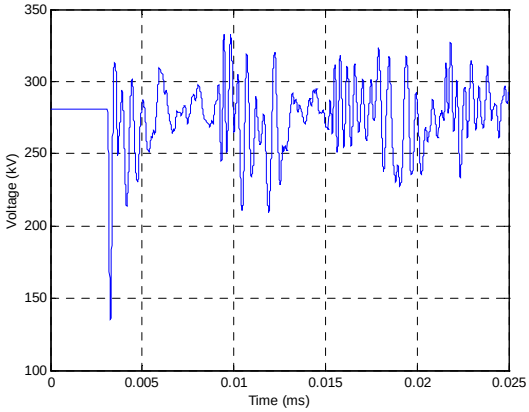

a. The voltage seen at the terminal of Tr. #2

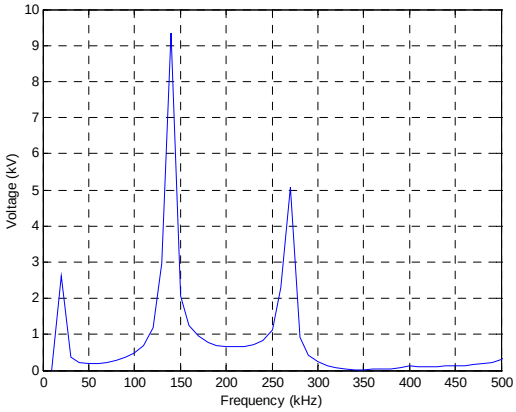

b. The frequency spectrum of Fig.3.8a

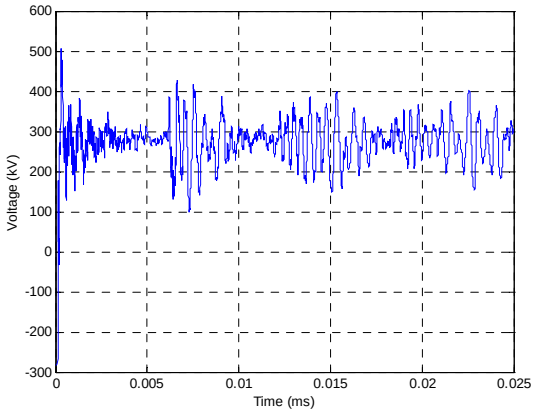

c. The voltage seen at starting bus side of DS 3625

Fig.3.8. The voltages due to DS 3625 restrike when Unit 2 is started by Unit 1

3.4.2. Case 2 – Unit 5 Started by Unit 1

When Unit 5 is started by Unit 1 using the Back-to-Back starting method, the following switching sequence is used:

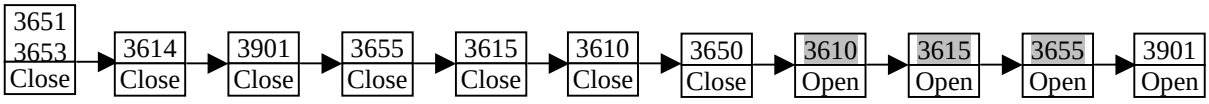

The switching operations shaded may generate high overvoltages, including:

- VFT resulting from CB 3610 restrikes;
- VFT resulting from DS 3615 and 3655 restrikes.

3.4.2.1. CB Restrike Due to CB 3610 Opening

Fig.3.9a and 3.9b shows the voltage waveform seen at the terminal of Tr.#1 and its frequency spectrum. The overvoltage is 2.47 pu, and the maximum rate of rise dv/dt is 1.09 MV/us. The predominant resonant frequency is still 88 kHz and 231 kHz. The voltage seen at the terminal of Tr.#5 is shown in Fig.3.9c, and the overvoltage is 2.40 pu. The overvoltage is a little smaller and smoother than at Tr.#1, but it is still severe for the insulation of Tr.#5. Fig.3.9d shows the voltage at the GIS side of CB 3610, and the overvoltage is 1.64 pu.

3.4.2.2. DS Restrike Due to DS 3615 and DS 3655 Opening

VFT seen at the terminal of Tr.#5 is shown in Fig.3.10, 3.11 and Table 3.2. Results show that VFT resulting from DS 3615 restrikes has little effects on the insulation of Tr. #5. Similar to the restrike of DS 3645, DS 3655 restrikes generate higher VFT with higher voltage change due to longer float starting bus, making Tr. #5 more vulnerable to breakdown.

3.4.3. Discussion

With analysis of the simulation results using back-to-back starting, conclusions are drawn below:

- The characteristics of the VFT seen at the transformer terminals due to DS restrikes are related to the length of the float starting bus bar. The longer the floating bus, the higher maximum overvoltage and maximum voltage change, but the maximum rate of rise is similar, around 1.0 ~ 1.6 MV/us. Though very high frequency components of the VFT are filtered by the oil-filled cable when the VFT reaches the transformer, the highest frequency seen at the transformer terminal can still be up to 5MHz.

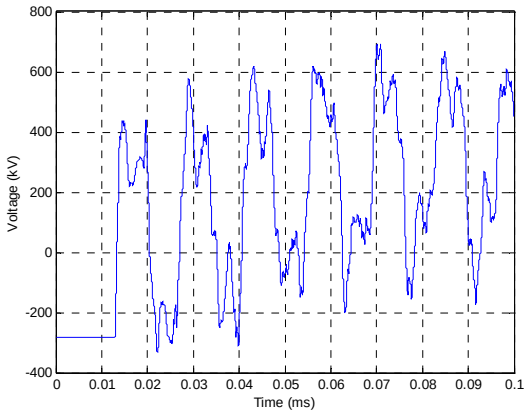

a. The voltage seen at Tr.#1 terminal

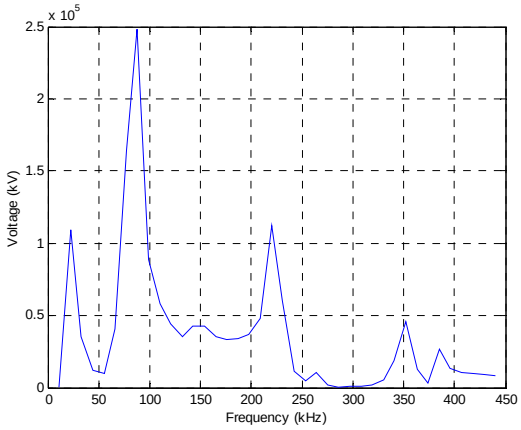

b. The frequency spectrum of Fig.3.9a

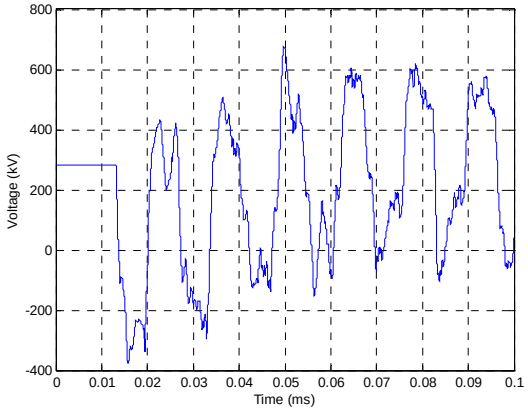

c. The voltage seen at Tr.#5 terminal

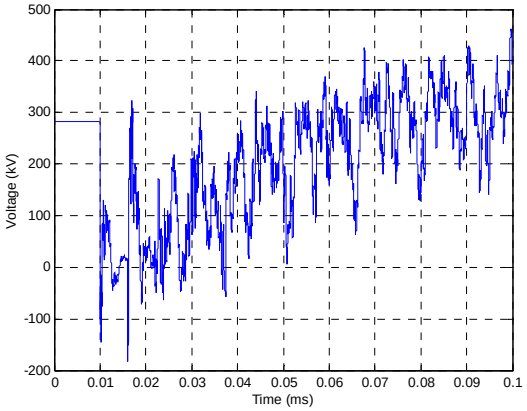

d. The voltage at the GIS side of CB 3610

Fig.3.9. The voltages due to CB 3610 restrike when Unit 5 is started by Unit 1

VFT due to DS 3615 or 3665 restrikes has little effect on the transformers because of its low overvoltage and small voltage change. However, VFT due to DS 3525, 3635, 3645, 3655, and 3901 are expected to be harmful to the associated transformer insulations due to the high voltage change and high rate of rise, which may generate extremely non-linear voltage distribution along the windings or excite partial winding resonance. The following cases will generate higher VFT and require more attentions, Unit 4 and Unit 5 started by Unit 1, and Unit 3 started by Unit 6. VFT due to DS restrikes may contribute to the Tr. #4 failure.

- Though CB restrikes happens just occasionally, they do overstress the transformer insulation due to frequent CB switching. Particularly, the exposure of the driving units, Unit 1 or Unit 6, to CB restrikes is more than twice or three times the other units. This may be a

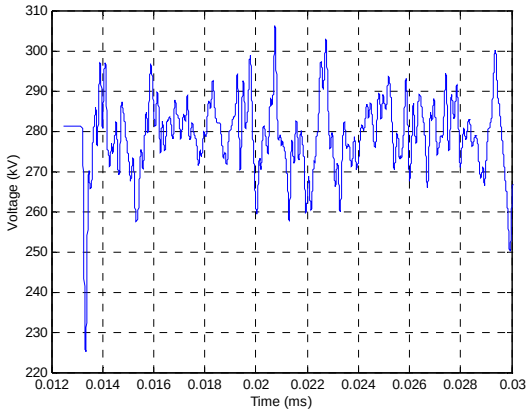

Fig.3.10. VFT seen at the terminal of Tr.#5 due to DS 3615 restrike when Unit 5 is started by Unit 1

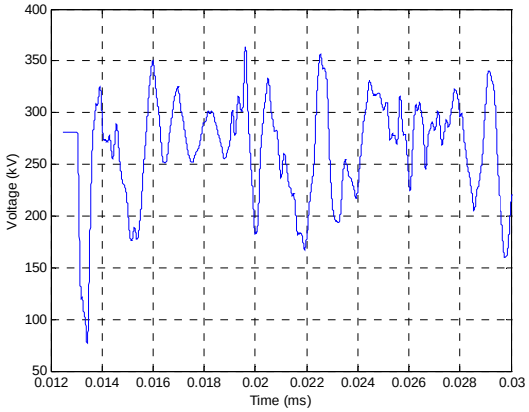

Fig.3.11. VFT seen at the terminal of Tr.#5 due to DS 3655 restrike when Unit 5 is started by Unit 1

Table 3.2. VFT seen at the Tr. #5 terminal due to DS 3615 and 3655 restrikes when Unit 5 is started by Unit 1

	The maximum VFT (pu)	The maximum voltage change (kV)	Resonant frequency (kHz)	Fig.
DS 3615 restrike	1.09	55.9	140.0	Fig.3.10
DS 3655 restrike	1.36	204.1	137.8, 482.6, 609.0	Fig.3.11

major cause of Tr. #1 successive failures. VFT due to CB restrikes generates high overvoltage with low resonant frequency, which may coincide with the characteristic frequencies of the transformer winding. VFT due to CB restrikes is much more severe than due to DS restrikes.

3.5. Simulation of Switching Transients When Units Are Disconnected from the GIS

The switching sequences are given in Appendix B. Switching transients are expected only due to CB restrike when CBs are opened to isolate the units from the GIS. Here CB 3610 restrike is simulated when CB 3610 is opened at the generation mode. For other similar CB switching operations, the analysis procedure is the same.

CB 3610 restrike may occur when Tr.#1 is disconnected from the GIS at the generation mode. The simulation circuit is similar to Chapter 3.4.1.2, while the starting bus is not included here. Only Unit.1 is assumed to be in service while other units are standstill. Switching transient seen at the terminals of Tr.#1 due to CB 3610 restrike is shown in Fig.3.12. The maximum overvoltage is 2.81 pu (790.1 kV), and the maximum rate of rise is about 1.54 MV/μs.

Assuming that all units are in service, switching transients seen at transformer terminals are shown in Fig.3.13 due to CB 3610 restrike. The resulting maximum overvoltages at each transformer terminals are shown in Table 3.3. The resonant frequency is about 80.43 kHz.

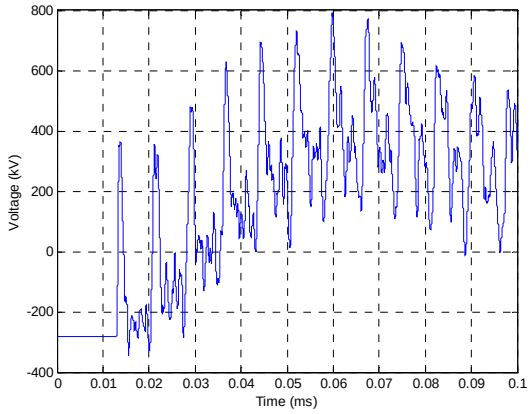

Fig.3.12. Switching transient seen at the Tr.#1 terminal due to CB 3610 restrike when Unit 1 is disconnected from the GIS

Table 3.3. Switching transients at the tranformer terminals due to CB 3610 restrike

	Peak value in pu	Peak value in kV
Tr.#1	2.71	764.4
Tr.#2	2.10	592.0
Tr.#3	1.81	509.6
Tr.#4	1.48	416.2
Tr.#5	1.59	447.8

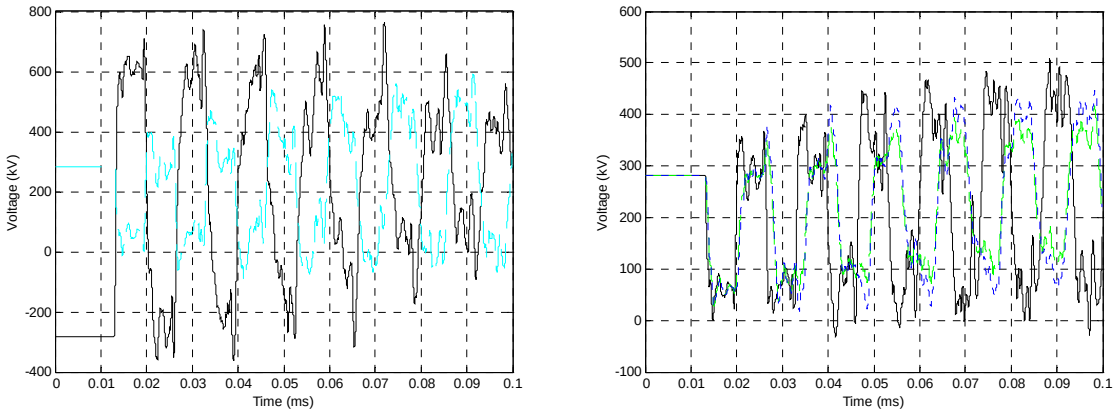

a. Tr.#1 (Solid), Tr.#2 (Dash) b. Tr.#3 (Solid), Tr.#4 (Dash), Tr.#5 (Dot)

Fig.3.13. Switching transients seen at transformer terminals due to CB 3610 restrike if all transformers are in operation

3.6. Frequency Scan of the Transformer HV Winding

In order to study the possibility of resonance in the transformer HV winding, a frequency scan is done using the detailed transformer HV winding model. The HV winding is modeled as two 10x10 inductance matrixes shown in Fig.3.14. The capacitance and inductance values were provided by the manufacturer. The current with the magnitude of 1 Amp is injected into the HV terminal, H_1, and the neutral, H_0 is grounded. The frequency range is 60 Hz ~ 250 kHz.

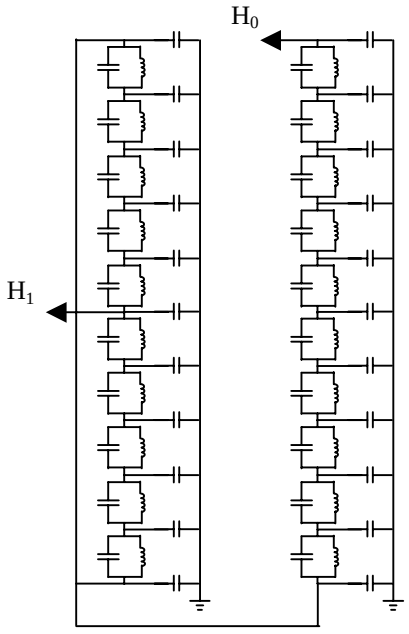

Fig.3.14. Transformer HV winding Model

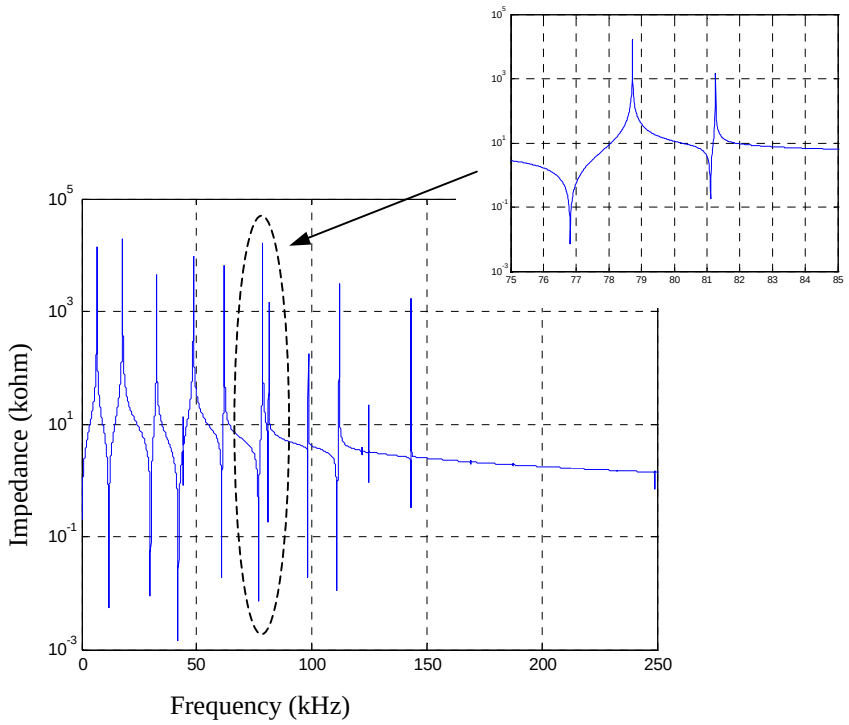

Fig.3.15. The driving point impedance of the transformer HV winding

The input impedance of the HV winding is shown in Fig.3.15. The winding nature frequencies include 76.8 kHz, 78.7 kHz, 81.1 kHz, 81.3 kHz, and 143.5 kHz. Some of them are very close to the cable natural frequency of 84 kHz. Compared to Fig.3.6, 3.9 and Table 3.2, it is possible that partial resonance may be excited in the HV winding in the case of CB or DS restriking.

3.7. Approach to Mitigate the Effects of Switching Transients and VFT on GSU Transformers

Due to its duration and magnitude, VFT produced by DS switching may not cause surge arresters to conduct. However, a surge capacitor paralleled with the arrester may find its place in the protective scheme as a wave modifier that softens the VFT front at transformer terminals and improve the VFT distribution along the transformer windings. It is also helpful for absorbing the sharp spikes of VFT due to CB restriking since surge arresters do not act quickly enough to prevent the switching transients with steep front. Therefore, installing an

additional surge capacitor at the GSU transformer HV terminal might be very useful to mitigate the effects of VFT due to DS and CB restriking [Gree91].

It is well known that surge capacitors have been applied in the protection of motors in LV and MV levels to reduce the risk of inter-turn insulation failure due to lightning or switching transients. However, there are several concerns when applying such surge capacitors in the protection of high voltage transformers as the case the case under study. These concerns are related to the capacitance value, capacity, cost, and possibility of failure of the surge capacitors themselves [Alfu94].

The capacitance is usually about 0.2 to 0.5 μF in motor protection schemes. The capacity of the capacitor banks will be about 9.0 to 22.4 MVar if the same value is applied in the 345 kV network, which is impractical due to installation space and cost. On the other hand, capacitors with small capacitance values could not satisfy requirements of voltage spike reduction.

As shown in Fig.3.16 and 3.17, when an additional 8 nF capacitor is installed at the transformer terminals, the maximum voltage change and the peak value of the VFT are dramatically reduced due to DS restriking. However, the peak value of switching transients due to CB restriking keeps almost the same, only the resonant frequency decreases a little, and this in turn increases the possibility of partial resonance in the HV winding. With the increment of the capacitance, transients due to both DS and CB restriking will be further reduced. Here 8 nF is chosen because such kind of HV capacitors could be easily obtained. For example, the capacitance of some 345 kV CCVTs is also 8 nF.

In the studied case, in order to lower the VFT at the GSU transformer terminals, application of surge capacitors is a feasible alternative due to space limitation and cost, if the suitable capacitance value is selected.

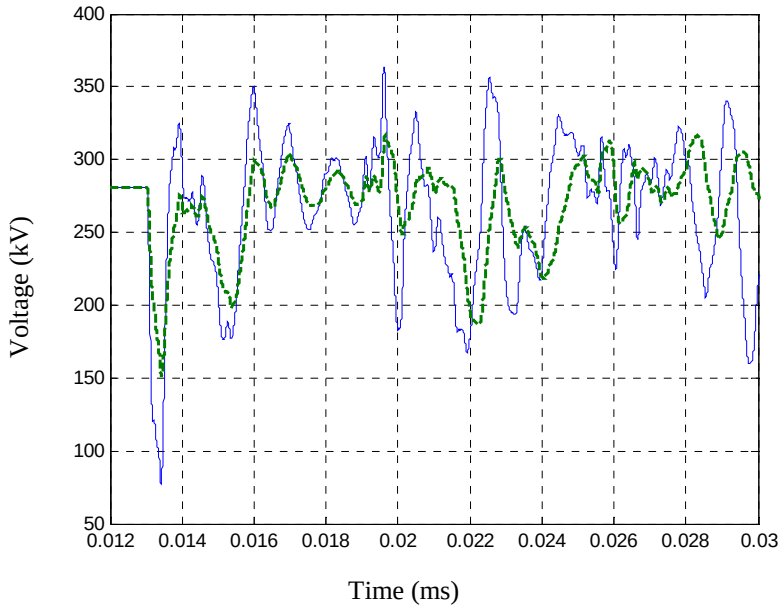

Fig.3.16 VFT seen at the Tr.#5 terminal due to DS 3655 restriking when Unit 5 is started by Unit 1

Solid line – Original VFT waveform in Fig.3.11
Dash line – VFT with an additional 8 nF capacitance attached at the Tr.#5 terminal.

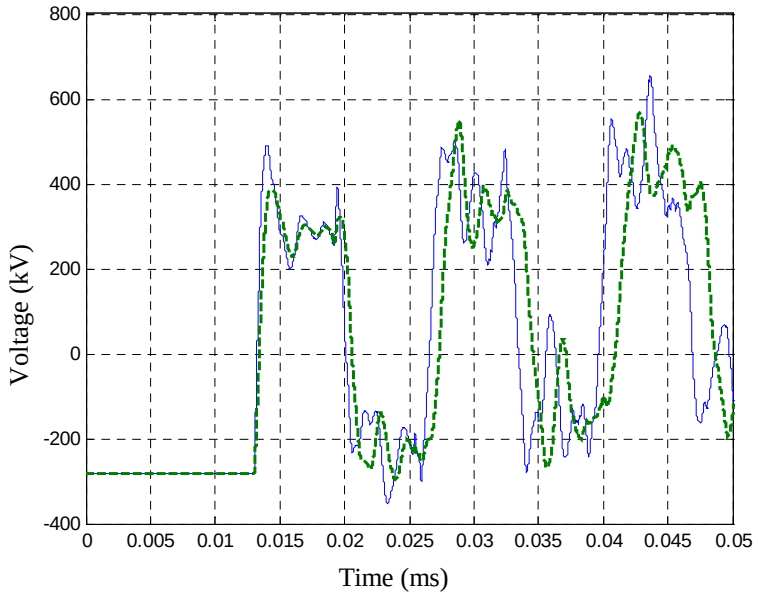

Fig.3.17. The switching overvoltage at the Tr.#1 terminal due to CB 3610 restriking when Unit 2 is started by Unit 1

Solid line - The original voltage waveform in Fig.3.6a.
Dash line – The voltage with an additional 8 nF capacitance attached at the Tr.#1 terminal.

3.8. Summary and Discussion

Various CB and DS switching operations are frequent in the routing or occasional operations in the plant. The main task in this study is to simulate and analyze the transients due to the routine operation of CB and DS. The routine operation sequences include:

- Switching sequence using back-to-back;
- Switching sequence using SFC;
- Switching sequence when disconnecting from the system.

All transient overvoltages obtained will be analyzed to determine the peak voltage, the maximum voltage change, the maximum rate of rise of the overvoltage, and predominant frequencies. The conclusions are drawn below.

1). Current chopping due to SF6 CB opening results in very small overovoltges in the studied cases, and should have little effects on the transformer operation.

2). Frequent VFT is expected to occur when the BTB starting method is used to start units, since disconnecting the floating starting bus is often done by the DS. The characteristics of the VFT seen at the transformer terminals due to DS re-strikes are related to the length of the float starting bus bar.

- The longer the floating bus is, the more charges remain on the bus, and the maximum overvoltage and maximum voltage change are larger, as defined in Fig.3. However the maximum rate of rise is similar, around 1.0 ~ 1.6 MV/us.

- Though very high frequency components of the VFT are filtered by the oil-filled cable when the VFT reaches the transformer, the highest frequency seen at the transformer terminal can still be up to 5MHz.

- The maximum VFT peak value can be up to 1.42 pu. The peak value of VFT usually is not large and may not be the direct cause of transformer main insulation.

- The maximum rate of rise of VFT is expected to be harmful to the associated transformer insulations, since they may generate extremely non-linear voltage distribution along the transformer windings, or excite partial-winding resonance due to high frequency components. The maximum voltage change can be up to 204 kV, which may overstress the insulation between turns.

- VFTs usually are not related to the transformer insulation direct breakdown, they may deteriorate the insulation gradually and result in transformer failure eventually.

- VFT due to DS 3615 or 3665 re-strikes usually has little effect on the transformers because disconnecting only a very short floating bus is involved. However, VFT due to DS 3525, 3635, 3645, 3655, and 3901 are expected to be harmful to the associated transformer insulations since the floating buses disconnected can be about 60 meters long. The following cases will generate higher VFT and requires more attention, Unit 4 and Unit 5 started by U1, and Unit 3 started by Unit 6. The VFT generated due to DS restrikes may contribute to the Tr.#4 failure.

3). Though CB restrikes occur only occasionally, they do overstress the transformer insulation due to frequent CB switching in this plant. Switching transients due to CB restrikes is much more severe than from DS restrikes. Particularly, the exposure of the driving units, Unit 1 or Unit 6, to CB restrikes is more than twice or three times the other units. This could be a major cause of Tr.#1 successive failures. Transients due to CB restrikes affect the transformer insulation in two ways:

- It could generate high overvoltage with the peak value of up to 2.7 pu which may directly result in the transformer insulation breakdown.

- It could excit resonance in the cable/transformer circuit or partial winding resonance in the transformer winding. The cable natural frequency of about 84 kHz is the dominant frequency of the overvoltage seen at the transformer terminal due to CB restrike. In Chapter 3.6, the frequency scan of the detailed transformer HV winding shows that several natural frequencies of the winding are near 80 kHz. It is very close to cable natural frequency.

4). When units are disconnected from GIS, CB restrike may produce overvoltages at the transformer terminals. The results are similar to 3).

5). Application of surge capacitors at GSU transformer terminals is a feasible alternative to mitigate the effects of the VFT on GSU transformers.

CHAPTER 4
STUDY OF LIGHTNING OVERVOLTAGE EFFECTS ON GSU TRANSFORMERS

This chapter presented the effects of lightning overvoltages on GSU transformers. Simulation showed that the current surge arrester configuration provides inadequate lightning protection to the GSU transformers, and the approach to lower the lightning transients at the transformer terminals is suggested.

4.1. Introduction

4.1.1. Characterization of Lightning Overvoltages Seen by GSU Transformers

In the pumped storage plant described in Chapter 3, it is suspected that lightning resulted in the first failure of Tr.#1 since it was thunderstorm weather when the failure happened. Therefore, in order to study if the current surge arrester configurations provide enough protection to GSU transformers, lightning overvoltage seen at the transformer terminal is simulated when lightning directly strikes the transmission line. As shown in Fig.3.1, surge arresters are installed only on the supply and load sides of the GIS in the plant. The transformer is connected to the GIS through a cable of 630 m, and no arresters are installed in the vicinity of the transformer. The effect of arrester location on lightning overvoltages at the transformer terminals is also analyzed.

4.1.2. Field Lightning Statistics

Some field statistical data between 1990 and 1996 are given as follows.

1). Isokeraunic level (IKL) (the number of thunderstorm days per year) is 55, which is specifically extracted from this plant area of about 20x20 km^2. The ground flash density, N_g, is about 5.99 flashes/km^2/year according to Eq.2.3. Furthermore, the average number of

flashes collected by a transmission line, N_s, is calculated approximately from Eq.4.1 [Elah90]:

$$N_s = N_g (28h^{0.6} + b)/10 \quad (4.1)$$

where h is the tower height (m), b is the overhead ground wire separation distance (m), and N_g is flashes/100 km/year. If the tower height is 28.1 m and the overhead ground wire separation distance is 11.0 m, the average number of flashes on a 345 kV transmission line in the plant area is approximately 1.3 flashes/km/year given in Eq.4.1.

2). Cumulative probability of lightning peak currents in the plant area is shown in Table 4.1. Fig.4.1 shows that cumulative probability of lightning peak currents is fitted quite well with Eq.2.1.

Table 4.1. Cumulative probability of lightning peak currents in the plant area

Lightning peak current (kA)	Cumulative probability (%)
10	98
15	90
20	80
25	70
30	60
35	50
40	40
45	33
50	28
60	20
70	12
80	10
90	7
100	5
150	2
160	1

4.2. Simulation Strategy

Simulation is done based on the field configuration when the first Tr.#1 failure happened. GIS Bus 1, 3, and 4 were in service, and Bus 2 was standstill, shown in Fig.3.1. Only the

transmission line to Chung-Liao 3 was in service. The plant power was supplied by SSTR 2, which was connected to Bus 4. Only Unit 1 was at generation mode with an output of 150 MW. The lightning current is modeled by a waveform of 1.2/50 us, 30 kA, and negative polarity, paralleled with a 400 ohm lightning channel surge impedance. The lightning current magnitude is chosen according to the field statistics. The software, ATP-EMTP was used for lightning simulation. The type 15 double-exponential surge function described in Eq.4.2 was used to model the lightning current,

$$I = Amp \bullet (\exp(A \bullet t) - \exp(B \bullet t)) \tag{4.2}$$

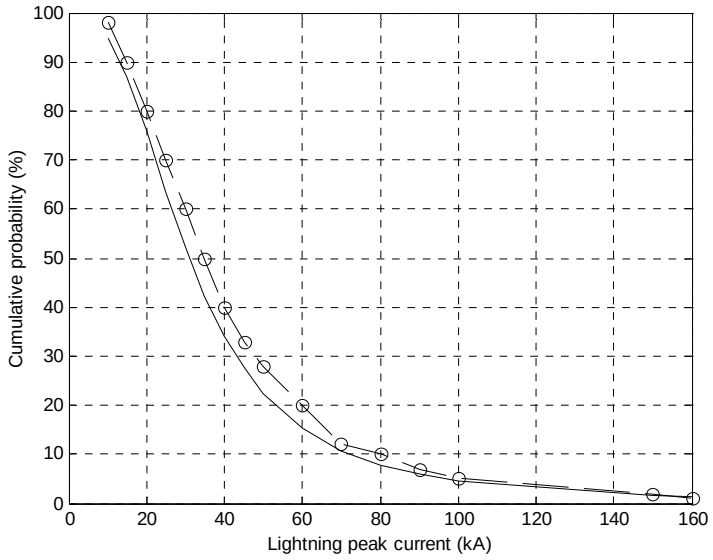

Fig.4.1. Cumulative probability distribution of lightning peak currents in the plant area
Dash line – Statistical data in the plant area.
Solid line – Results obtained from Anderson equation in Eq.2.1.

where Amp = 30.0 kA, A = -2.7E6 s^{-1}, B = -1.38E4 s^{-1}. The lightning current is injected directly at the transmission line 200 m far away from the GIS. The lightning injection part of the simulation circuit is shown in Fig.4.2. The time step is 2.5 ns and the maximum calculating time is 0.125 ms.

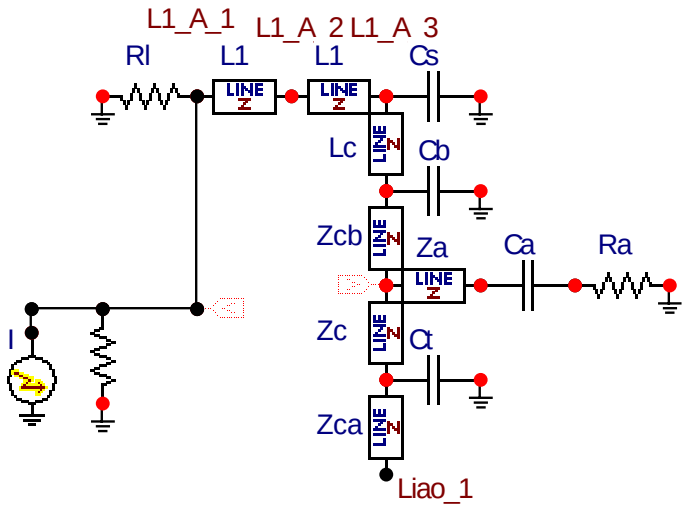

Fig.4.2. Lightning current injection simulation

The component modeling is the same as in the switching case, referred in Table 3.1, except for surge arresters. In the lightning study, the arrester is modeled as a non-linear resistance taking into account different sparkover voltages and V-I characteristics according to the behavior of the time to crest of the incoming waves [Work92a]. The rated voltage of the arrester is 312 kV, and its MCOV (maximum continuous operating voltage rating) is 209 kV.

The lightning overvoltage is analyzed in three cases: 1). No any arresters are installed in the plant; 2). The arresters are located as the original configuration shown in Fig.3.1; 3). Extra arresters are installed at the transformer terminals based on Fig.3.1.

Here the voltages seen at the following points are of concern: 1). V1 - the voltage at the Tr.#1 terminal; 2). V2 - the voltage at the GIS arrester terminal connected to Tr.#1; 3). V3 - the voltage at the injection point of the lightning current.

4.3. Case 1 - All Arresters Are Disabled

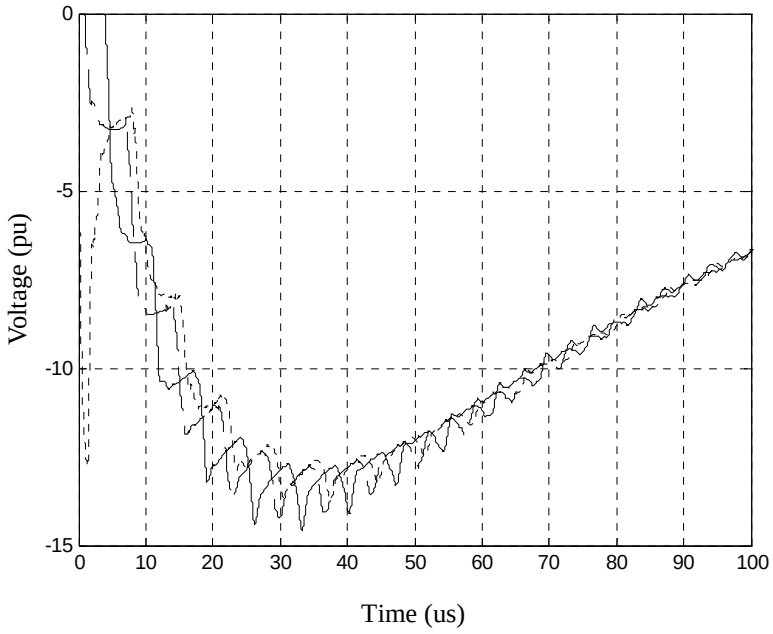

Fig.4.3. Lightning overvoltges at the Tr.#1 terminal and other nodes in Case 1
(V1- Solid; V2- Dash; V3- Dot)

As shown in Fig.4.3, without arresters, the overvoltage observed at the Tr.#1 terminal can reach up to 14.56 pu, much larger than the transformer BIL of 3.73 pu (1050 kV). Due to wave propagation in the cable, there is a 3.3 μs time delay between V1 and V2. The notch in the voltage V3 resulted from the wave negative reflection at the interface between the GIS bus and the overhead transmission line, and between the GIS bus and the cable.

4.4. Case 2 - The Original Arrester Configuration

The overvoltages are shown in Fig.4.4, though the voltage at the arrester terminal is reduced dramatically due to arrester trigger, the voltage at the Tr.#1 terminal is still very high because of wave reflection, and can be up to 4.21 pu, almost double magnitude at the arrester terminal. It is worth noting, that even with the arrester installed, the lightning overvoltage seen at the Tr.#1 terminal is still higher than the transformer BIL in the studied case. Moreover, a frequency of 84 kHz dominates this overvoltage, which is exactly the natural frequency of the cable of 630 m length. The lightning can then excite resonance in the cable/transformer circuit or partial winding resonance in the transformer winding. It can be

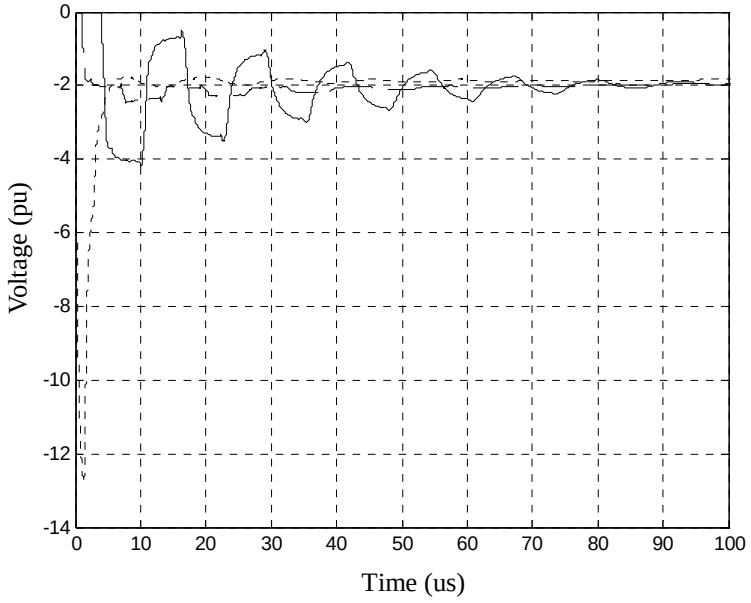

Fig.4.4. Lightning overvoltges at the Tr.#1 terminal and other nodes in Case 2
(V1- Solid; V2- Dash; V3- Dot)

concluded that current arrester configuration provides less lightning protection to the GSU transformer.

4.5. Case 3 - An Extra Arrester Is Installed at the Tr.#1 Terminal

If an extra arrester is installed at the Tr.#1 terminal, the overvoltage at the Tr.#1 terminal is dramatically decreased below the transformer BIL, just 2.29 pu, as shown in Fig.4.5. Compared to Case 2, installing surge arresters at the transformer terminals is necessary for suppressing harmful lightning overvoltages.

4.6. Analysis of Lightning Overvoltage Simulation

Simulation shows that the GIS side arresters do not provide enough protection to the transformers, making transformer insulation vulnerable to lightning surges. This can be a possible cause of Tr.#1 HV winding insulation failure.

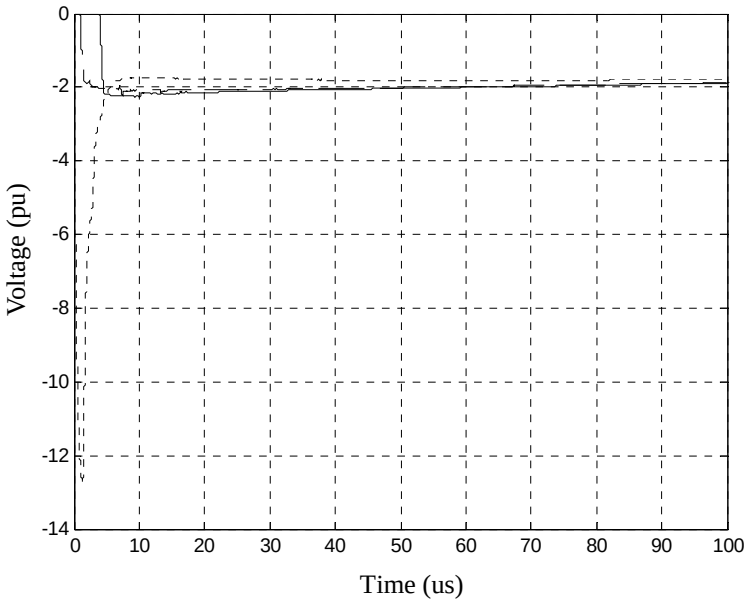

Fig.4.5. Lightning overvoltges at the Tr.#1 terminal and other nodes in Case 3
(V1- Solid; V2- Dash; V3- Dot)

Several factors may contribute to a transformer failure due to lightning strokes [Bick86], including: 1) very high magnitude of the overvoltage; 2) nonlinear voltage distribution along the winding, which could result in high voltage between turns; 3) resonance or partial-winding resonance in the HV winding if they coincide with the excitation frequencies.

The study shows that arresters installed at the transformer terminals can help reducing the overvoltage seen at the same transformer terminals to a level below the BIL. However, due to space limitation in the field, it is difficult to install new arresters near the GSU transformers.

4.7. Approach to Lower the Lightning Overvoltages at Transformer Terminals

In order to lower the lightning overvoltages at the GSU transformer terminals, an approach without installation of new arresters is suggested here. Simulation shows that, if more transformers are connected to the GIS, much smaller overvoltages will appear at each transformer terminals for a given magnitude of the injected lightning current. Two reasons contribute to the overvoltage reduction. When more cables are connected to the GIS in

parallel, the equivalent cable surge impedance becomes smaller, the peak value of the overvoltage appearing at the transformer terminals is reduced dramatically due to negative reflection. Another factor is, with more transformers connected to the GIS, more arresters are also connected to the network, and it is helpful for absorbing more lightning energy by the arresters, hence reducing the maximum overvoltages at each transformer terminal.

Fig.4.6 shows the overvoltage at the Tr.#1 terminal when other transformers are connected to the Bus 1 or Bus 3 one by one, when the lightning current directly strikes the transmission line with the same circuit configuration as in Case 2. The peak value is also illustrated in Table 4.2. It shows that if more than two units are put into operation, the lightning overvoltage at transformer terminals can be reduced to a level below the BIL in the

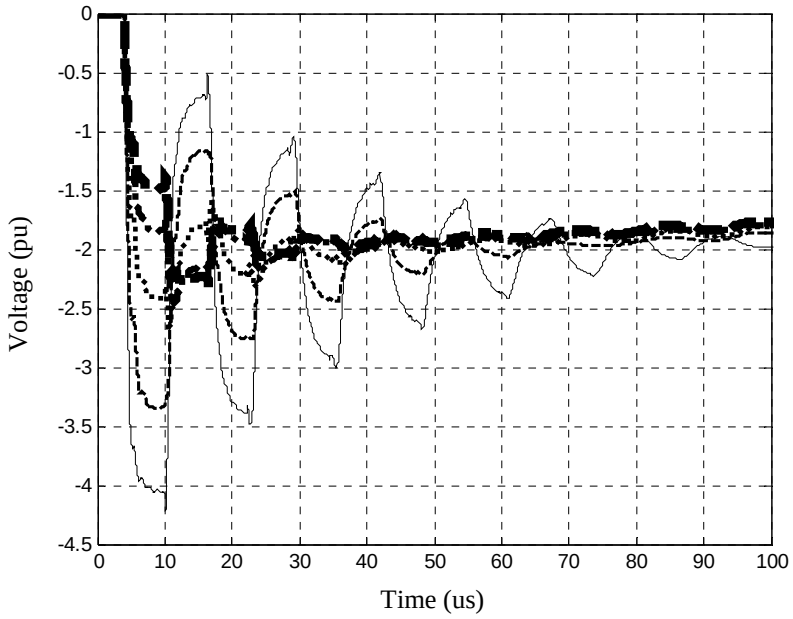

Fig.4.6. Lightning overvoltages at the Tr.#1 terminal when other transformers are connected to the GIS buses one by one.

Solid - Only Tr.#1 is in operation.
Dash - Tr.#2 is then connected to Bus 1.
Dot – Tr.#3 is then connected to Bus 1.
Dash-Dot - Tr.#4 is then connected to Bus 3.
Dash with the line width of 4 - Tr.#5 is then connected to Bus 3.

studied case. The study indicates that lowering the equivalent surge impedance on the cable side (more in parallel) is more effective in reducing the over-voltage peak than adding more arresters on transformer side for other transformers.

Table 4.2. The overvoltage peak value at the Tr. #1 terminal

	Voltage peak value (kV)	pu
Only Transformer 1	1187.0	4.21
Transformer 1 and 2	943.7	3.35
Transformer 1, 2 and 3	757.4	2.69
Transformer 1, 2, 3 and 4	700.4	2.49
Transformer 1, 2, 3, 4 and 5	641.7	2.28

This suggests the idea that when the stormy weather is coming, in order to reduce lightning overvoltage at transformer terminals, an effective alternative is to run more units which in fact will connect more transformers to the GIS. It should be noted that lowering the equivalent surge impedance of the cable is more effective to reduce the overvotlage peak than adding more arresters.

4.8. Summary and Discussion

In order to find out the possible causes contributing to GSU transformer failures in a large pumped storage plant, and most importantly, avoid such failures in the future, the extensive review and simulations were done in Chapter 2, 3 and 4. Based on the analysis, the conclusion are given below:

1). Some CB and DS switching may produce harmful overvoltages on the associated transformer insulations. The detailed discussion is given in Chapter 3.

2). Commutation voltage spikes and harmonics always exist when starting the unit using static frequency converter (SFC). Thanks to Sebastian Rosado’s work [Rosa01], simulation shows that SFC operation has little effects on the GSU transformer operation, either harmonics or commutation spikes.

3). Simulation of the direct lightning stroke in this chapter shows that the current arrester configuration does not provide enough protection to the GSU transformers, making transformer insulation vulnerable to lightning surges. Arresters installed at the transformer terminals can help reducing overvoltages seen at the same transformer terminals. The study also indicates that when the stormy weather is coming, in order to reduce lightning overvoltages at transformer terminals, an effective alternative is to run more units. This results in a lower equivalent surge impedance of the cable.

CHAPTER 5
STUDY OF HARMONICS AND REACTIVE POWER CONSUMPTION FROM GIC SATURATED TRANSFORMERS

Compared to effects of electrical transients on power transformer insulation, geomagnetically induced currents (GIC) may affect transformer operation in a different way. GIC are can cause severe transformer half-cycle saturation. This chapter introduces a simplified method based on the equivalent magnetizing curve of the transformer to estimate harmonic currents and Mvar due to transformer half-cycle saturation. The simulation methods are validated with observational and field test data for transformers experiencing half-cycle saturation.

5.1. Introduction

The earth-surface-potential induced by geomagnetic storms causes geomagnetically-induced-currents (GIC) to flow in the large-scale electric power systems. GIC enter and exit the power system through the grounded neutrals of wye-connected transformers that are located at opposite ends of a long transmission line. Geomagnetically induced current (GIC) is a quasi-direct current, and can result in a high level of half-cycle saturation when present in a transformer. A transformer with the half-cycle saturation becomes a rich source of even and odd harmonics and draws significant inductive MVar from the power system, and may further cause reactive power overloading, overheating, false relay tripping, etc [Arbe89]. In March 1989, the entire Quebec area experienced a blackout lasting more than nine hours, and a large transformer at a nuclear plant in the US was damaged due to the GIC. As the severity of solar storms peaks about every 11 years, the Northern hemisphere are expected to face particularly serious vulnerability problems during the solar cycle beginning from last year, real time GIC forecast and evaluation is very important to avoid the power system blackouts during the solar storm.

As a key part of real time GIC forecast and evaluation, it is important to accurately model the behavior of multiple individual transformers experiencing differing levels of GIC in a

large scale model. This chapter studied and validated the simplified transformer models to modeling the AC reaction of the transformer due to saturation on the network.

Staged tests have been performed to study the harmonics and reactive power consumption during transformer saturation [Lesh93 and Kapp89]. Several simulation methods have also been developed to calculate harmonic currents and MVar intake of transformers resulting from GIC. These include the FEM based models [Lush91], and the magnetic circuit models [Wall91]. These methods are usually accurate but complicated and require detailed design information that is generally not available.

To estimate harmonic currents and MVar with only the given GIC and the nameplate information of the transformer, it is necessary to look for simplified methods that will provide sufficient accuracy for large-scale network models of storm impacts. Results of the model are presented in this chapter is to validate a simplified approach for transformers with different core design. Harmonics and the MVar consumption of transformers with different core design are analytically compared, and a simple formula is obtained to evaluate the MVar consumption directly with the given GIC, which is helpful for on-line GIC monitoring. The effect of the transformer parameters on the GIC induced saturation is also discussed, such as the voltage, MVA, and the normal exciting current.

5.2. Description of the Simplified Approach

5.2.1. Assumptions

The following assumptions are given to simplify the problem.

1). The nameplate information of the transformer is known, including the rated voltage and MVA, auto or normal, phase numbers, core configuration, and the typical excitation current percentage.

2). The input GIC is known and divides equally between three phases, either in single-phase transformer banks or three-phase transformers. In the case of autotransformers, it is especially important that the GIC flowing in all terminals (including ground or neutral) be known so that an effective GIC in the transformer can be derived.

3). The AC and DC flux only flows in the core and the leakage flux is ignored, except for the transformer with three-phase, 3-legged, core form. Iron loss and copper loss are also ignored, and then the formula below can be obtained.

Assume that the normal phase voltage $u(t)$ and induced electro-motive force (EMF) $e(t)$ of the exciting winding are fundamental-frequency positive-sequence and known, the AC linkage $\psi_{ac}(t)$ resulting in $e(t)$ is

$$\psi_{ac}(t) = -\int e(t)dt = -\int (-u(t))dt = \omega^{-1} \cdot \sqrt{2} U_1 \sin(\omega t) \tag{5.1}$$

where U_1 is the RMS value of $u(t)$. If the DC linkage ψ_{dc} induced by GIC exists, then the total linkage $\psi(t)$ in the transformer core can be represented by the exciting current $i(t)$.

$$\psi(t) = \psi_{ac}(t) + \psi_{dc} = F(i(t)) = F(i_{ac}(t) + I_{dc}) \tag{5.2}$$

where $i_{ac}(t)$ is the AC component of $i(t)$, I_{dc} is the value of GIC per phase, the function F is the equivalent ψ-i magnetizing curve of the transformer.

Provided that $\psi_{ac}(t)$, I_{dc}, and the function F are known, ψ_{dc} and $i_{ac}(t)$ could be calculated from Eq.5.2 by using an iteration algorithm called binary search method [Xuw93]. FFT is used to find harmonic currents from $i_{ac}(t)$, and the MVar Q is given below:

$$Q = 3 * U_1 * I_1 \tag{5.3}$$

where I_1 is the fundamental component of $i(t)$.

5.2.2. Iteration Algorithms

For a single phase transformer, the magnetizing curve $\psi(I)$ can be easily obtained from an iteration procedure called binary search method described below for solving Eq.5.2. This method is based on the fact that DC component in the exciting current $i(t)$ is equal to the applied GIC, I_{dc} [Xuw93].

1). Set the search range from $\psi_{dc} = 0$ to $\psi_{dc} = F(I_{dc})$ and initial guess for ψ_{dc} is equal to $F(I_{dc})/2$. AC flux $\psi_{ac}(t)$ is computed point by point in time domain. Here ten cycles of the 60 Hz waveform are needed to get the enough FFT accuracy, from $t = 0$ to $t = 10 \cdot 2\pi/\omega$. The sampling points can be equal to 2^k that is convenient to FFT, k is the order (k = 1, 2, 3 ...). Here k = 12.

2). The exciting current waveform $i(t)$ can be obtained point by point from Eq.5.2. The DC component of $i(t)$ (that is, I_{dc}') is calculated with Discrete Fourier Transformation which effectively gives:

$$I_{dc}^{'} = \frac{1}{n}\sum_{p=1}^{n} i(t_p) \tag{5.4}$$

where n is sampling points and $i(t_p)$ is the current value at the p-th point.

3). If $I_{dc}' > I_{dc}$, then ψ_{dc} is set at the mid-value in the range (0, $F(I_{dc})/2$) again; If $I_{dc}' < I_{dc}$, then ψ_{dc} is set at the mid-value in the range ($F(I_{dc})/2$, $F(I_{dc})$) again; If the search range is sufficiently small, a ψ_{dc} with an acceptable accuracy is obtained and the search process can be stopped. Otherwise the process is redirected to Step 2).

Once ψ_{dc} is obtained, $i_{ac}(t)$ can be calculated point by point in time domain from Eq.5.2, then harmonic currents are found.

5.2.3. Treatment of Auto Transformers

Auto transformers can be modeled as two-winding transformers as long as an effective GIC or DC current I_{dc}' is used for the unequal flow of GIC in the series and common windings [Bote89].

$$I_{dc}' = (kI_{dc1}+I_{dc})/(k+1) \quad (5.5)$$

Where I_{dc1} and I_{dc} are the GIC flowing in the series winding and the common winding, respectively. $k = V_H/V_L$-1. V_H and V_L are the terminal voltages on the HV and the LV side of the auto transformer. In the analysis below, only two-winding transformers are discussed assuming that auto transformers have already been represented by two-winding transformers.

5.2.4. Simplified Algorithm for Single-phase Transformers

The process of estimating harmonic currents for the single-phase transformer is straight-forward since it involves only one common main flux path that can be represented by a non-linear inductance. The magnetizing curve ψ-I can be given directly from the no-load voltage-current V-I curve of the exciting winding according to Eq.5.1, either core form or shell form. The typical magnetizing curve can be replaced by a proxy using a piecewise linear representation as shown in Fig.5.1a, k_1 and k_2 are the slopes of the lines. As a rule of thumb,

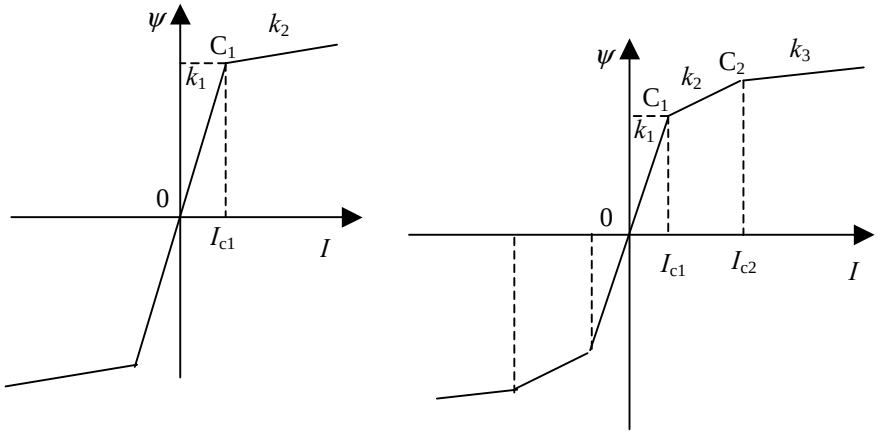

(a) Single phase (b) Three-phase, shell form

Fig.5.1. The equivalent magnetizing curve of the transformer

I_{c1} is equal to 1.1* $\sqrt{2}\, I_{exc}$ at the knee of the magnetizing curve. I_{exc} is the RMS value of the normal exciting current.

5.2.5. Treatment of Three-phase Transformers

Since the AC and DC flux path are different for three-phase transformers, the different equivalent magnetizing curve should be given for different core designs. Here the DC flux per phase is assumed to be equal for the sake of simplification. Since very few three-phase transformers with 7-legged, shell form are in use, the analysis about this kind of transformers is not considered below.

1). Three-phase, shell form. The equivalent ψ-I curve is represented by five straight lines, other than three lines, in order to roughly describe the complicated AC and DC flux coupling in the core. As shown in Fig.5.1b, the slope k_1 and the first knee C_1 are determined according to the rated voltage and the normal exciting current similar to the case of the single-phase transformer. The slope k_2, k_3, and the second knee C_2 are determined by field results. Since the path of DC flux induced by GIC is different from the AC flux path, a scaled GIC which would have the same effect as the original GIC in the core is considered in Eq.5.2.

2). Three-phase, 3-legged, core form. Similar to the case of three-phase, shell form, the different values of the slope k_2, k_3, the second knee C_2, and the scaling factor of GIC are determined by test results.

3). Three-phase, 5-legged, core form. Supposed that the positive-sequence AC flux only exists in the main legs and the magnetic path per phase can be roughly shown in Fig.5.2a. The DC flux flows between the side leg and the main leg as shown in Fig.5.2b. Here S is the cross-section area of the main leg, and that of the side leg is half of the main leg. L is the leg height. The equivalent AC and DC magnetizing curves are shown in Fig.5.1a. The AC curve can be found according to the no-load V-I curve of the transformer, and the DC curve is obtained below.

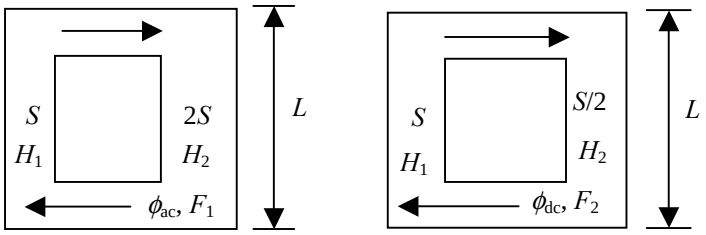

(a) AC magnetic path (b) DC magnetic path

Fig.5.2. The simplified magnetic path of the three-phase, 5-legged, core form transformer

Provided that F_1 is the AC magnetic-motive force (MMF) in Fig.5.2a, the first slope k_{ac} of the AC magnetizing curve is given below.

$$F_1 = NI_{ac} = H_1L + H_2L$$
$$= \mu l * \psi/S + \mu l * \psi/(2S) = \mu l/S*(1.5\psi) \quad (5.6)$$

$$k_{ac} = \psi/(NI_{ac}) = (2/3)*S/(\mu l) \quad (5.7)$$

Where I_{ac} is the AC exciting current, H_1 and H_2 are the magnetic strength of the legs, ψ is the AC linkage, N is the turn number of the exciting winding. The effect of yokes is ignored. F_2 is the DC MMF in Fig.5.2b, and I_{dc} is the DC current per phase, then the first slope of the DC magnetizing curve k_{dc} is shown below.

$$F_2 = NI_{dc} = \mu l * \psi/S + \mu l * \psi/(0.5*S) = \mu l/S*(3\psi) \quad (5.8)$$

$$k_{dc} = \psi/(NI_{dc}) = (1/3)*S/(\mu l) = k_{ac}/2 \quad (5.9)$$

Refer to Fig.5.1a, the linkage ψ at the knee of the DC magnetizing curve in Fig.5.2b is the same as the the case in Fig.5.2a. The second slopes of the magnetizing curves in Fig.5.2a and 2b are determined according to test results.

The DC flux ϕ_{dc} is first found by using Eq.5.2 and the magnetizing curve in Fig.5.1a. The DC current in Eq.5.2 should be one and a half of GIC per phase because the half of DC flux in Phase B contributes to the magnetic circuit in Fig.5.2b. Assume that $\psi_{ac}(t)$ in Eq.5.2 is still the normal operating AC flux. The exciting current $i(t)$ is given by applying the magnetizing curve in Fig.5.2a with the obtained ϕ_{dc} and normal $\psi_{ac}(t)$.

The normal exciting current I_{exc} can be estimated from the rated load current of the transformer, usually fall into 0.2% - 0.5% for large power transformers.

5.3. Verification of Simulation Results

The simulation results were compared with test results to verify the feasibility of the simplified method. Because of the presence of load, the exciting current of the transformer becomes superimposed upon the load current, and the fundamental component of the exciting current is difficult to measure accurately [Kapp89]. As shown in Table 5.1, only the second harmonic current is compared with the test results for different core designs, except for the single-phase core and shell form [Kapp89 and Elect85]. The deviation between the simulated and test results is also given for different GIC values. The maximal deviation is within 30% and most of them are within 10%. The deviation for single-phase shell form and three-phase 5-legged core form is smaller than for three-phase shell form and three-phase 3-legged core form.

Fig.5.3 shows the simulated exciting current waveform and the frequency spectrum with a GIC of 11.5 A per phase for the single-phase core form transformer. The measured transformer is 400 MVA, 512/242 kV. The exciting current is 0.32 A [Bote89]. The simulated result agreed also well with the test result. It shows that the simplified method is feasible with adequate accuracy for all core designs.

5.4. Case Analysis and Comparison

Table 5.1. The comparison of the second harmonic current of transformers with different core design between the simulated and measured results

GIC (A)	*	25	50	75	100	150	225	300
Measured results (RMS, A)	(a)	10.6	19.8	27.9				
	(b)	2.69	4.24	7.21	7.78			
	(c)	1.41	2.97	6.22	9.05			
	(d)			18.2		35.5	49.5	56.1
Simulated results (RMS, A)	(a)	11.1	21.5	32.1				
	(b)	2.5	4.4	7.0	9.2			
	(c)	1.6	3.8	6.1	8.3			
	(d)			17.8		33.0	46.0	58.0
Deviation (*100%)	(a)	4.7	8.6	15.1				
	(b)	7.1	3.8	0.1	18.3			
	(c)	13.5	28.0	1.9	8.3			
	(d)			2.2		7.0	7.1	3.4

* The value of GIC is in neutral.

(a) The measured transformer is 360 MVA, 500/230 kV, single-phase, shell form [Kapp89]. The exciting current is 0.001 p.u.

(b) The measured transformer is 200 MVA, 230/115 kV, three-phase, shell form [Kapp89]. The exciting current is 0.0026 p.u.

(c) The measured transformer is 200 MVA, 230/115 kV, three-phase, 3-legged, core form [Kapp89]. The exciting current is 0.0026 p.u.

(d) The measured transformer is 750 MVA, 525/303 kV, three-phase, 5-legged, core form [Elect85]. The exciting current is 0.0004 p.u.

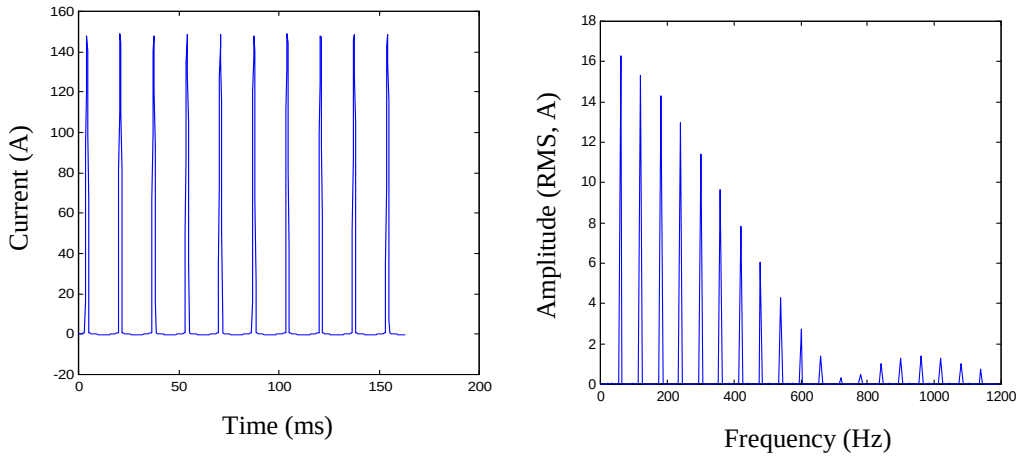

(a) The exciting current waveform (b) The exciting current harmonics

Fig.5.3. The simulated exciting current for a GIC of 11.5 A per phase (single-phase, core form transformer)

A series of simulations were performed to compare the GIC effect on transformers with different core design based on the simplified method. For easy comparison in the following case analysis, the transformer parameters are set constant for different core designs.

MVA: 300 MVA

Voltage: 500/230 kV

Frequency: 60 Hz

The exciting current: 0.42 A

Our study shows that the effect of GIC is similar for the single-phase shell form and single-phase core form if the above parameters are used, so the core designs compared include: single-phase, three-phase shell form, three-phase 3-legged core form, three-phase 5-legged core form. The GIC range of interest per phase is from 0 to 40 A with the increment of 1 A. Various outputs for each core design and different GIC are obtained and compared, such as the exciting current harmonics, MVar consumption.

5.4.1. The Exciting Current Harmonics

The variation of the exciting current peak and harmonics with the increasing GIC are shown in Fig.5.4 and Fig.5.5. The exciting current peak increases nonlinearly with GIC for all core designs, and the increasing rate is also different. For a fixed GIC, the exciting current peak for single-phase is always the highest, and a decreasing order for other core designs is three-phase 5-legged core form, three-phase 3-legged core form, three-phase shell form.

The harmonics variation in Fig.5.5 has the same trend as the case of the exciting current peak. It should be noted that the fundamental and second harmonic currents are linear with GIC in the calculated range for all types of core design. The harmonics become nonlinear with the increase of GIC if the harmonics order is higher. This can be explained below.

As shown in Fig.5.3a, if GIC is five times more than the peak of the normal exciting current, the normal exciting current can be ignored and the exciting current waveform can be approximately represented by a periodical triangle wave as shown in Fig.5.6. Here A is the exciting current peak, $f = 1/T$ is the fundamental frequency, k_1 and k_2 are the slopes. The

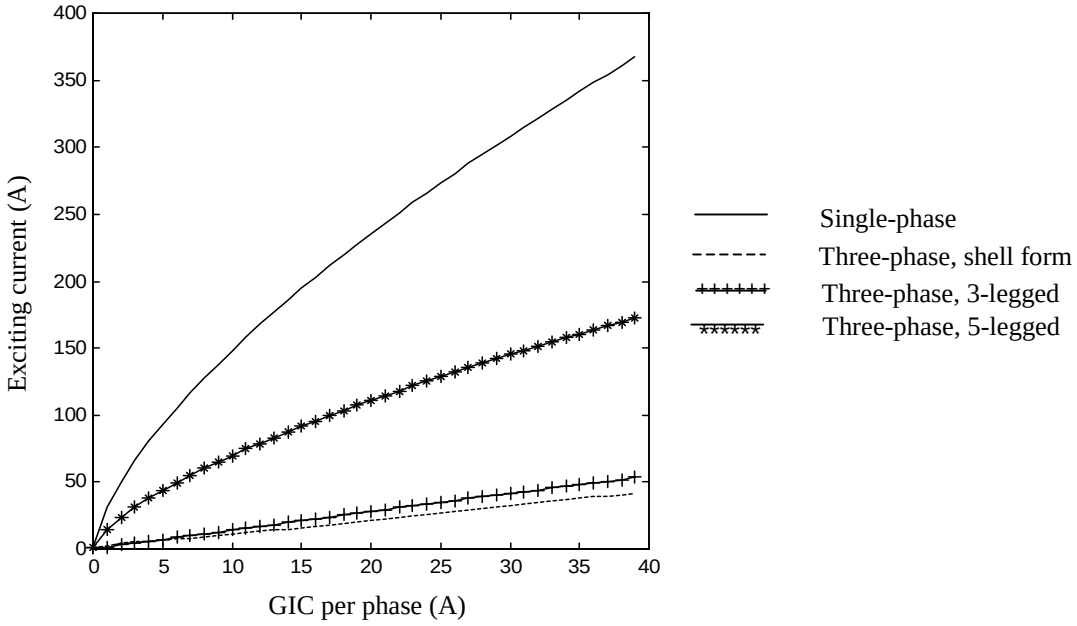

Fig.5.4. The variation of the exciting current with the input GIC per phase

duration of the triangle pulse t_d is equal to t_2-t_1, then $t_1 = T/4 - t_d/2$, and $t_2 = T/4 + t_d/2$. GIC per phase can be obtained by the triangle area S divided by the period of T, that is,

$$\text{GIC} = S/T = (A \cdot t_d/2)/T \tag{5.10}$$

The exciting current $i(t)$ and its Fourier series are given below.

$$i(t) = \begin{cases} A(1 + (t - T/4) \cdot 2/t_d) & t_1 < t < T/4 \\ A(1 - (t - T/4) \cdot 2/t_d) & T/4 < t < t_2 \\ 0 & \text{others} \end{cases} \tag{5.11}$$

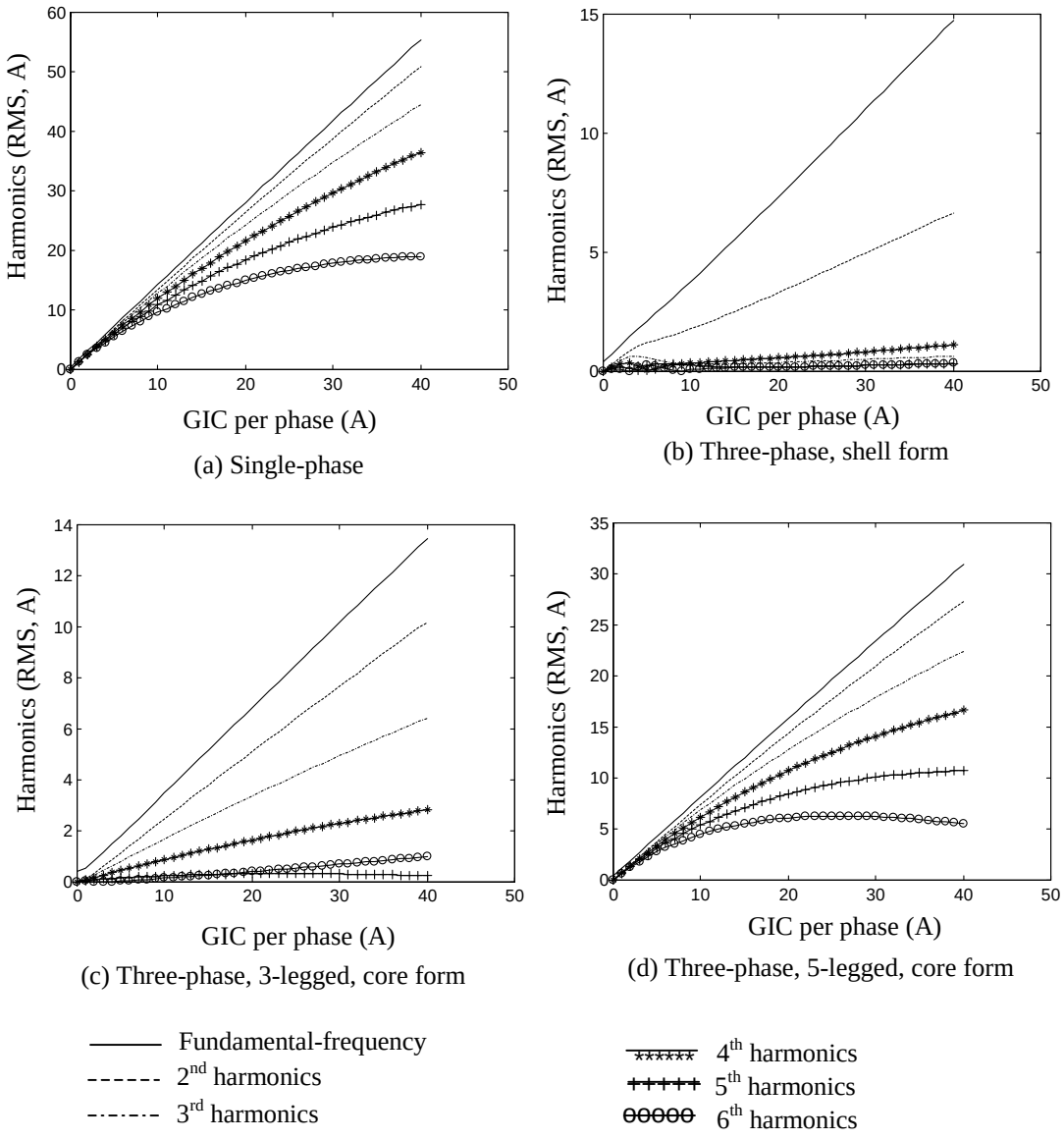

Fig.5.5. The relationship of the exciting current harmonics and GIC for transformers with different core design

$$I_{\mathrm{n}} = \frac{1}{T}\int_0^T i(t)\cdot\exp(-jn\omega_0 t)\,dt$$

$$= \frac{1}{T}\cdot\exp(-jn\omega_0\frac{T}{4})\cdot \mathrm{A}\cdot\frac{t_{\mathrm{d}}}{2}\cdot\left[\frac{\sin(n\omega_0\frac{t_{\mathrm{d}}}{4})}{n\omega_0\frac{t_{\mathrm{d}}}{4}}\right]^2 \qquad (5.12)$$

$$= \mathrm{GIC}\cdot\exp(-jn\omega_0\frac{T}{4})\cdot\left[\frac{\sin(n\omega_0\frac{t_{\mathrm{d}}}{4})}{n\omega_0\frac{t_{\mathrm{d}}}{4}}\right]^2$$

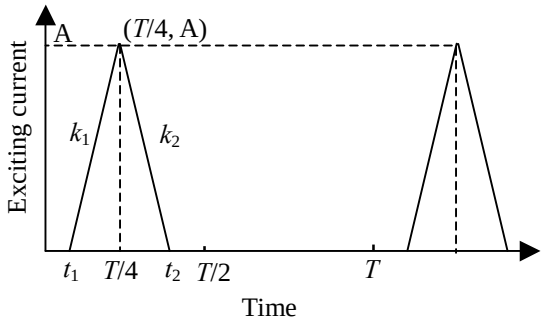

Fig.5.6. The approximate waveform of the exciting current in case of the transformer saturation

Where $\omega_0 = 2\pi/T$, n = 1,2,3… Eq.5.12 means that not only the fundamental component I_1, but also all other harmonics are of good linear relationship with GIC. The magnitude of the harmonics falls off as $1/n$. In fact, since the duration t_d does also vary with the increase of GIC, this results in the nonlinear relationship between the higher order harmonics and GIC. This has been verified by field measurements [Lesh93].

Fig.5.5 also shows that the even harmonics increase dramatically with the increase of GIC, different from the case of the transformer over-excitation. Half-cycle saturation, caused by the presence of GIC, will produce significant levels of even harmonics. The detection of even harmonics serves as a reliable indicator of the presence of GIC and half-cycle saturation.

5.4.2. Reactive Power Consumption

The MVar consumption of the transformer is calculated by using Eq.5.3. As shown in Fig.5.7, the variation of the MVar consumption is also linear with the increase of GIC for the sake of the fundamental component of the exciting current. The MVar drawn by the transformer can be easily estimated by using the following formula according to Fig.5.7.

$$Q\ (\text{MVar}) = k_1 * \text{GIC} + Q_0 \qquad (5.13)$$

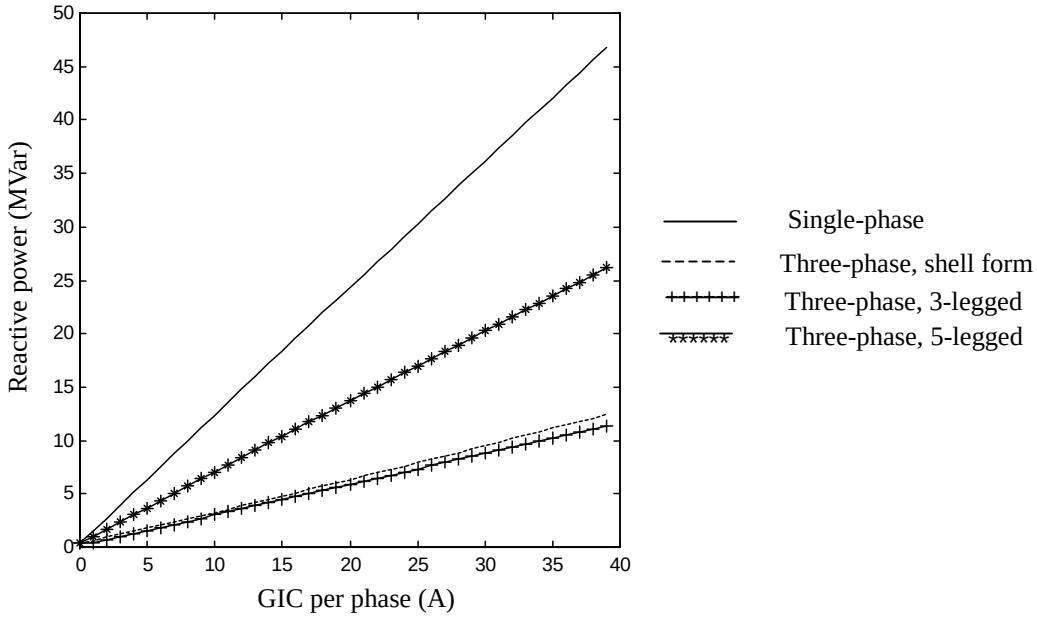

Fig.5.7. The variation of the MVar consumption with the input GIC per phase

Table 5.2. The value of k_1 and k_2 for different core

Core design	k_1	k_2
Single phase	1.18	0.97
Three-phase, shell form	0.33	1.91
Three-phase, 3-legged, core form	0.29	1.13
Three-phase, 5-legged, core form	0.66	1.01

Here Q_0 is the reactive power consumption from the normal exciting current and the value of GIC is in neutral. The value of k_1 is given in Table 5.2 for different core designs.

With the increase of GIC, the MVar consumption for all types of core design increases in different speed. They can be ranked to reflect the decreasing susceptibility to GIC below.

Single phase

Three-phase, 5-legged, core form

Three-phase, shell form

Three-phase, 3-legged, core form

The reason that the MVar based order is different from the exciting current peak based order is, that the distribution of the harmonics for each core design is different for a fixed GIC. Although the exciting current peak for three-phase shell form is smaller than that for three-phase 3-legged core form, the fundamental component is higher than the latter.

Fig.5.8 shows the relationship between the second harmonic current and the reactive power. A good linear relationship between the MVar consumption and the second harmonic current also exists for the calculated range of GIC and this has been verified on-site [Lesh93]. The formula below can be used to estimate the MVar consumption if the second harmonic current is detected.

$$Q \text{ (MVar)} = k_2 * I_2 + Q_0 \qquad (5.14)$$

I_2 is the RMS value of the second harmonic current. The value of k_2 is given in Table 5.2. Since the variation of 4^{th} and 6^{th} harmonics is nonlinear with the increase of GIC, no suitable formula can be obtained to estimate the MVar consumption by 4^{th} or 6^{th} harmonics.

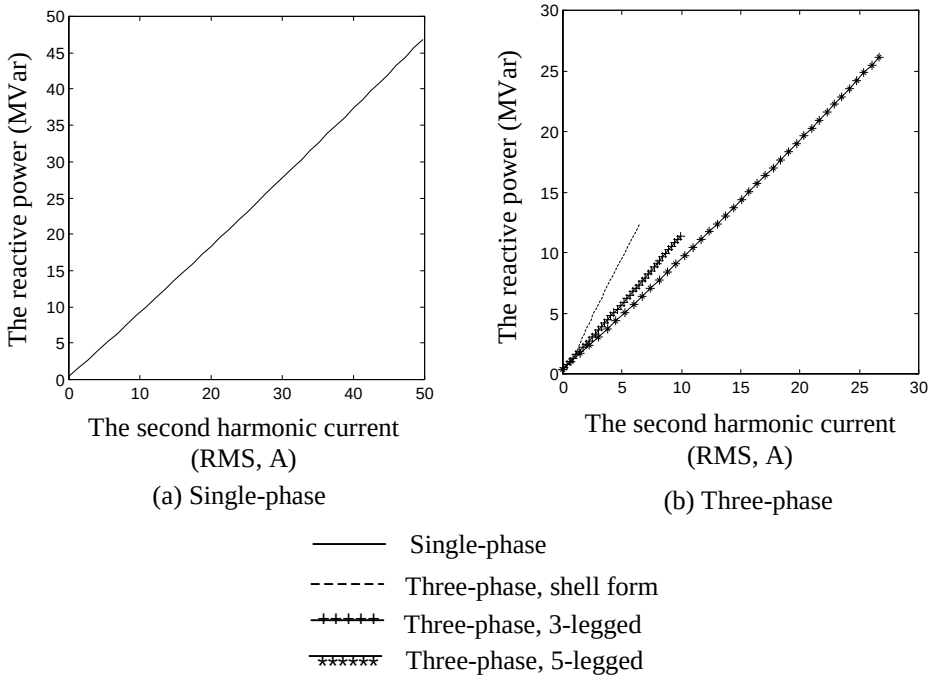

Fig.5.8. The variation of the MVar consumption with the second harmonic current

5.4.3. The Indicator of Transformer Saturation

A new partial harmonic distortion index, *PHD*, can be defined below to measure the GIC induced saturation.

$$PHD = \frac{\sqrt{\sum_{i=2}^{N} I_i^{\,2}}}{I_1} \tag{5.15}$$

Here I_i (i = 1,2, … N) is the RMS value of the harmonics. As shown in Fig.5.9, the *PHD* variation with the increase of GIC is different for different core designs. It revealed an interesting phenomenon that *PHD* increases dramatically when GIC increases up to a limit of about 1.0 A. It means that transformers enter definite saturate at this point. *PHD* may be used

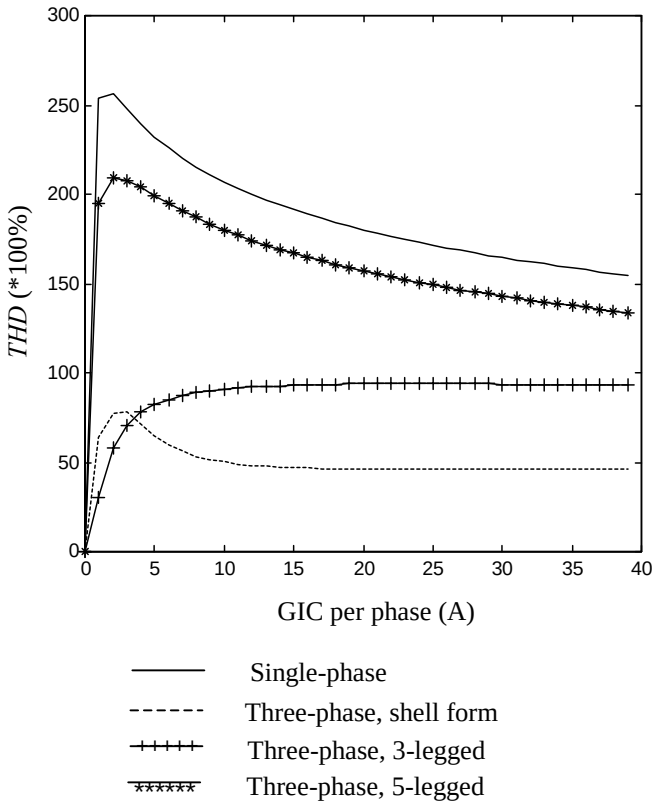

Fig.5.9. The variation of *THD* with the input GIC per phase

as an index to show when transformers begin saturating.

In fact, since the knee of the equivalent magnetizing curve is usually set at $1.1*\sqrt{2}I_{\text{exc}}$, transformers will begin to saturate if GIC exceeds 0.1 times the peak of I_{exc}. This GIC value is the lower limit when *PHD* begins to increase dramatically.

Since the odd harmonic components are affected by many factors, the accurate measurement of them that are caused by GIC alone is impossible. A nominal *PHD*' can be applied as the index to show the on-set of GIC induced saturation.

$$PHD' = \frac{\sqrt{I_2^2 + I_4^2 + I_6^2}}{I_{exc}} \tag{5.16}$$

5.5. Discussion of Factors Affecting GIC Induced Saturation

The above analysis is based on the constant transformer parameters for all types of core design, such as the rated voltage, MVA, and power frequency. In fact, these parameters also affect the GIC induced saturation of the transformer. Study shows that the GIC induced saturation is determined by both the no-load characteristics and the core design of the transformer [Albe93, Lesh93, and Albe81]. The no-load characteristics, that is, the magnetic characteristics of the transformer, will vary if the voltage, MVA, and power frequency are changed, and the GIC induced saturation trend is also changed. The effect of these transformer parameters on GIC induced saturation is discussed below.

1). The effect of power frequency. According to the transformer theory, EMF is proportional to the product of the turn number of the exciting winding *N*, power frequency *f*, and flux density *B*. Assume that the normal exciting current and the rated voltage, that is, EMF, were kept constant, only frequency is changed from 60 Hz to 50 Hz, then the product of *N* and *B* has to increase 1.2 times. Two possibilities that the effect of frequency on the GIC induced saturation exist. If *N* increases 1.2 times, but the cross-section area of the core is also enlarged to keep *B* constant, then the saturation trend of the transformer is not changed. That

is, the ratio of the slopes in Fig.5.1 will be constant, although the linkage ψ at the knee of the equivalent magnetizing curve will be 1.2 times higher than the case of 60 Hz according to Eq.5.1. The effect of GIC on the transformer saturation is the same as the case of 60 Hz.

If N and the core design are kept constant, that is, the transformer is the original one, only the frequency is reduced, then B has to increase, the transformer becomes overexciting and the normal operation point will exceed the unsaturated range. This means, the transformer has already saturated even without the input GIC. Since the transformer saturation caused by over-excitation is full-cycle saturation, only odd harmonics exist. If GIC is injected, the saturation becomes unsymmetrical, even harmonic components begins to increase. Fig.5.10 shows the waveform of the exciting current and the harmonics in this case, the transformer and the input GIC is the same as Fig.5.3. Since the transformer is overexciting, odd harmonic components are larger than even components.

2). The effect of the rated voltage. If the rated voltage decreases and the normal exciting current is kept constant, N will be reduced. Similar to the case of power frequency, two possibilities also exist. If the cross-section area of the core is set constant, the normal flux density B, and then the linkage ψ will decrease. The saturation margin increases and the transformer is less susceptible to GIC. On the other hand, if the cross-section area of the core is reduced and B is set constant, the saturation trend of the transformer is unvaried, and the effect of GIC will be still unchanged. The MVar consumption will decrease with the reduced voltage in both of cases according to Eq.5.3. Especially for the last case, the MVar consumption will decrease proportional to the rated voltage.

3). The effect of the operating voltage. If the transformer is original one, all parameters are set constant, only the operating voltage is changed, and the saturation margin is also changed. If the operating voltage is reduced 10% from 500 kV to 450 kV for the single-phase transformer in case of Fig.5.5, the saturation margin increases. The MVA consumption will decrease 10.43% and I_1 will decrease 0.48% when GIC in neutral is 75 A. If the operating voltage is added 10% to 550 kV, the MVA consumption increases 10.51% and I_1 increases 0.46%.

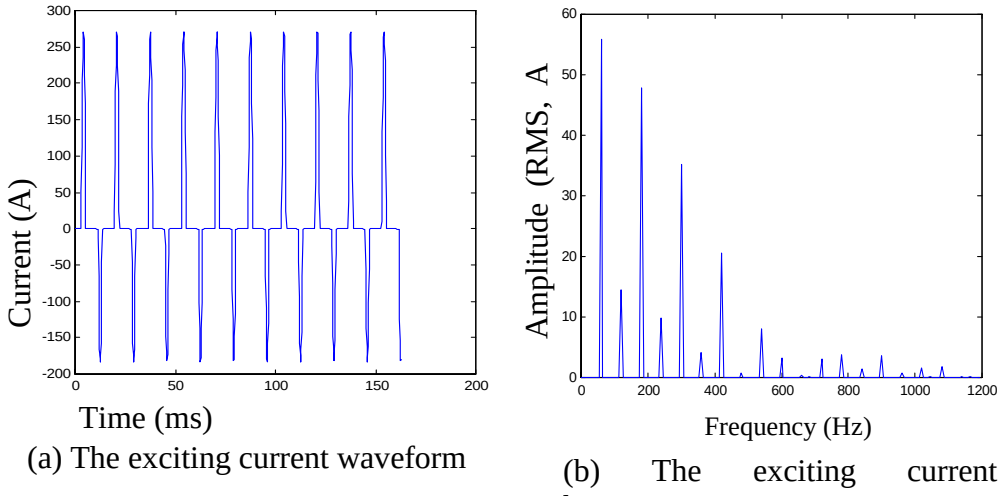

(a) The exciting current waveform (b) The exciting current

Fig.5.10. The exciting current for a GIC of 11.5 A per phase
(512/242 kV, single-phase, core form transformer, *f*=50 Hz)

4). The effect of the normal exciting current. The effect of I_{exc} on the transformer saturation is not significant. Provided that the normal AC linkage ψ_{ac} ($\psi_{ac} = N\phi_{ac}$, ϕ_{ac} is the AC flux in the core.) is set constant and MMF is unchanged, only the normal exciting current increases. N has to decrease, the flux ϕ_{ac}, then B will increase. The transformer is easier to saturate. Both the MVar consumption and harmonics will increase. For the single-phase transformer in case of Fig.5.5, I_{exc} is added 10%, from 0.42 A to 0.462 A, the MVA consumption and I_1 will increase 0.2% when GIC in neutral is 75 A, I_2 will increase 0.45%. If I_{exc} is added 50% to 0.63 A, the MVA consumption and I_1 will increase 0.89%, I_2 will increase 1.67%.

5). The effect of the rated MVA. The effect of MVA on the transformer saturation trend is not definite. Since large power transformers are designed to meet the specification of particular customers, which always focus on specifying the cost of losses, regardless of the no-load characteristics, it is difficult to define the relationship between MVA and the no-load characteristics of the transformer.

5.6. Other Related Issues

5.6.1. Calculation of the Time Constant

Fig.5.11 is a sample network used to estimate the time constant. It illustrates the power system and earth-surface-potentials (ESP) model. T_1 and T_2 are two 500 kV single phase transformer. The length of the HV line is about 400 km. Here L_{m1}, L_{m2}, R_{m1}, R_{m2}, and R_{t1}, R_{t2} are the exciting inductance, core loss resistance and the coil resistance of T1 and T_2, respectively. L_l and R_l are the inductance and resistance of the line. R_{g1} and R_{g2} are the earth resistance. Suppose ESP can be represented by an idea voltage source and 6 V/km, so DC voltage source is step voltage, U_0=2400 V. AC voltage source is shown in Eq.5.17.

$$u(t) = \sqrt{2}E_0 \sin(\omega t + \alpha) \tag{5.17}$$

R_m is ignored and the simplified circuit is shown in Fig.5.11c, R=R_l+R_{t1}+R_{t2}+R_{g1}+R_{g2}, and L= L_l+L_{m1}+L_{m2}. The injected GIC I_{dc} is represented by DC voltage source in Fig.5.11d.

$$I_{dc} = (U_0/R) \bullet 1(t) \tag{5.18}$$

In Fig.5.11d, when t<0, the transformer is in AC steady state with the excitation of $u(t)$, the exciting current $i(t)$ is

$$i(t) = \sqrt{2}\frac{E_0}{\sqrt{R^2 + (\omega L)^2}} \sin(\omega t + \alpha - \theta) \tag{5.19}$$

$$\theta = tg^{-1}\frac{\omega L}{R} \tag{5.20}$$

When GIC is injected into the network, the exciting current $i(t)$ is

$$i(t) = \sqrt{2}\frac{E_0}{\sqrt{R^2 + (\omega L)^2}} \sin(\omega t + \alpha - \theta) + I_{dc}(1 - e^{-t/\tau}) \tag{5.21}$$

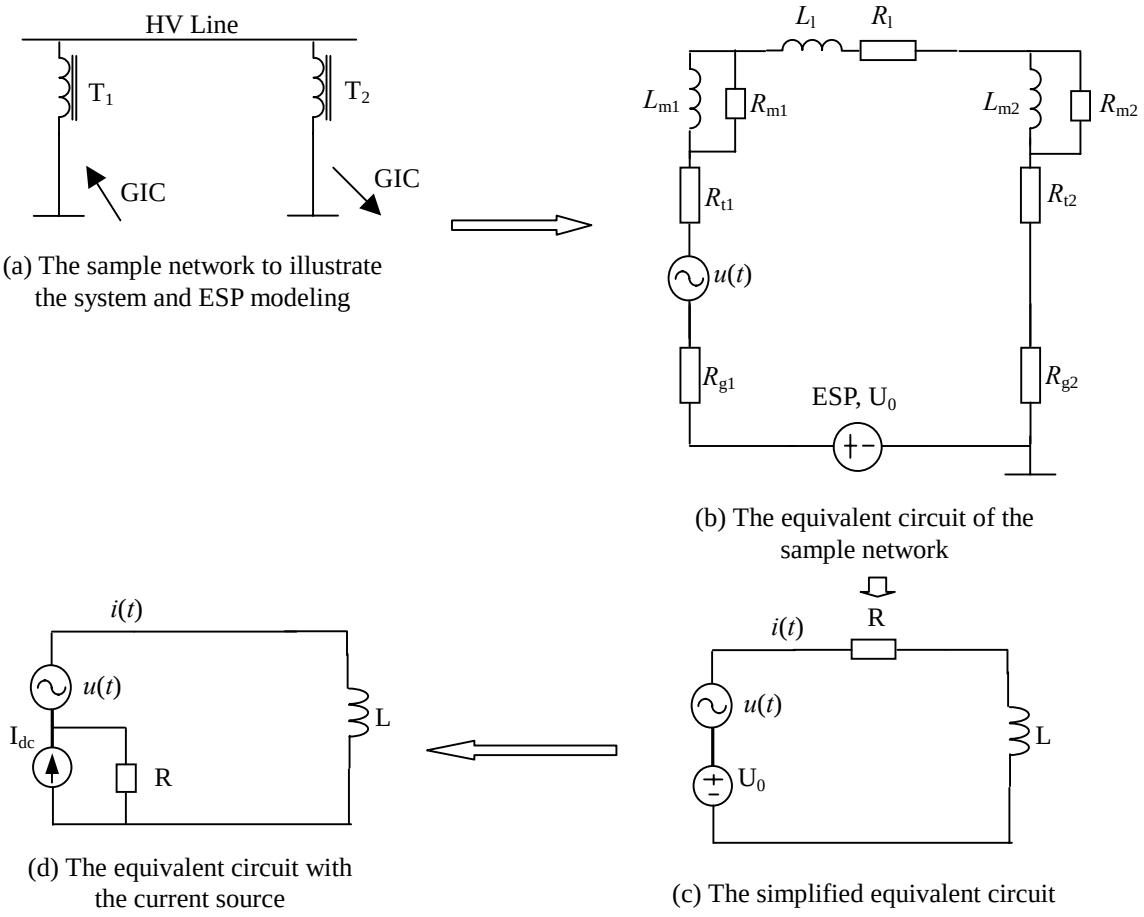

(a) The sample network to illustrate the system and ESP modeling

(b) The equivalent circuit of the sample network

(c) The simplified equivalent circuit

(d) The equivalent circuit with the current source

Fig.5.11. The model of the sample network with GIC

The time constant τ is

$$\tau = L/R \tag{5.22}$$

Eq.5.21 shows that the time constant τ of the network determines the saturation speed of the transformer. Actually L_m varies with the saturation level of the transformer and decreases with the increase of transformer saturation. The value given by Eq.5.22 is greater than the actual time needed to saturate a transformer. We can assume a constant L_m for convenience.

Suppose $R_{g1} = R_{g2} = 1.0$ ohm [Albe92], $R_{t1} = R_{t2} = 2.0$ ohm, $R_l = 0.0726 \bullet 400 = 29.0$ ohm, L_l=0.53 H. Because the transformer becomes saturated when GIC is injected, the exciting inductance decreases several times from the original value, here assume that $L_{m1} = L_{m2} =$

500.0 H. Then R = 35 ohm, L = 1000.53 H, τ = 28.6 s, the injected GIC step current is 68.6 A.

If the grounding electrode is a long thin cylinder with the length of 10 m and the diameter of 0.04m, the resistance R_{g1} is about 10 ohm [Cizh79]. Then the total resistance R equals to 53 ohm, τ=18.9 s. That is, the transformer will reach 63.2% saturation when t = τ = 18.9 s, and 86.5% when t=2τ=37.8s, and 95.0% when t=3τ=56.7s.

5.6.2 The Impact of dI_{dc}/dt

Suppose GIC in Fig.5.11d can be represented below

$$I_{dc} = U_0 / R\,(1 - e^{-t/\tau_2}) \cdot 1(t) \tag{5.23}$$

The time constant τ_2 reflects GIC change rate, then the current $i(t)$ is

$$i(t) = \sqrt{2}\,\frac{E_0}{\sqrt{R^2 + (\omega L)^2}}\sin(\omega t + \alpha - \theta) + I_{dc}\left(1 - \frac{\tau_1}{\tau_1 - \tau_2}e^{-t/\tau_1} + \frac{\tau_2}{\tau_1 - \tau_2}e^{-t/\tau_2}\right) \tag{5.24}$$

Here τ_1 is the time constant of the line/transformer combination in Fig.5.11. Eq.5.24 indicates that τ_1 and the time constant of GIC τ_2 together will determine the saturation speed of the transformer.

Assuming that τ_1 is equal to 18.9s, and τ_2 is equal to 5.0s, the relationship of the transformer saturation level and time is given in Fig.5.12, which indicate that the transformer will be 50% saturated at t=19s, and 95% saturated at t =60s.

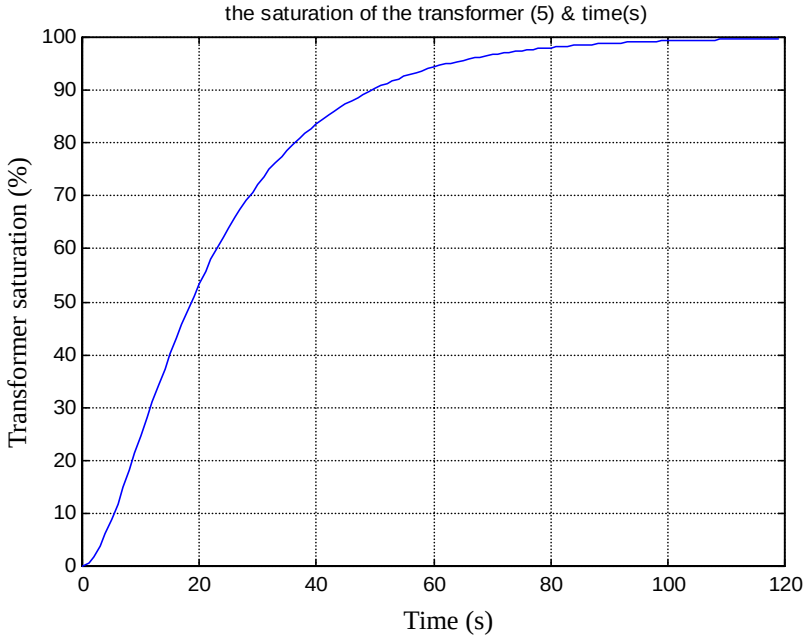

Fig.5.12. The relationship of the saturation of the transformer and time

5.6.3. The Impact of the Initial High Peak of GIC Waveform on Transformer Saturation

When GIC has an initial high peak followed by a lower value, the saturation of the transformer will decrease to a lower level with a smaller (shorter) time constant because of the smaller exciting inductance L_{m}.

For example, if the injected GIC is shown as Fig.5.13, assume that the exciting inductance of the transformer is L_{m2} when GIC changes from 10 A to 2 A, and the exciting inductance is L_{m1} when GIC changes from 0 to 10 A at the beginning. L_{m2} is lower than L_{m1}. According to Eq.5.21, the exciting current $i(t)$ is

$$i(t)=\sqrt{2}\frac{E_0}{\sqrt{R^2+(\omega L)^2}}\sin(\omega t+\alpha-\theta)+I_{\mathrm{dc1}}(1-e^{-t/\tau_1})\cdot 1(t)+I_{\mathrm{dc2}}(1-e^{-(t-T)/\tau_2})\cdot 1(t-T) \quad (5.25)$$

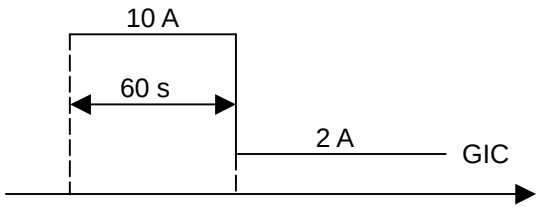

Fig.5.13 The variation of GIC

Here I_{dc1} = 10 A, I_{dc2} = -8 A. This means an equivalent GIC of 2 A is injected when t = T = 60 s. Suppose the inductance L in the first item in Eq.5.25 is unchanged, L=1000 H. τ_1 and τ_2 are the time constant of the power network, and T is the time when GIC changes.

$$\tau_1 = L_{m1}/R \quad (5.26)$$

$$\tau_2 = L_{m2}/R \quad (5.27)$$

Similar to Problem 1, suppose the total resistance R is equal to 53 ohm, L_{m1}=1000.53 H, then τ_1=18.9 s. That is, when GIC of 10 A is injected at the beginning, the transformer will reach 63.2% saturation when $t = \tau_1$ = 18.9 s, and 86.5% when t=2τ_1 =37.8s, and 95.0% when t=3τ_1=56.7s.

When the time is 60 s, another GIC of –8 A is injected to the transformer. Assuming that L_{m2}=L_{m1}/5=200.1 H because of the transformer saturation, then τ_2=3.78 s. That is, the transition time of GIC from 10 A to 2 A is about 3τ_2, 11.3 s.

If E_0 = 408 kV, the frequency is 60 Hz, α=0, θ=$\tan^{-1}(\omega L/R)$=π/2, then the waveform of the exciting current is shown in Fig.5.14.

5.6.4. The Impact of Transformer Load on the GIC Caused Harmonics and MVars

For a given GIC, the harmonics generated by the transformer is independent of its load. However, the harmonic voltage is affected by the loads.

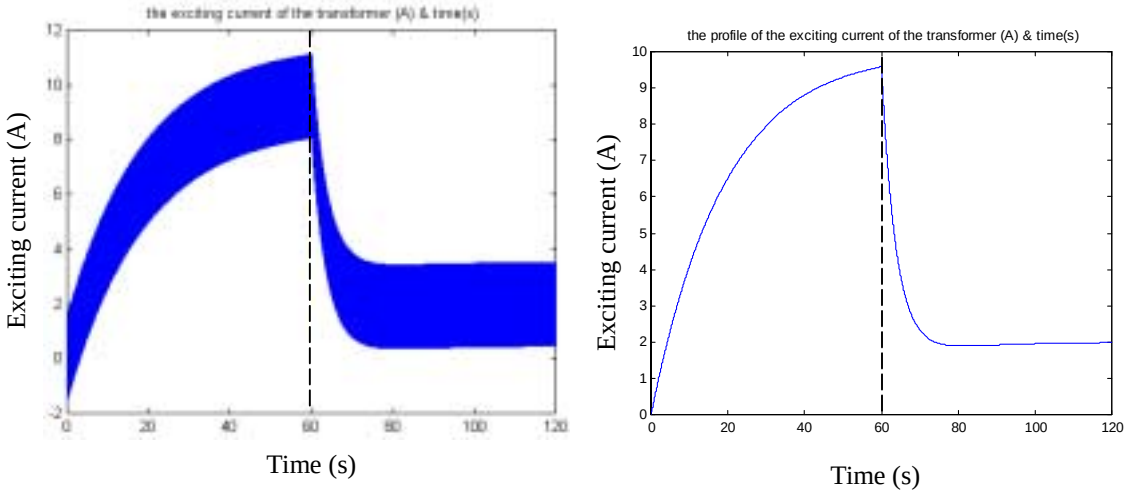

Fig.5.14. The waveform of the exciting current and its profile

5.7. Summary

To estimate harmonic currents and MVar with only the given GIC and the nameplate information of the transformer, this chapter developed a simplified method based on the equivalent magnetizing curve for transformers with different core design. Compared with test results, the simulation method is feasible with adequate accuracy.

The effect of GIC on transformers with different core design is analyzed based on the simplified method. The relationship between the harmonics, the MVar consumption and GIC are illustrated. Simulation shows that the fundamental component of the exciting current and the reactive power are linear with GIC, making the evaluation of the MVar consumption directly with the given GIC possible. Partial harmonic distortion, *PHD* can be applied as a good indicator to show when the transformer begins saturating with the input GIC. The effect of the transformer parameters, such as the voltage, frequency, the exciting current, and MVA, on the GIC induced saturation is also discussed.

CHAPTER 6
VIRTUAL HOSPITAL FOR POWER EQUIPMENT

Analysis and diagnosis of transformer abnormalities or failures discussed in the prior chapters heavily relies on previous experience and information related to equipment testing, diagnosis, and maintenance. Information technology opens new doors in this area with powerful and convenient information sharing capabilities. This chapter introduces the concepts and prototype development of a Virtual Hospital (VH) for Power Equipment, which will collect a variety of transformer or other equipment abnormities and failures, and provide integrated diagnostic tools for specific power equipment based on the Internet.

6.1. Introduction

6.1.1. Motivation

Power equipment diagnosis and maintenance plays a key role in keeping one of our national critical infrastructures in good health and is essential to the electric power industry. With the rapid development of deregulation and privatization in the power industry, convenient acquisition of diagnosis and maintenance information has become increasingly important for electric power companies to optimize repair intervals, reduce the maintenance cost, and increase operating efficiency [Worke00, Oppe99, and Wray97]. However, valuable experiences and knowledge of power equipment diagnostics and maintenance were not systematically collected and shared up to now. Very often they are just kept by the maintenance division of utilities or maintenance service providers that are rarely shared with others outside the organization.

Until recently, such information was usually available only in print form distant from field or office, and the barriers to access the information were quite high, especially for the field personnel and maintenance service [Senb00]. For consultants and researchers, it is also impossible to have the extensive historical case studies about equipment faults or failures, since many of them are scattered in publications or kept by utilities for internal reference.

Systematical and extensive collection of diagnosis and maintenance knowledge and information is essential for the power equipment maintenance community to provide easy maintenance information access and retrieval [Hayn96].

From the 1990s, the development and widespread use of the Internet has been opening up new windows to the power equipment maintenance community. Timesaving information retrieval, extraction and quick decision-making are enabled with minimum efforts due to the open system and cross-platform architecture supported by the Internet [Levi99, Gold00, and Smit94]. Comprehensive diagnosis and maintenance information of power equipment can be easily accessed worldwide through the World-Wide-Web (WWW), and interoperability will be greatly enhanced between the community members, which makes troubleshooting a much easier task [Pipe00]. Furthermore, e-commerce stemming from the Internet is increasingly adopted in order to lower the cost of doing business through lower transaction cost. Maintenance strategies are also dramatically altered with E-commerce involvement [Grai00].

However, existing equipment diagnosis and maintenance information on the Internet is poorly organized, scattered, and of questionable authority. Although some maintenance service providers do have Web sites promoting commercial services in diagnosis and networked maintenance management [StraMa, TeleGl, and EnerCo], diagnostic techniques and test data are usually not widely shared. As a consequence, duplication in research and development is the norm, draining the resources that could have been used to develop new diagnostic and maintenance techniques.

Development of digital library techniques enables the Internet based virtual hospital for power equipment, due to its abilities to effectively retrieve information, to preserve and extend discourse, as well as to provide richer contexts for people to interact with information [ForLib, ArmsWi, and LynCl]. Digital library is not merely equivalent to a digitized collection of maintenance materials with information management tools, it is rather an environment to bring together collections, services, and community members in support of the full life cycle of creation, dissemination, and preservation of information in this community. Such an enriched digital library can also include an online service exchanger to

conveniently bridge the maintenance service providers with service seekers. The traditional way individuals and organizations behave, communicate, and conduct their affairs is expected to be altered in this community with the application of digital library [Mcmi99], as they are increasingly turning to the Internet-based repositories as the primary source of information about power equipment maintenance.

6.1.2. Purpose of the Virtual Hospital

Inspired by the virtual hospital in medicine [Hayn96 and Phoh96], the concept of an Internet based Virtual Hospital (VH) for Power Equipment is proposed. The benefits of such a VH include but are not limited to:

1). supporting and promoting worldwide information sharing on tests, diagnosis, and maintenance of power equipment, and integrating state of the art diagnosis and maintenance information in the routine work of field maintenance personnel and maintenance service providers;

2). promoting distance training, continuing education and remote diagnosis wherever the Internet is accessible, and providing an easy starting point as well as in-depth study links for diagnosis of power equipment failures or abnormalities;

3). providing a convenient communication channel for the power equipment maintenance community through the Internet; and

4). providing a test bed and promoter of newly developed technologies of diagnosis and maintenance. These objectives will be accomplished by identifying the applications necessary and designing and implementing an information architecture to support these needs.

The VH tries to simplify access to state of the art diagnosis and maintenance information, speed up the information extraction and service transaction, integrate the knowledge and

information into the routine equipment diagnosis and maintenance, thereby reducing operation and maintenance (O&M) costs to optimize use of resources through utilization of new maintenance processes, technologies and experiences.

6.2. Internet Applications in Equipment Diagnosis and Maintenance

Internet applications in power equipment maintenance fall into three categories: remote condition monitoring, remote diagnosis, and networked maintenance.

6.2.1. Remote Condition Monitoring

Currently there are two types of remote condition monitoring configurations. One is through the high-speed real-time Local Area Network (LAN) within substations and plants such Ethernet or FDDI. Monitoring systems for power equipment, remote terminal units (RTUs), and other control components, are connected to the LAN as intelligent electronic devices (IED). Protection, control, monitoring, and other secondary functions are integrated together into this communication network. Intelligent functions are incorporated into IEDs, which can be accessed through substation or plant servers [Prou99, GESA, and Yasu98]. This kind of configuration is more suitable to new substations and plants with less wiring, fast response, and easy maintenance. However, high upgrading cost may be required for the existing substations or plants.

Another approach is by setting up the substation server as the interface between Internet/Intranet and monitoring systems in the substation. Monitoring systems are wired to the server separately or using the existing links [Pomm98]. An Internet based transmission substation monitoring system is used for remote substation vision [Chan99]. Remote online monitoring via Internet for power transformers or break circuits is also developed [Siem00 and StraMa].

6.2.2. Remote Diagnosis

Several maintenance companies or utilities have already taken advantage of Internet in remote equipment diagnosis and maintenance. Currently the basic mode is, field personnel or monitoring systems automatically upload the condition information of the operating power equipment to the server in maintenance companies or maintenance divisions in utilities. A central group of highly skilled maintenance engineers will analyze and evaluate equipment condition using various diagnostic methods and their experiences, then analysis results and maintenance action recommendations are documented to issue back to the customer's Web page or related field technicians via E-mail or file transfers. Several companies now provide such remote diagnosis services [EnerCo, Entek, and Hoga99]. Special Internet based information management system example for both equipment diagnosis and predictive maintenance [MainWeb] is also available. Remote capabilities enhance the diagnosis efficiency and maximize productivity with expert diagnostic services for reduced travel costs and lower downtime.

Another emerging mode is developing the remote diagnosis center, in which the proven diagnostic tools are collected and integrated together. Maintenance engineers and field technicians can access these tools via Internet for their own evaluation of power equipment. Currently it has been developed for rotating machine and other mechanical equipment diagnosis [Lingso], however, no similar tools exist for power equipment diagnosis.

6.2.3. Networked Maintenance

Internet enables development of the networked maintenance database. One company [DataSys] has developed a Web based CMMS (Computerized Maintenance management System), MP2Weblink for many kinds of management functions such as assets, work orders, materials, maintenance, etc. MP2Weblink server will store all information into several databases, maintenance managers, engineers, and technicians can input or obtain information anywhere. EPRI is also developing a Maintenance Management Workstation (MMW) for optimizing maintenance work at transmission substations [EPRI00]. Beyond the work-order logging and tracking capabilities of conventional CMMS, MMW collects and stores data on equipment condition, analyzes performance, and prioritizes needed tasks. Maintenance

management can be made more convenient, more efficient, and easier to be integrated into the enterprise wide information system.

6.2.4. Trend of Internet Application in Equipment Maintenance

It is expected that Internet/Intranet based fault diagnosis and maintenance for power equipment will result in the following trends.

1). Standardization. If monitoring instruments and diagnostic tools have different communication interfaces and data formats, it will be very difficult for them to be integrated. Internet based interfaces and standard data formats provide an easy way to exchange/access data/information, therefore can result in tremendous savings in resources that should focus on validating existed diagnostic methods and developing new ones [Good98].

2). Networked management. Internet makes it possible to do remote monitoring, diagnosis, and networked maintenance of power equipment for multiple substations and power plants. The distributed information storage capability and integrated diagnostic techniques of Internet based maintenance management systems could push equipment management from individual solutions to a global approach.

3). Integration: Integration can be realized at four different levels: a) monitoring instruments; b) diagnostic techniques; c) maintenance strategy; and d) personnel management. Multi-parameter based monitoring instruments can be developed and integrated via Intranet as parts of the substation automation, and an integrated equipment monitoring network for a specific power system grid can be built. A virtual hospital can be developed to host existing diagnostic techniques for specific power equipment, and help reconstructing utility maintenance strategies. Reliability centered equipment maintenance strategies can be drawn from a global approach based on the more comprehensive evaluation of the equipment. With such an Internet based monitoring and maintenance network, many maintenance divisions can be consolidated into a few effective groups [Borl98 and Butl96]. A VH can host existing diagnostic techniques and play a critical role of integration.

4). Testbed of newly developed technologies, because it is low-cost and sometimes free of charge and easier to be evaluated.

6.2.5. Comparison Between the VH in Medicine and in Power

A successful case is the development of Virtual Hospital in Medicine launched in 1992 (http://www.vh.org). As a digital health science library, the virtual hospital makes the Internet a useful medical reference and a tool for health promotion and lifelong medical education. All information are transferred to HTML documents and stored in a multimedia database in a Web server, and one can access it worldwide. The Virtual Hospital provides access to textbooks, diagnostic algorithms, patient simulations, historical information, and patient instructional, etc. The information is organized in several separate indices for easy access.

Comparing power equipment with human subjects from the diagnosis and patient point of view, many similarities exist in test and monitoring methods, diagnosis and prognostic procedures, data analysis, and maintenance strategies. Even for the information management of diagnosis and maintenance, the strategies and procedures are also comparable [Jaak96, Dass98, Milo99, and Simp98]. Here the power equipment can be analogous to patients, and maintenance personnel are equivalent to the nurses or doctors, maintenance experts are the medical specialists. Therefore, the functions of a hospital can be virtually implemented in a VH for power equipment.

6.3. Concept of a Virtual Hospital (VH) for Power Equipment

6.3.1. Overview

Combined the history of various diagnostic tests, maintenance activities, and fault analysis could provide very valuable information for equipment life estimation and future apparatus design modifications. In an attempt to integrate information and historical cases of

power equipment diagnosis and maintenance, a new Internet based virtual hospital (VH) for power equipment is proposed conceptually and being developed. The VH is based on the use of a digital library, the Internet and IT techniques to permit the collection and exchange of information of the equipment, maintenance practices, test data and the diagnosis. The VH is an important tool to aid those affected by the loss of experienced engineers during the deregulation of the power industry and can be used to improve maintenance quality worldwide [Dong01a].

6.3.2. Who Can Be Served by the VH

The VH will serve the education purpose as well as power equipment maintenance community, which consists of people performing equipment maintenance (utility maintenance personnel, industry societies, manufacturers), those with the need to learn and study power equipment maintenance (students, educators and researchers), manufacturers, and maintenance experts (maintenance service providers, utilities, and developers automated diagnostic tools). Over time individuals in the community may play numerous roles.

Different community members play different roles in supporting and using the VH. The collection of processes that describe how each of these groups will use the VH, are shown in Fig.6.1.

- Maintenance service receiver can use the VH for education, remote diagnosis, solutions, service searching, and field experience uploading to the VH for sharing.

- Maintenance service provider can use the VH for speedy communication, sharing experiences and ideas, remote diagnosis and maintenance, expediting development of new techniques, modifying the design-based fault/symptom models, uploading general diagnosis and maintenance knowledge to the VH.

- Educators, Students, and Researchers can use the VH for distance education and training, reviewing new research activities, and uploading and sharing diagnosis and maintenance techniques and research results, retrieving equipment failure cases.

- Manufacturer (including equipment and instrument manufacturers) can use the VH for developing new test devices and measurement techniques, uploading equipment design data and parameters, retrieving the historical failure cases for modifying equipment design.

- Other maintenance communities can use VH as a reference to establish their own digital library and share common experiences and techniques.

Fig.6.2 also illustrates how the user interacts with the maintenance information. As an example, the procedure to diagnose a transformer failure is described below to show how the use case works.

1). Operator reports a transformer failure event;

2). An expert or service provider obtains the contract to determine the causes resulting in this failure;

3). Field maintenance worker takes the diagnostic tests to get some in-depth information using the measurement instrument;

4). Manufacturer and operator provide detailed equipment design and operation information;

5). The transformer is diagnosed and maintained;

6). All maintenance activities are documented as part of general knowledge to update the equipment design, operation, and maintenance.

6.3.3. VH Collections

This section will present detailed description of selected collection modules in the VH given in Fig.6.2.

- **Education collection center**

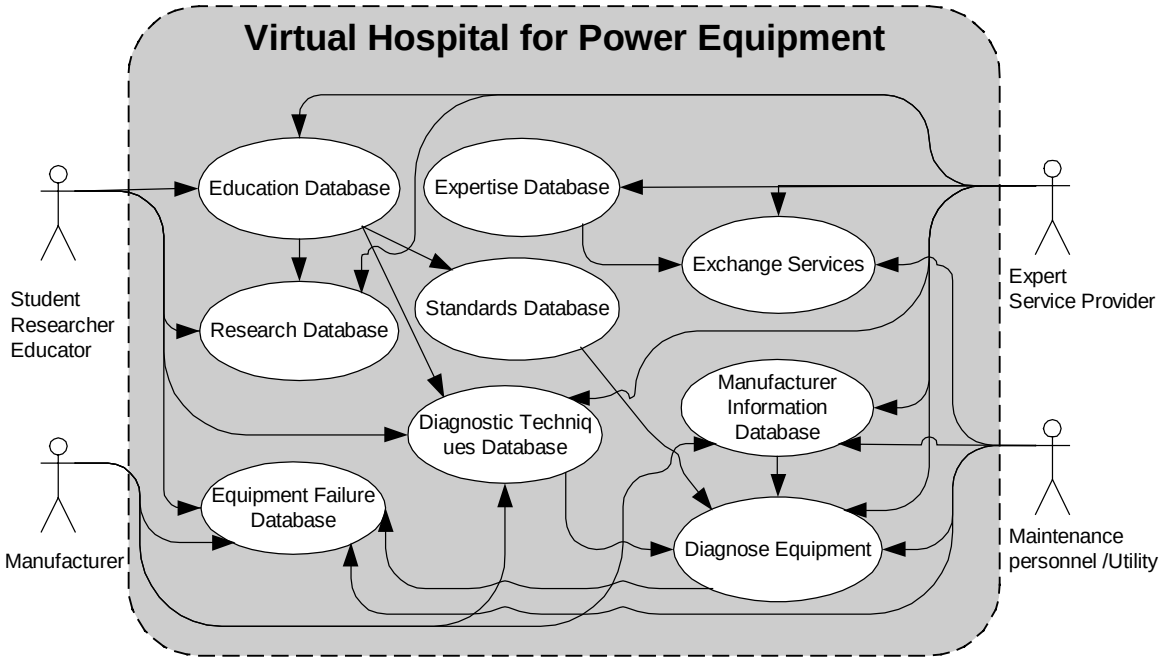

Fig.6.1. The overall use case diagram of the VH

To document general knowledge and basic educational materials related to diagnosis and maintenance for specific equipment. Textbooks, presentations, tutorials and lectures will be included. Text, image, audio, and other multimedia educational materials are used to make the knowledge easily understood for education and distance training.

• **Standard collection center**

To collect and organize all related standards including test procedures, diagnostic techniques, maintenance guides and recommendations, and general test results explanation. The standards come from IEEE, IEC, ANSI and other national standards organizations.

• **Typical collection case center**

To collect typical historical cases and test data related to equipment abnormalities or failures, and provide detailed failure analysis. For some equipment or parts, existing fault-tracking trees or design-based fault/symptom models will be improved and updated continually [Arno99]. Since many typical cases have been collected and analyzed by some IEEE Task Forces and CIGRE Working Groups, collaboration with them is very important to

enrich the case base. Data mining techniques will be applied to identify such fault models from the fault cases collection.

• **Diagnosis and maintenance center**

To include diagnostic techniques and maintenance management strategies. Diagnostic techniques include: expert system and artificial neural network based diagnostic algorithms, fuzzy or statistical diagnostic techniques, and etc. Maintenance strategies include failure mode effect analysis (FMEA), failure mode effect and criticality analysis (FMECA), reliability centered maintenance (RCM), trend analysis, life estimation, etc [Jans00 and Moub00]. An example of such tool is illustrated in Chapter 6.5. Since most diagnostic

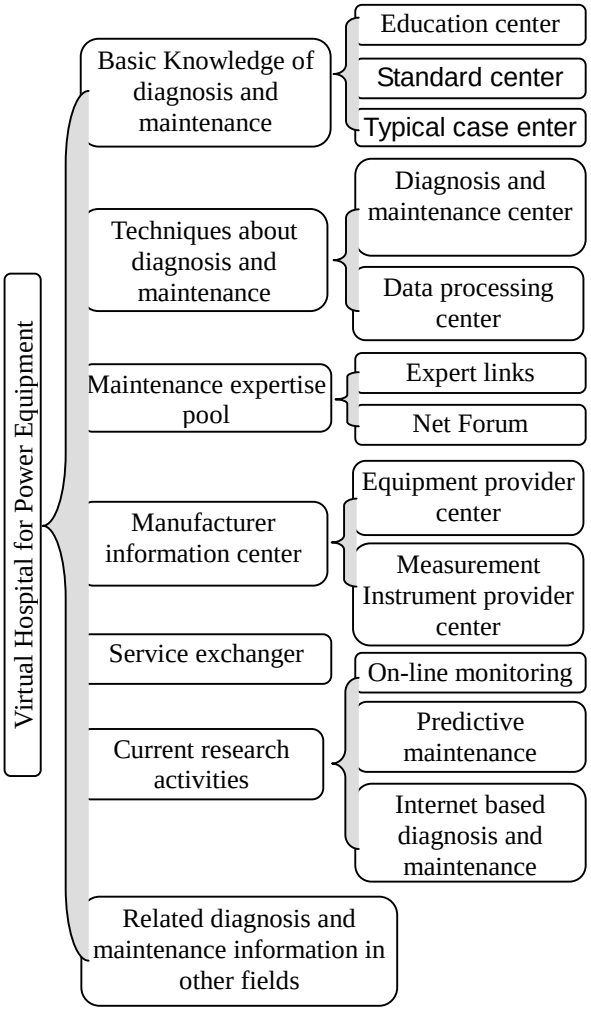

Fig.6.2. VH major contents

techniques are commercial products, their features and links are provided. This center may be critical in promoting integrated diagnosis if enough information is available. As a complement, a data processing center is also built to collect or index many signal processing techniques frequently used for data mining and feature extraction in standard format, such as time and frequency domain analysis, statistical and reliability analysis, pattern recognition, etc.

- **Maintenance expert pool**

To build a global expert database for links to maintenance personnel, maintenance service providers, maintenance experts, researchers, and manufacturers. Expert links will also support video-conferencing, chat, and newsgroup for distance diagnosis and information exchange. Expert pool makes the community members not only an information receiver, but also a contributor of knowledge and experience. Several expert pools have been successfully running in other fields, however the similar pool is not published so far [Askme].

- **Online service exchanger**

To bridge the worldwide diagnosis and maintenance service providers, measurement instrument manufacturers, with service seekers, and enable them conveniently do some service transactions via the Internet. Such an online service bridge provides a friendly Internet based agent to extend the service physical areas for service providers and give more selections for the service seekers who want to get better service. Currently such an agent mainly exists in other industries, such as stock, insurance, etc, but not yet in this community.

- **Technology news center**

To present state of the art research activities related to equipment diagnosis and maintenance, such as on-line monitoring, predictive maintenance, Internet/ Intranet based monitoring and diagnosis, networked maintenance management, etc [MaTa98]. Product review, evaluation, and recommendation services can also be part of the VH functions.

6.3.4. VH Architecture and Implementation

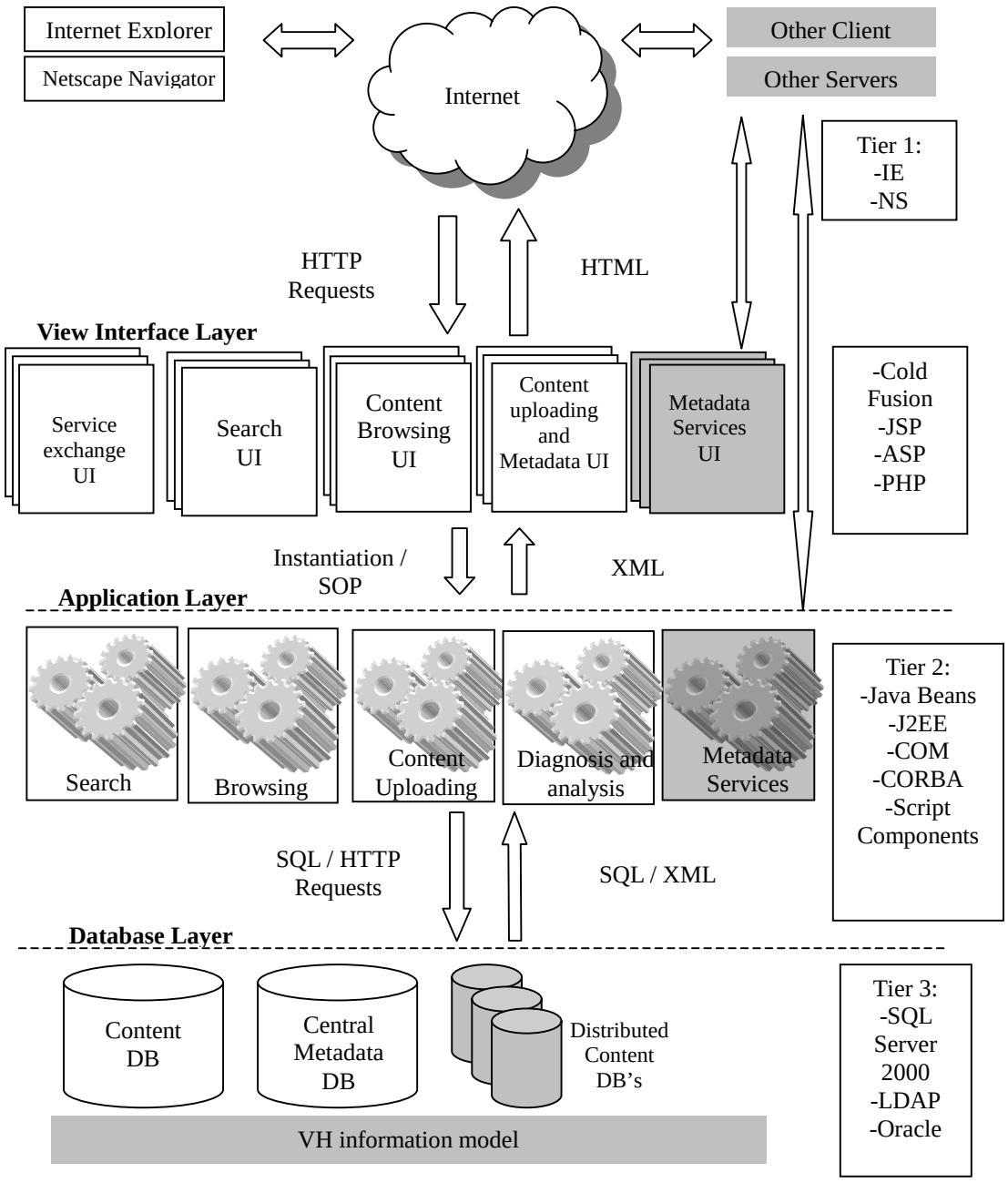

Fig.6.3. The VH application architecture

The VH is built upon the open Internet and WWW structures that allow for scalability, interoperability, and modifiability [Tyle99]. Simplicity, intuitive and open architecture are the guiding principles in the VH design and development. Similar to the virtual medical hospital concept, "from simple system, powerful and complex behaviors can emerge" [NavyMe]. The VH multi-tier architecture is shown in Fig.6.3, including: Database layer,

Access layer to bridge the database and the applications, Application layer to implement diagnosis and information update, View layer to implement user interfaces for various purposes, and Client layer to allow the user browse the information. XML is used primarily to format and present the VH materials as it provides a mechanism to impose constraints on the storage layout and logical structure, and is intended to meet the requirements of large-scale Web content providers for industry-specific markup, vendor-neutral data exchange. In order to organize the VH information, a comprehensive information model has been developed and illustrated in Chapter 6.4. A VH prototype has also been developed in Visual Basic for demonstration, as shown Fig.6.4, which is used to show the VH general diagnosis

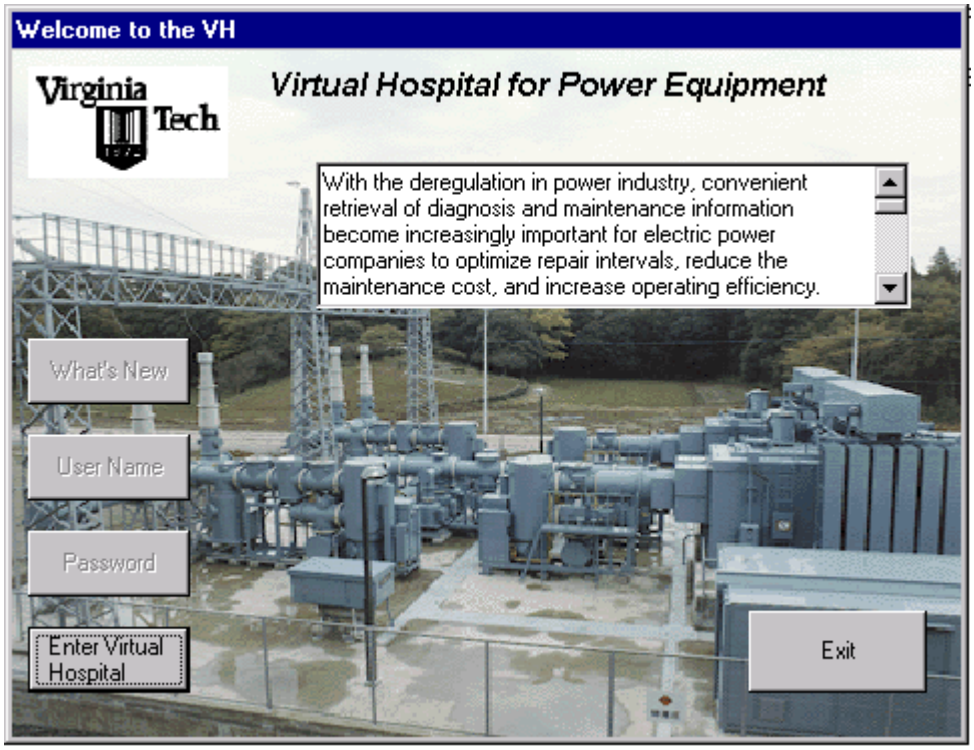

Fig.6.4. The VH prototype

application, and a Access database based on the information model is designed to support the VH prototype.

It should be noted, what the VH can provide is a collection (and linkage) of information, knowledge and techniques. The VH is not to replace the diagnostic and maintenance management tools currently used in power companies, but to complement and integrate the existing applications. Expanding and supporting the VH is the responsibility of the whole

maintenance community. Development of the VH is a time intensive process. Continuous updating and expanding is necessary and could be done overtime through joint effort with organizations such as EPRI and private sectors.

6.4. Information Model for Power Equipment Diagnosis and Maintenance

6.4.1. Introduction

Though many databases have been used to manage the maintenance information in recent years, they are developed individually and based on different information models, and a high barrier is in accessing and exchanging the data that has been collected by other parts of the organization or the third party [Matu99]. In order to provide the power equipment maintenance community a standard mechanism to exchange the maintenance information, a uniform information model is developed used to data organization, access, sharing, and archiving related to equipment diagnosis and maintenance. As shown in Fig.6.4, with this information model, maintenance information in the VH can be easily accessed and shared in a common way.

6.4.2. Analysis of Maintenance Information

6.4.2.1. Category of Maintenance Information

As shown in Fig.6.1 and 6.2, maintenance information can be usually categorized as follows [EPRI99]:

Equipment specification information

Information about manufacturer specification and installation of the equipment and its components.

Equipment maintenance information

Information about measurement data in various tests (e.g., performance or diagnostic tests), records of failure analysis and maintenance. Sometimes it is necessary to include the information related to measurement instruments.

Documentation information

Information about some general knowledge and standards associated with equipment measurement, diagnosis, and maintenance. Various measurement and diagnostic techniques are also considered part of documents.

Expertise information

Information about the contact information and skills of maintenance experts and researchers, which are crucial for successful equipment diagnosis.

6.4.2.2. CIM Extension

Since 1990s, the Electric Power Research Institute (EPRI) has developed the Common Information Model (CIM) which provides a comprehensive logical view of Energy Management System (EMS) information in a control center. Recently asset model extensions to the CIM are also being developed to support utility operations, including maintenance and work order management, with the purpose of modeling asset related information that needs to be exchanged among systems (e.g., EMS, Distribution Management System - DMS, Geographic Information System - GIS, work Management, etc.) [EPRI99]. However there are still some concerns to support the information to be exchanged for power equipment diagnosis and maintenance.

The CIM model was initially oriented towards support of transmission and generation from system operation of view, and only the equipment and its parameters related to the system operation are modeled. In terms of equipment diagnosis and maintenance, all high voltage power equipment and their components are concerned, including surge arresters that are not included in the CIM. For transformers, transformer oil and bushings should also be modeled.

Though the CIM provides detailed measurement entities and attributes to contain a heterogeneous collection of different types of measurements for a wide variety of equipment [Beck00], information about diagnostic testing, the measurement instruments and measurement techniques are not cared, which are key to support of equipment diagnosis. For example, two measurement techniques have been popular in the partial discharge (PD) measurement, wide-band detection with a unit of pC and narrow-band detection with μV. Different results will be obtained when the different PD detection method is applied, and it is possible that the wrong conclusion is given if the information about the PD measurement techniques was ignored during the information exchange.

Current asset extensions to the CIM cover the information included in the Computerized Maintenance Management System (CMMS), such as work task planning and scheduling. However, information about equipment diagnosis, historical failure cases, and diagnostic techniques, are not described. Furthermore, documentation and maintenance expertise are also part of the critical information to be exchanged. Therefore, it is important and necessary to develop a comprehensive information model specifically for power equipment diagnosis and maintenance.

6.4.3. Modeling of the Maintenance Information

Based on the CIM, the information model used for power equipment diagnosis and maintenance is defined and maintained using the Unified Modeling Language (UML) class diagram. As shown in Fig.6.5, the information model consists of several packages (or sub-models), including equipment, measurement, diagnosis, failure case, documentation, etc. The complete information model and detailed entity description are illustrated in Appendix D. The Package Person describes objects, such as skills and contact information of maintenance experts, while the Package ServiceExchange represents the information about the work task planning, scheduling, and ordering related to the experts. Both packages have been described in the asset model extensions to the CIM and not mentioned here. Other models are described in details as follows.

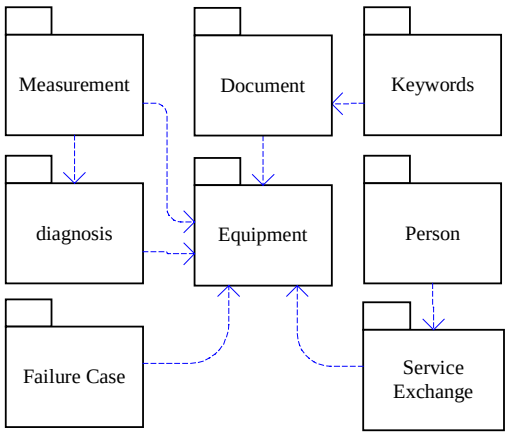

Fig.6.5. The logical view of the information model

6.4.3.1. Equipment Model

Equipment class represents not only the attributes related to the system operation included in the CIM, but also the information used for equipment diagnosis and maintenance. As an example, the transformer model is given in Fig.6.6. In order to promote and facilitate cooperative efforts between users and manufacturers to improve the reliability of power transformers, the transformer information that should be collected and reported has been defined in the IEEE Standard C57.117 [Guid88]. The transformer model in Fig.6.6 is the UML class diagram representation of the transformer population information, which is described in [Guid88].

From transformer diagnosis and maintenance of view, components supporting the transformer dielectric and mechanical strength, such as bushings, transformer oil, and cores, are critical to maintain the transformer in health, and have to be modeled. A component abstract class is defined to include all transformer and other equipment components to make the equipment description clear. The meaning of the entity attributes can be found in the Form 1 in [Guid88].

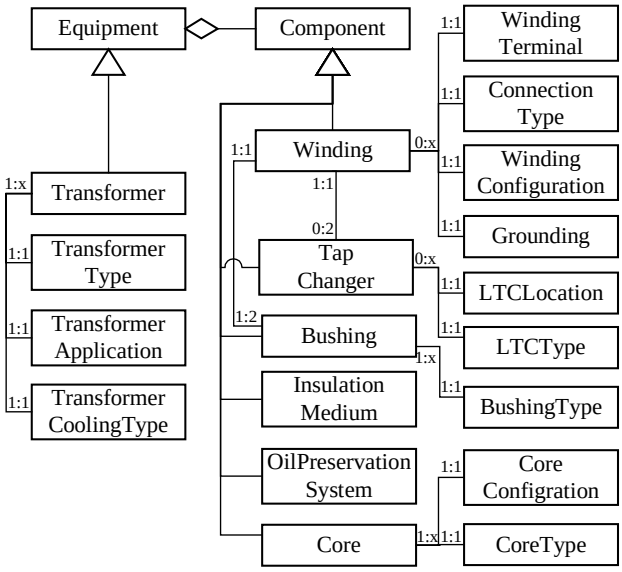

Fig.6.6. The transformer model

Similar representations can also be easily given to other power equipment, including generators /motors, cable, circuit breakers, gas insulated substation (GIS), arresters, potential transformers (PT), current transformers (CT), etc. It should be noted, that PTs and CTs are treated as the power equipment, not the measurement devices modeled in the CIM.

6.4.3.2. Measurement Package

There are several types of power equipment test and measurement, including acceptance tests, routing maintenance tests, diagnostic tests, etc. The equipment testing involves checking the insulation system, electrical properties, and other factors as they relate to the overall operation of the power system. Therefore, the parameters measured differ from equipment to equipment and may include electrical, mechanical, chemical, thermal, etc., quantities. The Package Measurement should model all information associated with equipment test and measurement.

As shown in Fig.6.7, Package Measurement consists of several entities to describe the measurement results, measurement techniques and instruments used.

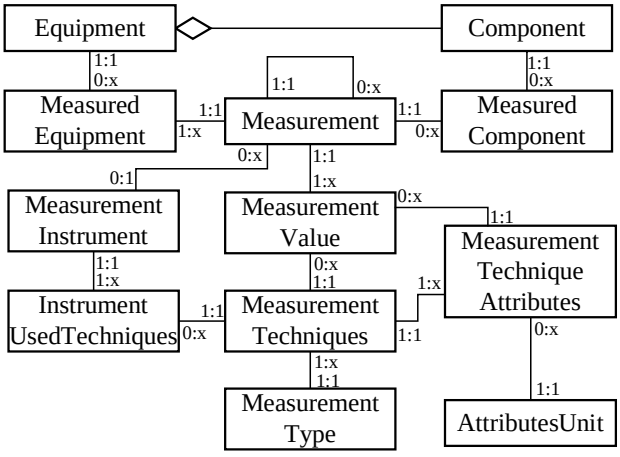

Fig.6.7. The measurement model

Entity Measurement represents the information about measurement time, reason, and interval. It plays as an index to search the particular test results and other information. Unlike modeling in the CIM, both equipment itself and measured components should be clarified for diagnosis and maintenance. The Entity Measurement has a recursive association to describe the relationship between measurement events.

Entity MeasurementType models all kinds of applied measurement types. According to IEEE Standard 62-1995, there are more than 50 diagnostic test items just for a power transformer and its components [Guid95]. For example, measurement of transformer oil includes water content, dissolved gas, dielectric strength, particle count, dielectric loss, power factor, interfacial tension, acidity, etc. Each test item may apply one or several techniques, which are modeled in the Entity MeasurementTechniques. The information about measurement techniques and types is important for failure analysis and result exchange.

Each measurement technique may result in one or several output parameters, which are modeled in the Entity Measurement-TechniqueAttributes. For example, measurement of dissolved gases in the transformer oil may produce several attributes, including H_2, CH_4, C_2H_6, C_2H_4, C_2H_2, etc. Entity AttributeUnit contains all units for the attributes, such as Amp, Volt, ppm, etc.

Depending on the measurement instrument and measurement techniques applied, a particular measurement may produce a number of results, which are contained in the Entity measurementValue, and are clarified by the measurement techniques and the specific attributes.

6.4.3.3. Diagnosis Package

All information about failure analysis and diagnostic tools is modeled in the diagnosis package as shown in Fig.6.8. Entity Diagnosis contains the information about a specific diagnosis event and involved measurement activities. The diagnosis results are described in the Entity DiagnosisReport, such as fault severity, fault location, fault types, and maintenance recommendations, depending on the diagnostic tool applied.

Recently a number of diagnostic applications are developed using artificial intelligence (AI) techniques, including artificial neural network, expert system, fuzzy logic, genetic algorithm, etc. They apply various measurement types for different equipment. Most of them

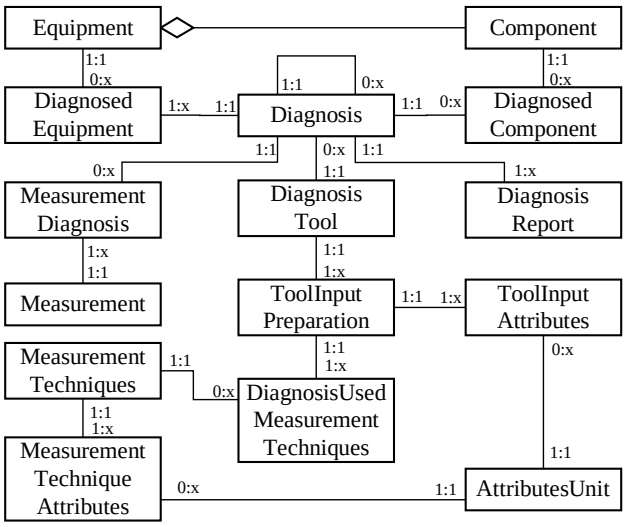

Fig.6.8. The diagnosis model

are lack of standard interfaces and difficult to share with the third party. This makes evaluation of the tools and exchange of the diagnostic results impossible.

This diagnosis package provides a mechanism to share the diagnostic tools and the results. The component concept that is popular in the software engineering is applied to model the diagnostic tool [CCAPI99]. A diagnostic tool plays like a black box, and just the following information is described in the model:

Source: Where the tool comes from and how to get it.

Features: The tool performance and purpose.

Input information: The involved measurement techniques and their attributes. When a tool is applied to diagnose the equipment or components, a set of measurement data may be used as the input information, which is defined in the Entity ToolInputPreparation and ToolInputAttributes. For example, a diagnostic tool implemented with the neural network and expert system requires measurement data originated from several types of tests, including partial discharge, dissolved-in-oil gas, water content, etc., used for power transformer diagnosis [Wang98]. Therefore, the relationship between the diagnosis tool and measurement techniques has to be defined.

The diagnosis model provides a open platform, any diagnostic tools and diagnosis reports can be easily stored in a relational database, and accessed or shared by other users or applications.

6.4.3.4. Failure Case Package

The information collection and reporting of equipment failure is important in equipment reliability analysis for users, manufacturers, or any maintenance organizations. For example, the data collection and reporting system for the transformer failure has been standardized in [Guid88]. Fig.6.9 shows the detailed failure case model, which is a class diagram representation of the Form 2 in [Guid88]. The model can also exactly describe other equipment failure case.

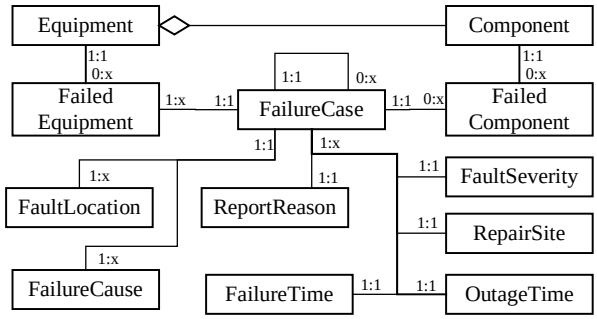

Fig.6.9. The failure case model

6.4.3.5. Documentation and Keywords

Equipment diagnosis and maintenance are usually conducted by various standards and historical experience. Modeling of such kinds of information is necessary to promote access and exchange of existing maintenance experience.

As shown in Fig.6.10, Entity Keywords defines the glossary of terms used in power equipment diagnosis and maintenance, which can be categorized into several types, including equipment, measurement, catalogue of defects and faults, etc. It is used to index other entities, such as documentation, measurement techniques, person skills, failure case, etc. Currently CIGRE Working Group 12.18 is working on systematizing a vocabulary, providing all keywords used to power transformer diagnosis and maintenance [Guui01].

Entity Document models the document features, such as title, author, and abstract. Entity DocumentCategory represents the document source, such as standards, white papers, instrument manus, or textbooks, etc. Entity DocumentType represents the document purpose, such as measurement, diagnosis, maintenance, equipment design, etc. Entity DocumentFormat describes the document formats, including text, pictures, movies, etc. Various documents can be clearly modeled using this package.

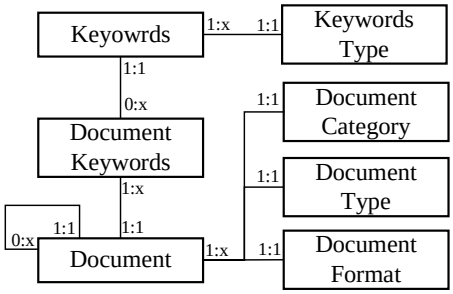

Fig.6.10. The documentation and keywords package

6.4.4. Advantages of the Information Model

The information model enables constructing the VH based on the Internet. It can satisfy the information storage, access, and exchange in the power equipment maintenance community. It can be a complement of the CIM and CMMS. When implementing a relational database using the information model for equipment diagnosis and maintenance in a utility or the VH, some information can be obtained from the CIM and CMMS through the views, such as equipment, person, and measurement.

Equipment diagnosis and maintenance information is often exchanged and shared between different utilities and service providers, even different countries, with the purpose of enriching the knowledge and experience of equipment diagnosis and maintenance. Similar to the CIM-XML, the information model can be represented in the XML RDF data model for convenient data exchange. For example, a type of power transformers produced by a specific manufacturer may be installed in several countries with different operation conditions and environments, all users and the manufacturer will benefit from sharing of the maintenance experience and failure analysis to update the equipment design and maintenance strategy.

6.5 Internet Based Fault Diagnostic Tool for Power Transformer

As an example of software tools available for transformer fault diagnosis in the VH, an Internet based interactive fault diagnostic tool is developed to remotely diagnose transformer faults. The embedded kernel in the tool is the Combined Artificial Neural Network and

Expert System tool (ANNEPS), developed at Virginia Tech for transformer fault diagnosis based on the dissolved gas-in-oil analysis (DGA) [Wang98 and Wang00]. Before the implementation of the Internet based tool is discussed, ANNEPS software is overviewed below.

6.5.1. ANNEPS Overview

DGA is a successful practice in transformer incipient fault diagnosis, which uses dissolved gas-in-oil concentrations and gassing rates to estimate the condition of a transformer. ANNEPS takes advantage of the self-learning and highly nonlinear mapping capability of ANN and the explicitly represented EPS rules in interpretation of DGA data. ANN could also acquire new experiences through incremental training from newly obtained data samples. The knowledge base of the expert system integrates IEEE and IEC guidelines and additional human expertise to ensure the available knowledge is used when insufficient data is available for the ANN training. An optimization mechanism is used to combine the output of the ANN and the expert system. When EPS detects a fault with high confidence and experience has shown that it usually does better than ANN for this type of fault, the mechanism ensures that the combined output of the ANNEPS gains more weight from the EPS; otherwise the combined output reflects the compromise of the two. The final diagnostic results are accompanied with maintenance action recommendations.

ANNEPS flowchart is shown in Fig.6.11. It consists of the following function modules:

- ANN-based normal/abnormal classifier, used to screen out abnormal cases for further diagnosis.
- Knowledge-based normal/abnormal classifier, used to screen out abnormal cases.
- ANN-based individual fault detector, used to detect each fault individually.
- Knowledge-based individual fault detector, used to detect each fault type individually.
- Combined fault diagnosis, used to integrate outputs of ANN- and EPS-based individual fault detectors.

- Maintenance action recommendation, used to estimate oil resample intervals and maintenance actions.

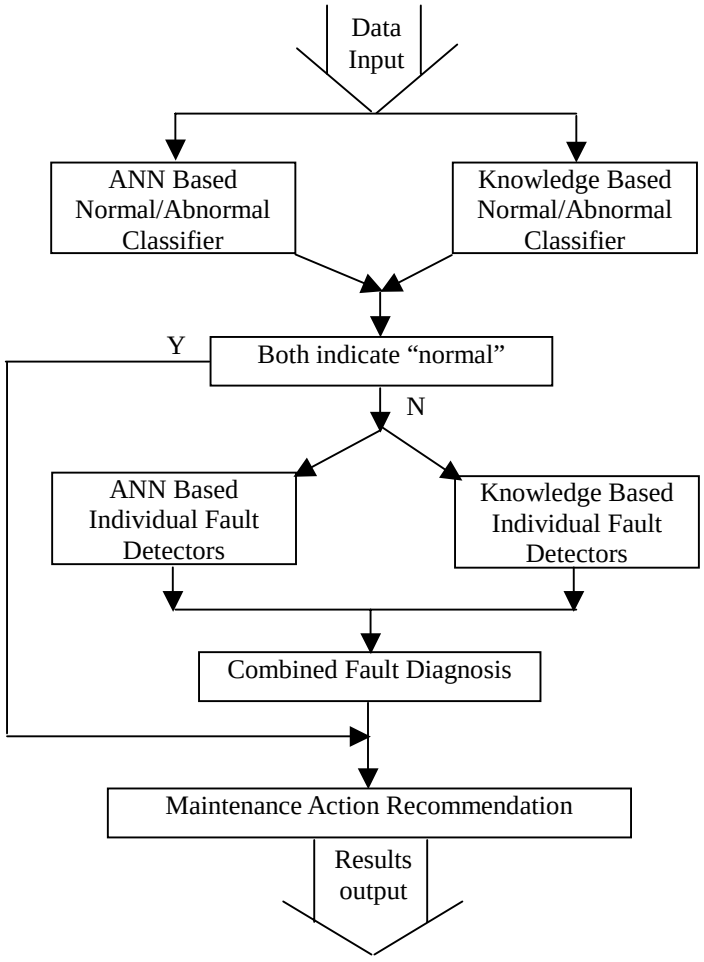

Fig. 6.11. ANNEPS flowchart

Input data includes all information related to transformer oil samples. Diagnosis outputs include diagnosed fault type, diagnosis confidence, oil resample interval, and maintenance action recommendations. The fault types are classified into the following categories:

- Normal (NR)
- Overheating of oil or cellulose (OH)
- Overheating of oil (OHO)

- Low energy discharge (LED)
- High energy discharge or arcing (HEDA)
- Cellulose degradation (CD)

Temperature range t of OH and OHO are further divided into four regions: $t < T1$, $T1 < t < T2$, $T2 < t < T3$, $t > T3$. Diagnosis confidence is represented by a real value in the range of [0,1]. Oil resample interval estimation is determined from both IEEE C57.104 and the key gas DGA method. The result is modified according to transformer size, voltage level, how critically the transformer is located, and other factors. Final recommendations are closely reflected in the oil resample interval output.

6.5.2. Implementation of Internet Based Diagnosis Tool

6.5.2.1. Diagnosis Procedure

As shown in Fig.6.12, the diagnostic tool uses Client/Server architecture. Client/Server describes the relationship between two computer programs in which one program, the client, makes a service request from another program, the server, which fulfills the request. The client/Server model provides a convenient way to interconnect programs that are distributed efficiently across different locations. Relative to the Internet, the Web browser is a client program that requests services (sending of Web pages or files) from a Web server or submits a HTML form to the server in another computer connected somewhere on the Internet. Transformer diagnosis is fulfilled according to the following procedures below:

1). The user anywhere in the world submits the transformer information and test data to the server at Virginia Tech via an HTML form.

2). The server parses the HTML form and returns a table including all input information to the user for confirmation.

3). The user checks and corrects the input information of the transformer, then sends the table back to the server.

4). The server prepares the input data file required by the diagnostic module, ANNEPS, according to the input information, then invokes ANNEPS execution module.

5). ANNEPS reads the input data file and diagnoses the transformer, then writes diagnostic results into an output file.

6). The server stores all transformer information into an ACCESS database, and sends the user a Web page to show the diagnostic results. The user can also download the result for further analysis.

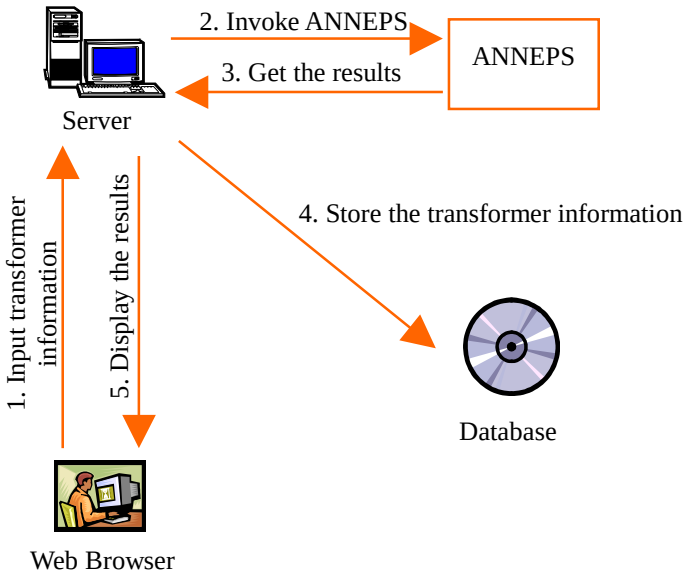

Fig.6.12. Flowchart of the Internet based fault diagnosis tool

Microsoft Active Server Pages (ASP) is used to realize the functions on Internet. ASP is a server-side scripting environment that can be used to create and run dynamic, interactive, high-performance Web server applications. An Active Server Page itself is simply a text file script with the extension **.**asp containing HTML, client and server side script in JavaScript, JScript or VBscript. The implementation behind the ASP page was intended as an open technology server-side framework, giving web developers the freedom to develop dynamic web sites using information accessed from the many COM-compliant data sources available to them [ASPHelp]. Details of this Internet based tool are introduced below.

6.5.2.2. Client Side

Users from anywhere in the world can access the transformer diagnostic tool via JavaScript enabled Web browser, either Internet Explorer or Netscape. What users will do is just inputting the transformer information in an HTML form and obtaining the results from the browser. The following transformer information is needed for diagnosis.

- Transformer general specifications

"Manufacturer", "Serial number", "Capacity", "Rated voltage", "Average load level", "Oil volume", "Oil preservation system", "Age", "Load tap changer (LTC) location", etc., used for results validation.

- Oil sample information

"Date sampled", used to set up gassing trend for historical comparison; "Oil sample identification number", used for index and documentation.

- Gas-in-oil concentrations and other test data

The gases in oil include CO_2, CO, H_2, CH_4, C_2H_6, C_2H_4, and C_2H_2. They are the key input parameters for diagnosis. Other parameters, such top oil temperature, power factor of oil, 2-furfural, acid number, interfacial tension, dissolved water, O_2, N_2, polarization degree, and partial discharge, are important to evaluate the transformer condition by ANNEPS. Users can input at most two sets of data sampled for trend analysis.

A JavaScript coded subroutine is executed by the user's browser to check and validate the input data before the data is submitted to the server. Gas-in-oil concentration data are limited to 0~100000 ppm.

6.5.2.3. Server Side

The Web server at Virginia Tech is Windows NT Server 4.0 with Microsoft Internet Information Server (IIS 4.0). A JScript subroutine will parse the HTML form from the client and generate the input data file for ANNEPS at the Web sever, and then another VBscript programmatic code is used to invoke the ANNEPS module to diagnose the transformer. Here

a special component, AspExec, is used to invoke the EXE module in ASP environment. AspExec component is developed by ServerObjects which allows ASP to execute DOS and Windows apps. The detailed code is shown below.

```
<%
…
‘Create the executor object.
Set Executor = Server.CreateObject("ASPExec.Execute")

‘Invoke ANNEPS module.
Executor.Application = "XXX\XXX.exe"

‘Set execution timeout.
Executor.TimeOut = 9000

‘Check if execution completed.
intResult = Executor.ExecuteWinAppAndWait
if intResult = 0 then
 …
%>
```

Here Object Executor is created to execute the ANNEPS module, and then check if the diagnosis completed. The diagnostic results are written into an output file by the ANNEPS module. All transformer information, data samples, and user information are saved into an Access database for retrieval and further analysis.

6.5.2.4. Result Display

The diagnostic results are returned and displayed in the client web browser. Diagnostic results include diagnosed fault type, diagnosis confidence, retest interval and maintenance action recommendations.

6.5.3. Discussion

This Internet based tool is the first DGA based diagnostic tool via the Internet for power equipment, and can be accessed at http://www.powerit.vt.edu/. The tool has been successfully used over 450 times over 12 months of international availability, and many users adopted this site for their routine diagnostic work. This clearly shows the feasibility of such diagnostic

tools, now what is needed in development of the VH, is to collect such tools to form a comprehensive diagnosis and maintenance tool for major power equipment.

6.6. Summary

Maximizing the share and exchange of diagnosis and maintenance information as well as techniques is critical for efficient and cost effective development of new techniques, modifying and updating the existing diagnostic techniques and maintenance strategies. The Virtual Hospital (VH) for Power Equipment discussed here meets such a need. The structure, contents, and operation of the VH are introduced in this chapter.

As a key part of the VH, a uniform information model is developed for data organization, access, sharing, and archiving related to equipment diagnosis and maintenance. The modeled information includes equipment and its components, measurement data, failure cases, and documentation. The sub-models are discussed in detailed. The developed information model can be a complement to the CIM and CMMS, and satisfy the information storage and exchange in the power equipment maintenance community.

As an example of diagnostic tools in the VH, an Internet based interactive fault diagnostic tool is developed for power transformers. The embedded kernel of the tool is the artificial neural network and expert system diagnosis tool based on the dissolved gas analysis information. From anywhere in the world one can access the diagnosis tool via Internet for their transformer diagnosis.

The VH caters to the deregulation of the power industry, and is instrumental in reconstruction of utility maintenance management and improving maintenance quality with a global approach. In fact, the VH is more than a digital library of existing diagnostic techniques; it is an Internet based dynamic information center. Many new ideas about diagnostic and maintenance techniques could be inspired while developing the VH. Continuous updating and expanding of the VH is necessary and could be later taken over by a number of organizations and private sectors.

CHAPTER 7
CONCLUSIONS

7.1. Conclusions

Two kinds of specific transformer failure or abnormality cases were systematically studied in the work of this dissertation, including extensive analysis of GSU (Generator-step-up) transformer failures in a pumped storage plant, and study of GIC (Geomagnetically induced current) effects on power transformers. Then, a new Internet based Virtual Hospital (VH) for power equipment is conceptually developed to help power equipment diagnosis and maintenance. The following conclusions highlight the results.

7.1.1. Analysis of GSU Transformer Failures in a Pumped Storage Plant

- The historical GSU transformer failures were extensively analyzed, and effects of abnormal electrical phenomena on the transformers were discussed. Some suggestions were given for the troubleshooting of the GSU transformer failures in the pumped storage plant.

- Special operation features in the pumped storage plant under study were analyzed, and three kinds of abnormal electrical phenomena associated with GSU transformers were studied, including switching transients and VFT (Very fast transients) in the GIS, lightning overvoltage, and harmonics and commutation spikes due to SFC (Static frequency converter) operation.

- Study of VFT in the GIS showed, frequent VFT is expected to occur when the back-to-back starting method is used to start units, since disconnecting the floating starting bus is often done by the DS. The conclusions included:

    1). The longer the floating bus is, the more charges remain on the bus, and the maximum overvoltage and maximum voltage change seen at GSU transformer

terminals are larger. The maximum VFT peak value can be up to 1.42 pu, which usually is not large and may not be the direct cause of transformer main insulation.

2). Due to high maximum rate of rise of the VFT and the maximum voltage change of up to 204 kV, some VFTs may overstress the insulation between transformer HV winding turns.

3). The following cases will generate higher VFT and requires more attention, Unit 4 and Unit 5 started by U1, and Unit 3 started by Unit 6. The VFT generated due to DS restrikes may contribute to the Tr.#4 failure.

- Though CB restrikes occur only occasionally, they do overstress the transformer insulation due to frequent CB switching in this plant. Particularly, the exposure of the driving units, Unit 1 or Unit 6, to CB restrikes is more than twice or three times the other units. This could be a major cause of Tr.#1 successive failures.

- Frequency scan of the detailed transformer HV winding model showed that several natural frequencies of the winding are near 80 kHz, which is very close to the cable natural frequency. It was possible that switching transients and VFT can excite the partial winding resonance in the transformer HV winding.

- Simulation showed that current chopping due to SF6 CB opening results in very small overovoltges in the studied cases, and should have little effects on the transformer operation.

- Simulation of the direct lightning stroke showed that the current arrester configuration does not provide enough protection to the GSU transformers, making transformer insulation vulnerable to lightning surges. This can be a possible cause of Tr.#1 HV winding insulation failure.

- In order to lower the lightning overvoltages at the GSU transformer terminals, an approach without installation of new arresters was proposed. Simulation showed that, if more

transformers were connected to the GIS, much smaller overvoltages would appear at each transformer terminals for a given magnitude of the injected lightning current due to the lower equivalent surge impedance of the cable. The study indicated that when the stormy weather is coming, in order to reduce lightning overvoltages at transformer terminals, an effective alternative is to run more units.

- Thanks to Sebastian Rosado's work [Rosa01], simulation showed that SFC operation has little effects on the GSU transformer operation, either harmonics or commutation spikes.

7.1.2. Analysis of GIC Effects on Power Transformers

- To estimate harmonic currents and MVar with only the given GIC and the nameplate information of the transformer for large-scale network models of sun storm impacts, a simplified method based on the equivalent magnetizing curve for transformers with different core design was developed and validated using test results.

- The effect of GIC on transformers with different core design was analyzed based on the simplified method. The relationship between the harmonics, the MVar consumption and GIC were illustrated. Simulation showed that the fundamental component of the exciting current and the reactive power are linear with GIC, making the evaluation of the MVar consumption directly with the given GIC possible.

- Study showed, partial harmonic distortion, *PHD* can be applied as a good indicator to show when the transformer begins saturating with the input GIC. The effect of the transformer parameters, such as the voltage, frequency, the exciting current, and MVA, on the GIC induced saturation was also discussed.

7.1.3. Study of the Virtual Hospital for Power Equipment

- In order to maximize the share and exchange of diagnosis and maintenance information, modify and update the existing diagnostic techniques and maintenance strategies, a new

Internet based Virtual Hospital (VH) for Power Equipment was conceptually developed. The structure, contents, and operation of the VH were discussed in details.

- As a key part of the VH, a comprehensive information model was developed for data organization, access, sharing, and archiving related to equipment diagnosis and maintenance. The developed information model can be a complement to the CIM and CMMS, and satisfy the information storage and exchange in the power equipment maintenance community.

- As an example of diagnostic tools in the VH, an Internet based interactive fault diagnostic tool was developed for power transformers. The embedded kernel of the tool is the artificial neural network and expert system diagnosis tool based on dissolved gas analysis (DGA).

7.2. Contributions

The major contributions are summarized below:

- A practical case of GSU transformer failures in the pumped storage plant was extensively studied. Abnormal electrical phenomena associated with GSU transformers, including switching transients and VFT, and lightning were modeled and simulated. Suggestions were given for troubleshooting of the GSU transformer failures. Mitigation of abnormal electrical phenomena effects on GSU transformers was proposed and studied. This can be a complete reference of troubleshooting of other similar transformer failures.

- A simplified method based on the equivalent magnetizing curve for transformers with different core design was developed and validated to estimate harmonic currents and MVar drawn by power transformers with a given GIC. A simple equation is derived to evaluate the MVar consumption with the fundamental component of the exciting current.

- An effective indicator was proposed using partial harmonic distortion, *PHD*, to show when the transformer begins saturating with the input GIC.

- The developed simplified method has been applied to a real time GIC monitoring system in the United Kingdom last year for a large power network with thousands of transformers [Erin01a and Erin01b].

- A new Internet based Virtual Hospital (VH) for Power Equipment was conceptually developed to share experience of power equipment diagnosis and maintenance, and update the existing diagnostic techniques and maintenance strategies.

- A comprehensive information model was developed for data organization, access, sharing, and archiving related to equipment diagnosis and maintenance.

- An Internet based interactive fault diagnostic tool was developed for power transformers based on dissolved gas analysis. From anywhere in the world one can access the diagnosis tool via Internet for their transformer diagnosis.

7.3. Future work

Some suggestions are given below for the future VH development.

- Develop the VH operation strategies for information collection, integration, consolidation, and dissemination.

- Establish the global maintenance expert pool in the VH as a bridge for members worldwide to share knowledge and experiences.

- Develop several information centers of the VH, including education center, standard center, and typical case center.

RELATED PUBLICATIONS

[1] Xuzhu Dong, Rosado S, Yilu Liu, Nien-Chung Wang, Tzong-Yih Guo, "Investigation of effects on internal insulation of main transformers in Mingtan operation environment," Monthly Journal of Taipower's Engineering, vol.637, pp.87-115, Sept. 2001.

[2] Xuzhu Dong, Sebastian Rosado, Yilu Liu, Nien-Chung Wang, E-Leny Line, Tzong-Yih Guo, "Study of abnormal electrical phenomena effects on GSU transformers (Part 1 of 2: Effects of switching transients)," submitted to IEEE Transactions on Power Delivery, Aug. 2001.

[3] Xuzhu Dong, Sebastian Rosado, Yilu Liu, Nien-Chung Wang, E-Leny Line, Tzong-Yih Guo, "Study of abnormal electrical phenomena effects on GSU transformers (Part 2 of 2: Effects of SFC operation and lightning)," submitted to IEEE Transactions on Power Delivery, Aug. 2001.

[4] Xuzhu Dong, Sebastian Rosado, Yili Liu, Nien-Chung Wang, Tzong-Yih Guo, "Transients seen at GSU Transformer terminals Part I: Historical case review," 2001 IEEE Power Engineering Society Winter Meeting, Ohio, vol.1, pp.312-317, Jan. 2001.

[5] Xuzhu Dong, Yilu Liu, John G. Kappenman, "Comparative analysis of exciting current harmonics and reactive power consumption from GIC saturated transformers," 2001 IEEE Power Engineering Society Winter Meeting, Ohio, vol.1, pp. 318-322, Jan. 2001.

[6] Xuzhu Dong, Zhenyuan Wang, Yilu Liu, P.J. Griffin, "Internet based fault diagnosis for power transformer," 2000 IEEE Power Engineering Society Summer Meeting, Seattle, Washington, July 2000.

[7] Abdel-Rahman Khatib, Xuzhu Dong, Bin Qiu, Yilu Liu, "Thoughts on future Internet based power system information network architecture," 2000 IEEE Power Engineering Society Summer Meeting, Seattle, Washington, vol.1, pp.155 –160, July 2000.

[8] Xuzhu Dong, Zhenyuan Wang, Bin Qiu, Ling Chen, Yilu Liu, "Internet based virtual hospital architecture for power equipment," 2001 IEEE Power Engineering Society Winter Meeting, Ohio, vol.2, pp.841-846, Jan. 2001.

[9] Xuzhu Dong, Zhenyuan Wang, Bin Qiu, Ling Chen, Yilu Liu, Deheng Zhu, Kexiong Tan, Fuqi Li, Du Lin, "Virtual hospital for power equipment on Internet," Proceedings

of 5th International Conference on Advances in Power System Control, Operation and Management (APSCOM - 2000), IEE, Hong Kong, Part vol.2, pp.359-63, 2000.

[10] Xuzhu Dong, Zhenyuan Wang, Yilu Liu, Deheng Zhu, "Internet Applications in fault diagnosis and predictive maintenance of power equipment," Proceedings of The First International Conference on Insulation Condition Monitoring of Electrical Plant (ICMEP'2000), China, pp.243-253, Sep. 2000.

[11] Xuzhu Dong, Zhenyuan Wang, Kyu-Min Rho, Yilu Liu, "Equipment fault diagnosis and related research at Virginia Tech," Proceedings of IX Substation Equipment Diagnostics Conference, EPRI, New Orleans, Feb. 2001.

[12] Xuzhu Dong, Yilu Liu, Frank A. LoPinto, Kevin P. Scheibe, Steven D. Sheetz, "Information model for power equipment diagnosis and maintenance," accepted by 2002 IEEE Power Engineering Society Winter Meeting.

VITA

Dr. Xuzhu Dong was born in Shaanxi Province, China. He entered Tsinghua University, China in 1988, spent nine half years and obtained his B.S., M.S., and Ph.D. degrees there in 1993, 1998, and 1998, respectively, all in High Voltage Engineering. He came to the United States in June 1998, first served as a research scientist, and then entered the Ph.D. program at the Department of Electrical Engineering, Virginia Tech, pursuing another doctoral degree.

Dr. Dong's research interests are electric power equipment condition monitoring and fault diagnosis, electrical transient analysis and lightning protection, power quality, and IT/Internet applications in power systems. He has authored or co-authored over 35 technical papers. He is a member of IEEE.

REFERENCES

[Harl00] J.W. Harley, V.V. Sokolov, "Diagnostic techniques for power transformers," EPRI Substation Equipment Diagnostics Conference IX, Feb. 2001.

[Alla91] D.J. Allan, "Power transformers – the second century," Power Engineering Journal, G0868, pp.5-14, Jan. 1991.

[Dong00] Xuzhu Dong, Zhenyuan Wang, Yilu Liu, P.J. Griffin, "Internet based fault diagnosis for power transformer," 2000 IEEE Power Engineering Society, Seattle, Washington, July 2000.

[Liu91] S.C. Liu, C.S. Hsieh, "The Mingtan pumped storage project in Taiwan," Water Power & Dam Construction, pp.9-15, Feb. 1991.

[Chia97] Jung-Chen Chiang, Chi-Jui Wu, Shih-Shong Yen, "Mitigation of harmonic disturbance at pumped storage power station with static frequency converter," IEEE Transactions on Energy Conversion, vol.12, no.3, pp.232-40, Sept. 1997.

[Kroo90] C. Kroon, "Large generator transformers," CIGRE, 12-208, 1990.

[PES98a] IEEE Power Engineering Society, Survey of Generator Step-up (GSU) Transformer Failures, IEEE, TP-132-0-101998, 1998.

[Kass96] S.D. Kassihin, S.D. Lizunov, G.R. Lipstein, A.K. Lokhanin, T.I. Morozova, "Service experience and reasons of bushing failures of EHV transformers and shunt reactors," CIGRE, 12-105, 1996.

[Flee94] J.A. Fleeman, J.H. Provanzana, J.M. Bednar, "AEP experience with repair and refurbishment of transformers and reactors," CIGRE, 12-204, 1994.

[Baty94] Yu.V. Batyayev, Yu.A. Dementyev, G.A. Dorf, V.M. Lavrentyev, I.L. Shleifman, "Analysis of the equipment damages and operation maintenance of classical-type EHV and UHV substations with an air insulation over 35-year operation," CIGRE, 23-105, 1994.

[Alla95] D.J. Allan, A. White, "Transformer design for high reliability," IEE Conference Publication, n406, pp.66-72, 1995.

[Lapw98] J. Lapworth, T. McGrail, "Transformer failure modes and planned replacement," IEE Colloquium Transformer Life Managemen, pp.9/1-7, 1998.

[Hend88] D.M.S. Henderson, W.A. Steele, J. Fyvie, E.F. Sharp, "Refurbishment of generator/motor units and main transformers at Cruachan Pumped Storage Power Station," International Conference on Refurbishment of Power Station Electrical Plant, IEE, pp.170-5, 1988.

[Saha99] T.K. Saha, M. Darveniza, Z.T. Yao, D.J.T. Hill, G. Yeung, "Investigating the effects of oxidation and thermal degradation on electrical and chemical properties of power transformers insulation," IEEE Transactions on Power Delivery, vol.14, no.4, pp.1359-67, Oct. 1999.

[Eber00] J.A. Ebert, "Power transformer operation at over and underexcitation, benefits and consequences," IEEE Transactions on Power Delivery, vol.15, no.1, pp.192-7, Jan. 2000.

[EPRI82] Electric Power Research Institute, 345 kV and Above Transmission Line Reference Book/Second Edition, 1982.

[Bick86] J.P. Bickford, A.G. Heaton, "Transients overvoltages on power systems," IEE Proceedings, vol.133, Pt. C, no.4, pp.201-225, May 1986.

[Gree91] Allan Greenwood. Electrical Transients in Power Systems, Second Edition, New York: Wiley, 1991, pp.116.

[Irav00] M.R. Iravani, A.K.S. Chaudhary, W.J. Giesbrecht, I.E. Hassan, A.J.F. Keri, K.C. Lee, J.A. Martinez, A.S. Morched, B.A. Mork, M. Parniani, A. Sharshar, D. Shirmohammadi, R.A. Walling, D.A. Woodford, "Modeling and analysis guidelines for slow transients. III. The study of ferroresonance," IEEE Transactions on Power Delivery, vol.15, no.1, pp.255-65, Jan. 2000.

[Past88] B.M. Pasternack, J.H. Provanzana, L.B. Wagenar, "Analysis of a generator step-up transformer failure following faulty synchronization," IEEE Transactions on Power Delivery, vol.3, no.3, pp.1051-8, July 1988.

[Sybi85] G. Sybille, M.M. Gavrilovic, J. Belanger, V.Q. Do, "Transformer saturation effects on EHV system overvoltages," IEEE Transactions on Power Apparatus & Systems, vol.PAS-104, no.3, pp.671-80, March 1985.

[Male88] R. Malewski, J. Douville, L. Lavallee, "Measurement of switching transients in 735 kV substations and assessment of their severity for transformer insulation," IEEE Transactions on Power Delivery, vol.3, no.4, pp.1380-90, Oct. 1988.

[Balt69] P.A. Baltensperger, P. Djurdjevic, "Damping of switching overvoltages in EHV networks-new economic aspects and solutions," IEEE Transactions on Power Apparatus & Systems, vol.pas-88, no.7, pp.1014-22, July 1969.

[Duba74] C. Dubanton, G. Gervais, "Switching overvoltages when closing unloaded lines. Effect of power and system configuration, statistical distribution," CIGRE, 33-05, 1974.

[Balt70] P. Baltensperger, E. Ruoss, "Switching overvoltages in EHV and UHV networks," CIGRE, 13-14, 1970.

[Gert78] R. Gert, J. Jirku, N.I. Lokhanina, V.S. Rashkes, "Phase-to-phase switching overvoltages in EHV systems," CIGRE, 33-03, 1978.

[Elki93] D.I. Elkins, A.C. Jain, T.E. McDermott, V. Rees, "Transients during 138-kV SF6 breaker switching of low inductive currents," IEEE Transactions on Industry Applications, vol.29, no.4, pp.721-7, July-Aug. 1993.

[Popo99] M. Popov, E. Acha, "Overvoltages due to switching off an unloaded transformer with a vacuum circuit breaker," IEEE Transactions on Power Delivery, vol.14, no.4, pp.1317-26, Oct. 1999.

[Kosm95] J. Kosmac, P. Zunko, "A statistical vacuum circuit breaker model for simulation of transient overvoltages," IEEE Transactions on Power Delivery, vol.10, no.1, pp.294-300, Jan. 1995.

[Mura77] M. Murano, S. Yanabu, H. Ohashi, H. Ishizuka, T. Okazaki, "Current chopping phenomena of medium voltage circuit breakers," IEEE Transactions on Power Apparatus & Systems, vol.PAS-96, no.1, pp.143-9, Jan.-Feb. 1977.

[Lee90] K.C. Lee, K.P. Poon, "Statistical switching overvoltage analysis of the first BC Hydro phase shifting transformer using the Electromagnetic Transients Program," IEEE Transactions on Power Systems, vol.5, no.4, pp.1054-60, Nov. 1990.

[Prei84] G. Preininger, "Resonance behaviour of high-voltage transformers," CIGRE, Proceedings of the 30th Session, pp.12.14/1-8, 1984.

[Nasr99] K. Nasrullah, "Voltage surge resonance on electric power network," 1999 IEEE Transmission and Distribution Conference. IEEE. Part vol.2, pp.687-90, 1999.

[Vaki95] M. Vakilian, R.C. Degeneff, M. Kupferschmid, "Computing the internal transient voltage response of a transformer with a nonlinear core using Gear's method. II. Verification," IEEE Transactions on Power Systems, vol.10, no.2, pp.702-8, May 1995.

[Pret84] R.E. Pretorius, P.V. Goosen, "Practical investigation into repeated failures of 400/220 kV autotransformers in the Escom network-results and solutions," International Conference on Large High Voltage Electric Systems. Proceedings of the 30th Session, CIGRE, pp.12.10/1-6, 1984.

[Sche84] A. Schei, K. Alstad, J.B. Sund, M. Rian, E. Nordrik, J. Hopperstad, "Resonant overvoltages in power station transformers initiated by switching transients in the connected cable network," CIGRE, Proceedings of the 30th Session, pp.12.7/1-8, 1984.

[Sabo88] A. Sabot, "Very fast transient phenomena associated with gas insulated substations," CIGRE, Proceedings of the 32nd Session, vol.2, pp.33-13/1-13, 1988.

[Mepe89] J. Mepelink, "Very fast transients in high-voltage GIS substations," Abb Review, no.5, pp.31-8, 1989.

[Fuji88] N. Fujimoto, F.Y. Chu, S.M. Harvey, G.L. Ford, S.A. Boggs, V.H. Tahiliani, M. Collod, "Developments in improved reliability for gas-insulated substations," Proceedings of the 32nd Session. International Conference on Large High Voltage Electric Systems, CIGRE, vol.1, pp.23-11/1-7, 1988.

[Okab91] S. Okabe, M. Kan, T. Kouno, "Analysis of surges measured at 550 kV substations," IEEE Transactions on Power Delivery, vol.6, no.4, pp.1462-8, Oct. 1991.

[Bogg84] S.A. Boggs, N. Fujimoto, M. Collod, E. Thuries, "The modeling of statistical operating parameters and the computation of operation-induced surge waveforms for GIS disconnectors," International Conference on Large High Voltage Electric Systems, Proceedings of the 30th Session, CIGRE, pp.13.15/1-7, 1984.

[Ogaw86] S. Ogawa, E. Haginomori, S. Nishiwaki, T. Yoshida, K. Terasaka, "Estimation of restriking transient overvoltage on disconnecting switch for GIS," IEEE Transactions on Power Delivery, vol.PWRD-1, no.2, pp.95-102, Apr. 1986.

[Lui94] C.Y. Lui, J. Hiley, "Computational study of very fast transients in GIS with special reference is effects of trapped charge and risetime on overvoltage amplitude," IEE Proceedings of Generation, Transmission & Distribution, vol.141, no.5, pp.485-90, Sept. 1994.

[Miri95] A.M. Miri, C. Binder, "Investigation of transient phenomena in inner- and outer systems of GIS due to disconnector operation," Proceedings of International Conference on Power Systems Transients, pp.71-6, 1995.

[Yana90] S. Yanabu, H. Murase, H. Aoyagi, H. Okubo, Y. Kawaguchi, "Estimation of fast transient overvoltage in gas-insulated substation," IEEE Transactions on Power Delivery, vol.5, no.4, pp.1875-82, Oct. 1990.

[Shib99] Y. Shibuya, S. Fujita, T. Shimomura, "Effects of very fast transient overvoltages on transformer," IEE Proceedings of Generation, Transmission & Distribution, vol.146, no.5, pp.459-64, Sept. 1999.

[Kres93] K. Kress, D. Konig, W. Muller, "Travelling waves as causes of internal resonance phenomena in coils and windings," CIGRE Proceedings of the 34th Session, CIGRE, vol.1, pp.12-303/1-7, 1993.

[Corn93] K. Cornick, B. Filliat, C. Kieny, W. Muller, "Distribution of very fast transient overvoltages in transformer windings," CIGRE Proceedings of the 34th Session, CIGRE, vol.1, pp.12-204/1-6, 1993.

[Gock98] E. Gockenbach, M. Aro, F. Chagas, K. Feser, J. Kuffel, R. Malewski, T. McComb, P. Munoz Rojas, G. Rizzi, "Measurements of very fast front transients," Electra, no.181, pp.70-91, Dec. 1998.

[Henr98] E.E. Henriksen, "Study of very fast transients overvoltages in transformers," Electra, no.179, pp.12-23, Aug. 1998.

[Mart96] H.J.A., Martins, A. Neves, I.B. Amorim, F. Maranhao, "The effect of fast transient overvoltages on 550 kV SF/sub 6//oil transformer bushings," Conference Record of the 1996 IEEE International Symposium on Electrical Insulation, IEEE. Part vol.2, pp.774-7, 1996.

[Mart91] H.J.A. Martins, V.R. Fernandes, R.S. Jacobsen, "Gas-insulated substation performance in Brazilian system," Gaseous Dielectrics VI. Plenum, pp.443-8, 1991.

[Dire82] A.J. Direne, M.P. Leme, P.C. Neves, "Failures in 500-kV and 138-kV bushings connected to gas-insulated switchgear," Doble Engineering Company, Sec. 4-301/4-301B, 1982.

[Dire84] A.J. Direne, M.P. Leme, A.L. Sica, W.J. Franca, "Investigation of the effects of switching transients generated in gas-insulated switchgear to 500-kV bushings and power transformers," Doble Engineering Company, Sec. 4-501/4-523, 1984.

[Naka97] K. Nakanishi, S. Fujita, H. Kurita, A. Kishi, T. Hasegawa, Y. Shibuya, "High frequency voltage oscillation in transformer windings and electrical breakdowns

properties of interturn insulation immersed in oil at VFT voltage," IEEE 1997 Annual Report. Conference on Electrical Insulation and Dielectric Phenomena, IEEE. Part vol.2, pp.490-3, 1997.

[Fuji98] S. Fujita, N. Hosokawa, Y. Shibuya, "Experimental investigation of high frequency voltage oscillation in transformer windings," IEEE Transactions on Power Delivery, vol.13, no.4, pp.1201-7, Oct. 1998.

[Mull83] W. Muller, W. Stein, "Behaviour of high voltage transformer windings on steep fronted input waves of nanosecond duration," Siemens Power Engineering, vol.5, no.5, pp.259-62, Sept.-Oct. 1983.

[Chow96] Pritindra Chowdhuri, Electromagnetic Transients in Power Systems, New York: Wiley, 1996.

[IEEEw93] IEEE working group report, "Estimating lightning performance of transmission lines. II. Updates to analytical models," IEEE Transactions on Power Delivery, vol.8, no.3, pp.1254-67, July 1993.

[Elah90] H. Elahi, M. Sublich, M.E. Anderson, B.D. Nelson, "Lightning overvoltage protection of the Paddock 362-145 kV gas-insulated substation," IEEE Transactions on Power Delivery, vol.5, no.1, pp.144-50, Jan. 1990.

[Wech88] K.H. Weck, "Special report for Group 33," Proceedings of the 32nd Session, International Conference on Large High Voltage Electric Systems, CIGRE, vol.2, pp.33.00/1-5, 1988.

[Lani98] C. Lanier, "A novel technique for the determination of relative corona activity within inverter-duty motor insulation systems using steep-fronted voltage pulses," Conference Record of the 1998 IEEE International Symposium on Electrical Insulation, IEEE, art vol.1, pp.229-36, 1998.

[Tana99] Y. Tanaka, T. Ono, M. Sampei, T. Obata, S. Tanabe, E. Tsuchie, T. Muraoka, "Long-term test of the equipment for +or-500 kV DC converter station," 1999 IEEE Power Engineering Society Summer Meeting. Conference Proceedings, IEEE, Part vol.2, pp.1152-7, 1999.

[Work96] Joint Working Group 12/14.10, "HVDC converter transformers," CIGRE, 12-202, 1996.

[Rick86] D.E. Rick, "Adjustable peed drive and power rectifier harmonics – their effect on power systems components," IEEE Transactions on Industry applications, vol. IA-22, no.1, pp.161-177, Jan. 1986.

[Kell99] A.W. Kelley, S.W. Edwards, J.P. Rhode, M.E. Baran, "Transformer derating for harmonic currents: a wide-band measurement approach for energized transformers," IEEE Transactions on Industry Applications, vol.35, no.6, pp.1450-7, Nov.-Dec. 1999.

[Dela96] A.C. Delaiba, J.C. de Oliveira, A.L.A. Vilaca, J.R. Cardoso, "The effect of harmonics on power transformers loss of life," 38th Midwest Symposium on Circuits and Systems. Proceedings, IEEE, Part vol.2, pp.933-6, 1996.

[Bish96] M.T. Bishop, J.F. Baranowski, D. Heath, S.J. Benna, "Evaluating harmonic-induced transformer heating," IEEE Transactions on Power Delivery, vol.11, no.1, pp.305-11, Jan. 1996.

[Ram88] B.S. Ram, J.A.C. Forrest, G.W. Swift, "Effects of harmonics on converter transformer load losses," IEEE Transactions on Power Delivery, vol.3, no.3, pp.1059-66, July 1988.

[Kras87] M.F. Krasil'nikov, A.M. Krasil'nikov, "Start-up system for pumping operation of the reversible units at the Dinorwig pumped-storage station," Gidrotekhnicheskoe Stroitel'Stvo, vol.21, no.5, pp.53-5, May 1987.

[Osbu92] G.D. Osburn, P.L. Atwater, "Design and testing of a back-to-back starting system for pumped storage hydrogenerators at Mt. Elbert Powerplant," IEEE Transactions on Energy Conversion, vol.7, no.2, pp.280-8, June 1992.

[Alle91] J. Allegre, G. Merouge, "Generator/motors for pumped storage plants," GEC Alsthom Technical Review, no.5, pp.59-66, April 1991.

[Harl81] J.M. Harley, "Static frequency converter controlled a.c. drives – state of the art and applications," Brown-Bouveri review, pp.31-39, 1981.

[Pete72] T. Petersson, K. Frank, "Starting of large synchronous motor using static frequency converter," IEEE Transactions on Power Apparatus & Systems, vol.PAS-91, no.1, pp.172-9, Jan.-Feb. 1972.

[Gran88] J. Grandl, A. Eriksson, J. Meppelink, C.V.D. Merwe, "Studies of very fast transients (VFT) in a 765 kV substation," CIGRE, 33-12/1-6, 1988.

[Esme88] P.C.V. Esmeraldo, F.M. Salgado Carvalho, "Surge propagation analysis: an application to the Grajau 500 kV SF/sub 6/ gas-insulated substation," Proceedings of the 32nd Session. International Conference on Large High Voltage Electric Systems, CIGRE, vol.2, pp.33-01/1-6, 1988.

[Cars91] S. Carsimamovic, R. Mahmutcehajic, "Computation of very fast transients in 400 kV gas insulated substations caused by disconnector switching," 6th Mediterranean Electrotechnical Conference. Proceedings, IEEE, vol.2, pp.1416-20, 1991.

[Lewi88] J. Lewis, B.M. Pryor, C.J. Jones, T. Irwin, L.C. Campbell, A. Aked, "Disconnector operations in gas insulated substations. Overvoltage studies and tests associated with a 420 kV installation," Proceedings of the 32nd Session. International Conference on Large High Voltage Electric Systems, CIGRE, vol.2, pp.33.09/1-8, 1988.

[Vino99] V. Vinod Kumar, M.J. Thomas, M.S. Naidu, "VFTO computation in 420 kV GIS, Eleventh International Symposium on High Voltage Engineering," IEE, Part vol.1, pp.319-22, 1999.

[Boec87] W. Boeck, R. Witzmann, "Main influences on the fast transient development in gas-insulated substations (GIS)," Proceedings of the Fifth International Symposium on High Voltage Engineering, vol.1, pp.12.01/1-4, 1987.

[Povh96] D. Povh, H. Schmitt, O. Valcker, R. Wutzmann, "Modelling and analysis guidelines for very fast transients," IEEE Transactions on Power Delivery, vol.11, no.4, pp.2028-35, Oct. 1996.

[Froh99] K. Frohlich, A. Carvalho, B. Avent, J. Bachiller, A. Bosma, J. Brunke, M. de Grijp, V. Hermosillo, H. Ito, J. Martin, A. Mercier, J. Patel, N. Poupardin, F. Salgado Carvalho, H. Schmidt, G. Schoonenberg, K. Suzuki, M. Waldron, "Controlled switching of HVAC circuit breakers: Guide for application lines, reactors, capacitors, transformers. I," Electra, no.183, pp.42-73, April 1999.

[Carv99] K. Frohlich, A. Carvalho, B. Avent, J. Bachiller, A. Bosma, J. Brunke, M. de Grijp, V. Hermosillo, H. Ito, J. Martin, A. Mercier, J. Patel, N. Poupardin, F. Salgado Carvalho, H. Schmidt, G. Schoonenberg, K. Suzuki, M. Waldron, "Controlled switching of HVAC circuit breakers. Guide for application lines, reactors, capacitors, transformers," Electra, no.185, pp.36-57, Aug. 1999.

[Work98] Working group 13.01, "State of the art of circuit-breaker modeling," Electra, No.181, pp.155-159, 1998.

[Pail99] J. Paillol, A. Gibert, V. Sabate, F. Isssac, J.C. Alliot, J.C. Kedzia, "Circuit breaker modelling in the EMC field," Eleventh International Symposium on High Voltage Engineering, IEE, Part vol.1, pp.327-30, 1999.

[Amur88] T. Amura, Y. Ichihara, Y. Takagi, M. Fujii, Tsuzuki, "Pursuing reduced insulation coordination for GIS substation by application of high performance metal oxide surge arrester," Proceedings of the 32nd Session, International Conference on Large High Voltage Electric Systems, CIGRE, vol.2, pp.33.04/1-6, 1988.

[Clay83] R.E. Clayton, I.S. Grant, D.E. Hedman, D.D. Wilson, "Surge arrester protection and very fast surges," IEEE Transactions on Power Apparatus & Systems, vol.PAS-102, no.8, pp.2400-12, Aug. 1983.

[Kim96] I. Kim, T. Funabashi, H. Sasaki, T. Hagiwara, M. Kobayashi, "Study of ZnO arrester model for steep front wave," IEEE Transactions on Power Delivery, vol.11, no.2, pp.834-41, April 1996.

[Erik86] A.J. Eriksson, H.J. Geldenhuys, H. Kroninger, S.M. Hefer, W.C. van der Merwe, "A study of lightning stresses on metal oxide surge arresters," International Conference on Large High Voltage Electric Systems, CIGRE: Proceedings of the 31st Session, CIGRE, vol.2, pp.33.08/1-8, 1986.

[Jin93] He Jin-Liang, Wu Wei-Han, "Adopting line surge arresters to increase lightning-withstand levels of transmission-lines," 1993 IEEE Region 10 Conference on Computer, Communication, Control and Power Engineering, IEEE. Part vol.5, pp.450-3, 1993.

[Pinc99] P. Pinceti, M. Giannettoni, "A simplified model for zinc oxide surge arresters," IEEE Transactions on Power Delivery, vol.14, no.2, pp.393-8, Apr. 1999.

[Work92a] IEEE working group 3.4.11, "Modeling of metal oxide surge arresters," IEEE Transactions on Power Delivery, vol.7, no.1, pp.302-9, Jan. 1992.

[Ardi92] A. Ardito, R. Iorio, G. Santagostino, A. Porrino, "Accurate modeling of capacitively graded bushings for calculation of fast transient overvoltages in GIS," IEEE Transactions on Power Delivery, vol.7, no.3, pp.1316-27, July 1992.

[Mart98] J.A. Martinez-Velasco, "ATP modelling of power transformers," ATP-EEUG News, pp.63-76, Aug. 1998.

[Qure93] S.A. Qureshi, A. Al-Arashi, "Transformer model for VFTO studies in gas insulated substations," Proceedings of 28th Universities Power Engineering Conference, vol.2, pp.977-80, 1993.

[Papa94] B.C. Papadias, N.D. Hatziargyriou, J.A. Bakopoulos, J.M. Prousalidis, "Three phase transformer modelling for fast electromagnetic transient studies," IEEE Transactions on Power Delivery, vol.9, no.2, pp.1151-9, Apr. 1994.

[Mart93] L. Marti, "Simulation of electromagnetic transients in underground cables using the EMTP," 2nd International Conference on Advances in Power System Control, Operation and Management, IEE, vol.1, pp.147-52, 1993.

[Mart88] L. Marti, "Simulation of transients in underground cables with frequency-dependent modal transformation matrices," IEEE Transactions on Power Delivery, vol.3, no.3, pp.1099-110, July 1988.

[Mere97] R.J. Meredith, "EMTP modeling of electromagnetic transients in multi-mode coaxial cables by finite sections," IEEE Transactions on Power Delivery, vol.12, no.1, pp.489-96, Jan. 1997.

[Alfu94] A. Al-Furaih, "Evaluation and testing of turn insulation of large AC motors," IEEE Industrial and Commercial Power Systems Technical Conference, pp.139-141, 1994.

[Rosa01] Sebastian P. Rosado, "Analysis of electric disturbances from the static frequency converter of a pumped storage station," Thesis, Virginia Polytechnic Institute and State University, 2001.

[Albe89] Vernon D. Albertson, "Geomagnetic disturbance causes and power system effects," 1989 IEEE Power Engineering Society Summer Meeting, pp.3-9, July 1989.

[Lesh93] R.L. Lesher, C.L. Wagner, W.E. Feero, "SUNBURST GIC Network," EPRI Report, RP-3211-01, Nov. 1993.

[Lush91] Shu Lu, Yilu Liu, "A fundamental analysis of transformer GIC magnetization using the finite elements approach," Proceedings of the American Power Conference, pp.1173-1178, April 1991.

[Wall91] R.A. Walling, A.H.Khan, "Characteristics of transformer exciting-current during geomagnetic disturbances," IEEE Transaction on Power Delivery, vol. 6, no. 4, pp.1707-1714, 1991.

[Xuw93] W. Xu, T.G. Martinich, J.H. Sawada, Y. Mansour, "Harmonics from SVC transformer saturation with direct current offset," 1993 IEEE Power Engineering Society Summer Meeting, 404-4 PWRD, pp.1-7, 1993.

[Bote89] D.H. Boteler, R.M. Shier, T. Watanabe, R.E. Horita, "Effcts of geomagnetically induced currents in the B.C. hydro 500 kV system," IEEE Transaction on Power Delivery, vol. 4, no. 1, pp.818-823, 1989.

[Kapp89] John G. Kappenman, "Transformer DC excitation field test & results," IEEE Power Engineering Society Summer Meeting, pp.14-22, July 1989.

[Elect85] General Electric Company, "High-voltage direct-current converter transformer magnetics," EPRI EL-4340, Dec. 1985.

[Albe93] V. D. Albertson, B Bozoki, WE Feero, John G. Kappenman, EV Larsen, DE Nordell, J Ponder, FS Prabhakara, K Thompson, R Walling, "Geomagnetic disturbance effects on power systems," IEEE Transaction on Power Delivery, vol.8, no.3, pp. 1206-1216, 1993.

[Albe81] V. D. Albertson, John G. Kappenman, N Mohan, GA Skarbakka, "Load flow studies in the presence of geomagnetically induced currents," IEEE Transaction on Power Apparatus and Systems, vol. PAS-100, no.2, pp.594-607, 1981.

[Albe92] V.D. Albertson, "Modeling and analysis of GIC, EPRI: TR-100450," Proceedings of Geomagnetically induced currents conference, pp.12-1-12-12, Jun. 1992.

[Cizh79] Feng Cizhang, Electromagnetic field, Educational Press, China, 1979, pp.115.

[Worke00] Working group 23.01, "questionnaire concerning aspects on planning, design, operation and maintenance of the future substation," Electra, pp 77-84, Aug. 2000.

[Oppe99] Laurie J. Oppel, Dennis Aronson, "Information Technology, Its increased importance in the power industry after deregulation," 1999 IEEE Power Engineering Society Summer Meeting, vol.2, pp 1196-9, 1999.

[Wray97] Ian Wray, "Surviving in the competitive power generation industry," Plant Services on the WEB, Oct. 1997.

[Senb00] Kanda S, Senba K, Nanakaya Y, Ikeda H, Kawai T, "Database management system for proactive maintenance (case study of steam turbine plant and switch-house equipment in Japan)," 2000 IEEE Power Engineering Society Winter Meeting, vol.1, pp 464 –469, 2000.

[Hayn96] Leonard Haynes, Renato Levy, Chujen Lin, Praveen Prasad, "Test and Maintenance information management standard," Conference Record on Test Technology and Commercialization, pp 390 –399, 1996.

[Levi99] Joel Levitt, "Maintenance and the Internet, Maintennace Technology,"

http://www.mt-online.com/current/01-99mis.html

[Gold00] Mark Goldstein, "Internet's Shake-Out with CMMS May Just Happen,"

http://www. facilitiesnet.com/NS/NS3a7ad.html

[Smit94] Smith T, Smith WL, "The North Carolina information highway," IEEE Network, vol.8, pp 12 –17, Nov.-Dec. 1994.

[Pipe00] James Piper, "A new spin on facility management,"

http://www.facilitiesnet. com/fn/NS/NS3b9gc.html

[Grai00] Grainger WW, "Trends and Issues in MRO Supply Purchasing and Management," http://www.plant-maintenance.com/maintenance_articles_ebiz.shtml

[StraMa] Maintenance Strategies Inc, "CStat on-line monitoring systems for substation equipment," http://msicorp.com/products.cfm

[TeleGl] Global Telemetry Systems remote monitoring service, http://www.onthelevel.com

[EnerCo] Cooper Energy Services, "Remote condition monitoring service (RCMS)," http://www. cooperenergy.com/

[ForLib] D-Lib Forum, http://www.dlib.org/

[ArmsWi] William Y. Arms, "Key Concepts in the Architecture of the Digital Library," http://www.dlib.org/dlib/July95/07arms.html

[LynCl] Clifford Lynch, "Interoperability, Scaling, and the Digital Libraries Research Agenda," http://www-diglib.stanford.edu/diglib/pub/reports/iita-dlw/main.html

[Mcmi99] Gail Mcmillan, "Digital library support distributed education or put the library in digital library," the 9th National Conference of the Association of College and Research Libraries, Apr. 1999.

[Phoh96] Shashi Phoha, "Using the national information infrastructure (NII) for monitoring, diagnostics and prognostics of operation machinery," Proceedings of the 35th conference on Decision and Control, pp.2583~2587, Dec. 1996.

[Prou99] Douglas Proudfoot, Dave Taylor, "How to turn a substation into a database server," IEEE Computer Applications in Power, pp.29-35, Apr. 1999.

[GESA] GE Industrial systems, "GESA: Substation Automation, " http://www.ge.com/industrialsystems/pm/brochure/gesa/index.htm

[Yasu98] Nemoto Yasunori, "Plant supervision and control network," Mitsubishi Electric Advance, vol.82, pp.10-13, March 1998.

[Pomm98] Itschner R, Pommerell C, Rutishauser M, "GLASS: Remote monitoring of embedded systems in power engineering," IEEE Internet Computing, vol.2, No.3, pp.46-52, May-June 1998.

[Chan99] Chan W.L., So A.T.P., Lai L.L, "Internet based transmission substation monitoring, IEEE Transactions on Power Systems," vol.14, No.1, pp.293-298, Feb. 1999.

[Siem00] Siemens, "Online monitoring for transformers based on Simatic hardware and software," http://www.ev.siemens.de/download/presse/ evg200001191e.doc

[Entek] Entek IRD, "Remote Program Management," http://www.heat. entekird.com/

[Hoga99] Sharon Hogarth, "Remote possibilities: Machine diagnostics at a distance," Manufacturing Engineering, pp.70-79, Feb. 1999.

[MainWeb] Maintenance Strategies Inc., "WebView 2000 TM," http://msicorp.com/ webview.cfm

[Lingso] He Lingsong, “Remote diagnosis expert system,” http://heliso.tripod.com/

[DataSys] Datastream Systems Inc, “MP2Weblink,”

http://www.dstm.com/ products/mp2.shtm

[EPRI00] Electric Power Research Institute, EPRI Report 2000.

[Good98] Gilbert RF, Goodin JL, Nelson K, “The benefits of a distribution automation system using the utility communications architecture (UCA),” the 42nd Annual Rural Electric Power Conference, pp.c3 -1-5, 1998.

[Borl98] Stuart H. Borlase, “Advancing to true station and distribution system integration in electric utility,” IEEE Transactions on Power Delivery, vol.13, No.1, pp 129-134, Jan. 1998.

[Butl96] Butler KL, “An expert system based framework for an incipient failure detection and predictive maintenance system,” Proceedings of International Conference on Intelligent Systems Applications to Power Systems (ISAP’96), pp 321 –326, 1996.

[Jaak96] Hannu Jaakkola, Pekka Loula, “Managing a virtual hospital,” IEMC’96, pp341-345, 1996.

[Dass98] Dassen WRM, Mulleneers RGA, van Dantzig JM, Gommer ED, Dijk WA, Haaksma J, Spruijt HJ, “Application of intranet and internet techniques in conducting clinical trials,” Computers in Cardiology, pp 477 –48, 01998.

[Milo99] Lupu E, Milosevic Z, Sloman M, “Use of roles and policies for specifying and managing a virtual enterprise,” Proceedings of Ninth International Workshop on Research Issues on Data Engineering: Information Technology for Virtual Enterprises (RIDE-VE '99), pp 72 –79, 1999.

[Simp98] Sheppard JW, Simpson WR, “Prototyping a diagnostic interface,” IEEE Systems Readiness Technology Conference (AUTOTESTCON '98), pp 276 –283, 1998.

[Dong01a] Xuzhu Dong, Zhenyuan Wang, Kyumin Rho, Yilu Liu, Nien-Chung Wang, Tzong-Yih Guo, Paul J. Griffin, “Equipment Diagnosis and Virtual Hospital Over the Internet,” EPRI Substation Equipment Diagnostics Conference IX, Feb. 2001.

[Arno99] Hale PS, Arno RG, Briggs SJ, “Operational maintenance data for power generation distribution and HVAC components,” IEEE Transactions on Industry Applications, vol.35, Issue.2, pp 282 –297, March-April 1999.

[Jans00] Janssen ALJ, “Life management of circuit-breakers,” Electra, pp 107-113, Aug. 2000.

[Moub00] John Moubray, “Reliability-centered Maintenance,” TWI Press, 2000.

[MaTa98] Ta-Kan Ma J, Tru-Ming Liu, Lo-Fu Wu, “New energy management system architectural design and Intranet/Internet applications to power systems,” 1998 International Conference on Energy Management and Power Delivery, IEEE, vol.1, p.207-12, 1998.

[Tyle99] David F. Tyler, “Java-based automated test systems: management considerations for an open architecture for test,” Conference of IEEE Systems Readiness Technology (AUTOTESTCON'99), pp 699 –706, 1999.

[NavyMe] The U.S. Navy Bureau of Medicine and Surgery, "Virtual Navy Hospital," http://www.vnh.org/

[Matu99] Robert Matusheski, "The role of information technology in plant reliability," P/PM Technology, June 1999. Available:

http://www.meridium.com/Press/magazines/meridium_ppm_tech.htm

[EPRI99] EPRI CCAPI Asset Modeling Team, Work Document, June 1999. Available: ftp://ftp.macro.com/epriapi/downloads/assets/

[Beck00] D. Becker, H. Falk, J. Gillerman, S. Mauser, R. Podmore, L. Schneberger, "Standards-based approach integrates utility applications," IEEE Computer Applications in Power, vol.13, issue 4, pp.13-20, Oct. 2000.

[Dors99] Paul Dorsey, Joseph Hudicka, Oracle8 Design Using UML Object Modeling, Oracle Press, 1999.

[Guid88] IEEE guide for reporting failure data for power transformers and shunt reactors on electric utility power systems, ANSI/IEEE Std C57.117-1986, Apr. 1988.

[Guid95] IEEE guide for diagnostic field testing of electric power apparatus - part 1: oil filled power transformers, regulators, and reactors, IEEE Std 62-1995, Aug. 1995.

[CCAPI99] CCAPI White Paper, 1999.

Available: ftp://ftp.macro.com/epriapi/downloads/CCAPI_white_paper/

[Wang98] Zhenyuan Wang, Yilu Liu, P.J. Griffin, "A combined ANN and expert system tool for transformer fault diagnosis," IEEE Transactions on Power Delivery, vol.13, No.4, pp.1224-1229, Oct. 1998.

[Guui01] P. Guuinic, J. Aubin, "CIGRE' work on power transformers," EPRI Substation Equipment Diagnostics Conference IX, Feb. 2001.

[Askme] Askme.comTM, http://www.askme.com

[Wang00] Zhenyuan Wang, Yilu Liu, Paul J. Griffin, "Neural Network and Expert System Application in Transformer Fault Diagnosis," IEEE Computer Applications in Power, vol.13, No.1, pp.50-55, Jan. 2000.

[ASPHelp] ASP help, http://asp-help.com/getstarted/

[Erin01a] I. Arslan Erinmez, Martin Croucher, David S. Crisford, "Advanced modeling techniques for assessment of geomagnetically induced current risks on the NGC transmission system," submitted to IEEE Transactions on Power Delivery, 2001.

[Erin01b] I. Arslan Erinmez, John Kappenman, William Radasky, "Implementatino of risk management measures for managing the geomagnetically induced current risks on the NGC transmission system," submitted to IEEE Transactions on Power Delivery, 2001.

APPENDIX A
TYPICAL SYSTEM DATA OF THE PUMPED STORAGE PLANT

A.1. 345 kV Network

Maximum short-circuit capacity under 345 kV:

- Three phase fault	37645 MVA (*)
- Single phase fault	34223 MVA (*)

Minimum short-circuit capacity under 345 kV:

- Three phase fault	13265 MVA (*)
- Single phase fault	8127 MVA (*)
- Aperiodic time constant	0.07 s
- Voltage range in normal operation	327 kV – 362 kV
- Maximum protection fault clearance time	500 ms

(*) These value take into account the short-circuit contribution of the six power units in Mingtan plant.

A.2. Main Transformer

Rated power	300 MVA
Primary rated voltage	16.5 kV
Secondary rated voltage	345 kV
Impedance voltage	14.5 % (±7.5%) (300 MVA basis)
Load loss	1200 kW
Connection	Ynd1

A.3. Generator/Motor

	Generator operation	Motor operation
Rated apparent power	300 MVA	300 MVA

Rated active power	270 MW	288 MW
Rated power factor	0.9	0.96
Rated speed	400 rev/min	

Reactances (basis 300 MVA)			Tolerance
- Direct-axis synchronous reactance	X_d	112.7%	±10%
- Direct-axis transient reactance	X'_d	28%	±15%
- Direct-axis subtransient reactance	X''_d	21%	+20%/-15%
- Quadrature-axis subtransient reactance	X''_q	23%	±20%
- Negative phase-sequence reactance	X_2	22%	±10%
- Zero phase-sequence reactance	X_0	12%	±15%

Time Constant	
- Direct-axis transient time constant in short-circuit T'_d	2.4 s
- Direct-axis subtransient time constant in short-circuit T''_d	0.052 s
- Aperiodic time constant T_a	0.31 s

A.4. 345 kV GIS

Rated voltage (kV)		345
Rated frequency (Hz)		60
Rated normal current (A)	Starting bus	2000
	Main bus	4000
	Feeder	4000/2000
Rated short-time withstand current (kA)		63 (3s)
Rated insulation level (kV)	Low frequency (60 Hz)	555
	Impulse	1300
Rated SF_6 gas pressure (kg/cm^2.G at 20 °C)	Circuit breaker	5.5
	Others	5.0
Rated control voltage (V)		DC125
Standard		ANSI

A.5. 345 kV 1 x 1250 MCM Paper-insulated, Aluminum-sheathed PVC Jacketed oil-filled Cable

Voltage			KV	345
Number of core				1
Sectional area of conductor			MCM	1250
Oil channel	Thickness of helix	(nom.)	mm	0.8
	Inner diameter of helix	(nom.)	mm	14.0
Conductor	Shape			Stranded circular with hollow
	Material			Annealed pain copper
	Outer diameter	(Approx.)	mm	37.2
Thickness of insulation (Including three layers of carbon black paper)		(ave.)	mm	26.29
Thickness of insulation shielding			mm	0.25
Aluminum sheath	Thickness of aluminum sheath	(ave.)	mm	2.4
Thickness of PVC jacket		(min.)	mm	3.6
Overall diameter of cable		(approx.)	mm	114
Weight of cable		(approx.)	kg/m	18
Volume of insulating oil		(approx.)	l/km	4000
Length			m	630

A.6. Station Service Transformer

- Rated power 36.66 MVA (FOA rating)
- Ratio 345 kV/13.8 kV
- Impedance voltage 14.75 % (±10%)
- Connection Ynd1

A.7. Surge Arrester

- Rated voltage 312 kV
- Nominal discharge current 10 kA

APPENDIX B

SWITCHING SEQUENCES IN THE PLANT

B.1. Switching Sequence Using Back-to-back

Several switching strategies are used for starting the units at pump mode as shown below. Here U means Unit and BTB means Back-to-back. The synchronizing requirements of CBs when switching to the system are that the speed is 400 rpm, the frequency is 60 Hz, and the output voltage of the unit is 16.5 kV.

B.1.1. Before DS 3635 Failure

1). U2 or U3 started by U1 using BTB, the switching sequence is:

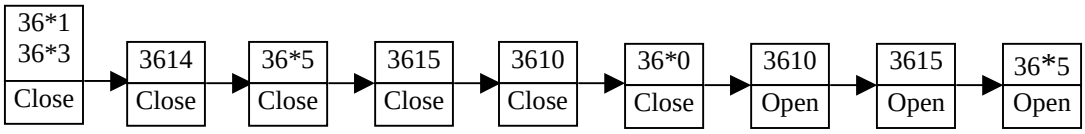

* for only U2 and U3.

2). U4 or U5 started by U1 using BTB, the switching sequence is:

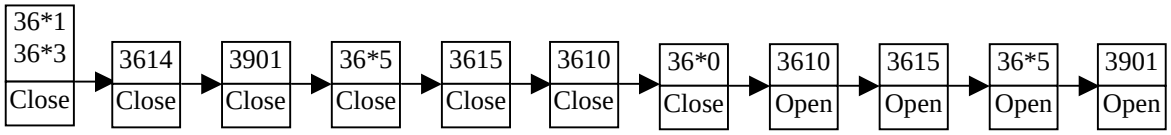

* for only U4 and U5.

B.1.2. After DS 3635 Failure

1). U2 or U3 started by U1 using BTB, the switching sequence is:

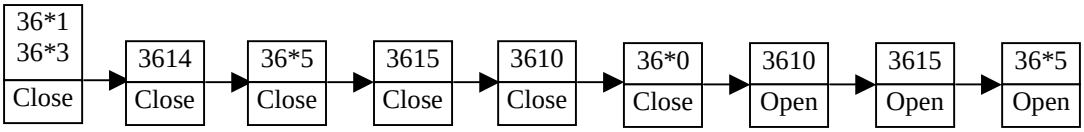

* for only U2 and U3.

2). U4 or U5 started by U1 using BTB, the switching sequence is:

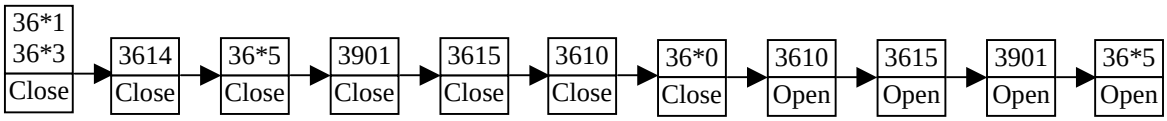

* for only U4 and U5.

B.1.3. After DS 3655 Failure, Only U3 Was Started by U1 or U5 Was Started by U6 Using BTB.

1). U2 or U3 started by U1 using BTB, the switching sequence is:

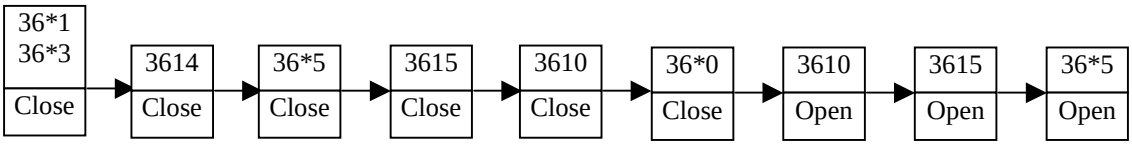

* for only U2 and U3.

2). U4 or U5 started by U1 using BTB, the switching sequence is:

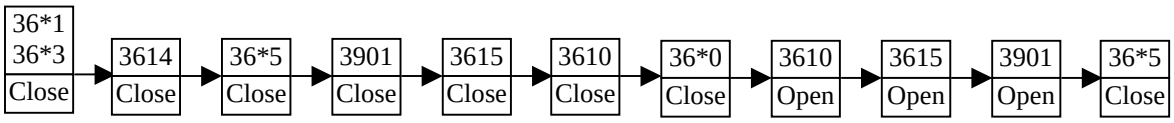

* for only U4 and U5.

B.1.4. After DS 3635 and DS 3655 Failure, Only U5 or U3 Were Started by U6 Using BTB Can Be Used.

1). U4 or U5 started by U6 using BTB, the switching sequence is:

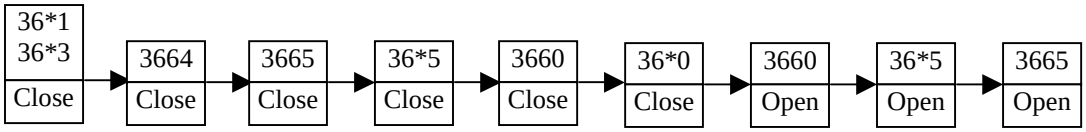

* for only U4 and U5.

2). U2 or U3 started by U6 using BTB, the switching sequence is:

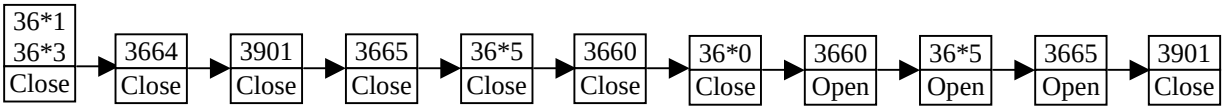

* for only U2 and U3.

B.2. Switching Sequence Using SFC

Usually SFC1 works for U1-3, and SFC for U4-6. As shown in Fig.1, when using SFC to start the units, the sequence used in field is:

1). SFC1 starting U4, U5, or U6 (* only for U4, U5, or U6)

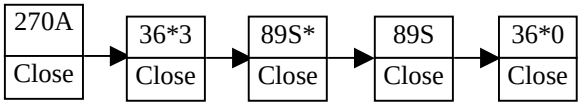

2). SFC1 starting U1, U2, or U3 (* only for U1, U2, or U3)

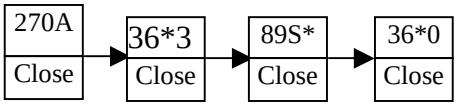

B.3. Switching Sequence When Disconnecting from the System

When the unit is at generation mode, the unit output is reduced first from 150 MW to 2 MW and 0 MVar, then CB 36*0 (* is 1 – 6) is opened. DS 36*1 and DS 36*4 are opened when the speed reaches 0 rpm.

When the unit is at pump mode, first the unit input is reduced to -100 MW ± 10% and 0 MVar, then CB 36*0 (* is 1 – 6) is opened. DS 36*1 and DS 36*3 are opened when the speed reaches 0 rpm.

APPENDIX C
TYPICAL SIMULATION CIRCUIT
(The example of CB 3610 re-strike when Unit 2 is started by Unit 1 using the back-to-back starting method)

C.1. The Complete Simulation Configuration

The simulation circuit includes Fig.C1 ~ C10.

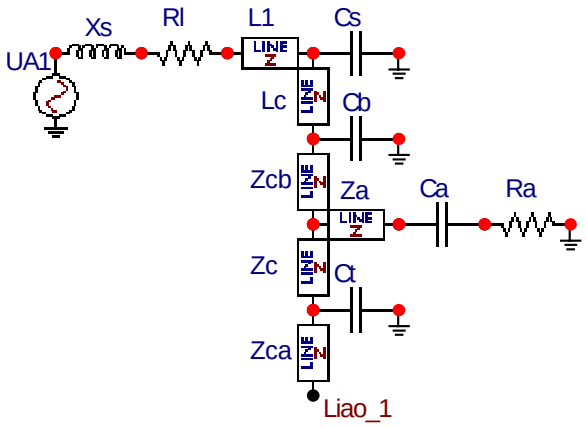

Fig.C1. Modeling of the GIS bus bay to Chung-Liao #1

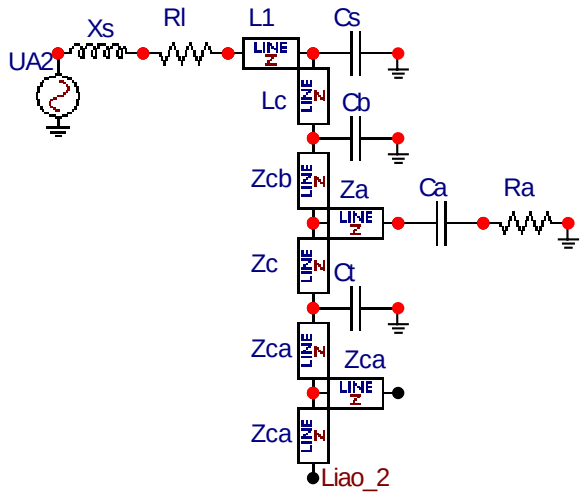

Fig.C2. Modeling of the GIS bus bay to Chung-Liao #2

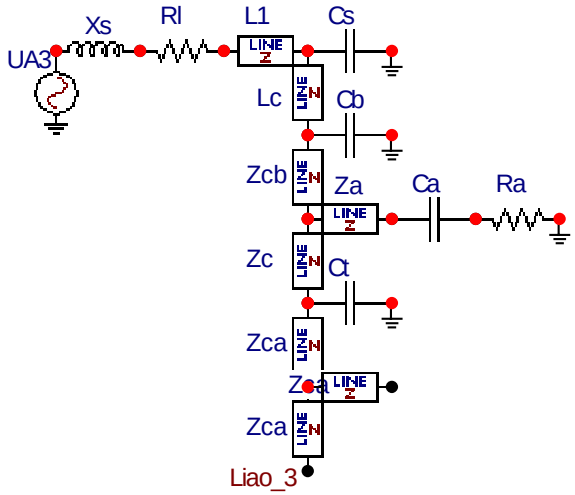

Fig.C3. Modeling of the GIS bus bay to Chung-Liao #3

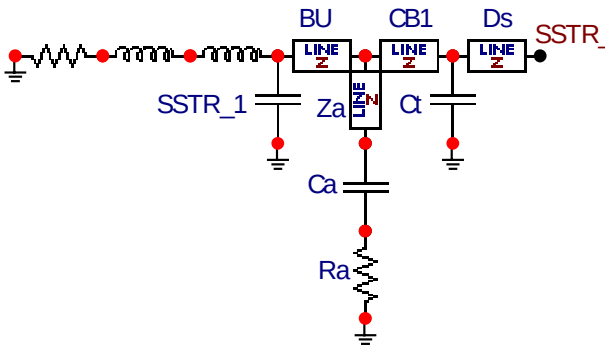

Fig.C4. Modeling of the GIS bus bay to SSTR #1

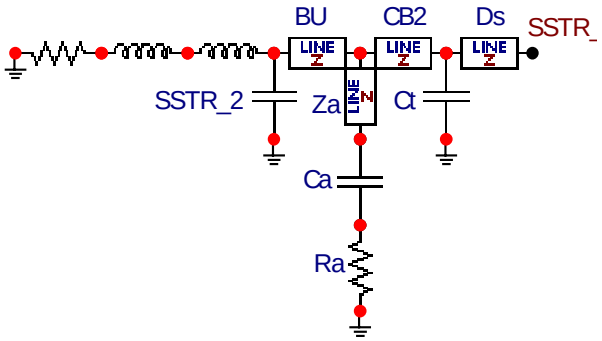

Fig.C5. Modeling of the GIS bus bay to SSTR #2

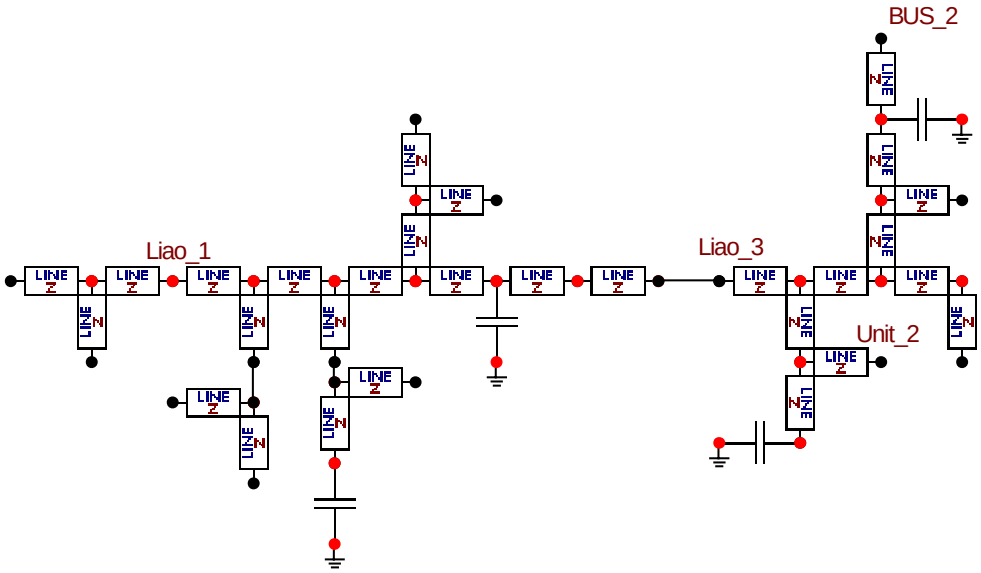

Fig.C6. Modeling of the GIS Bus 1 and Bus 3

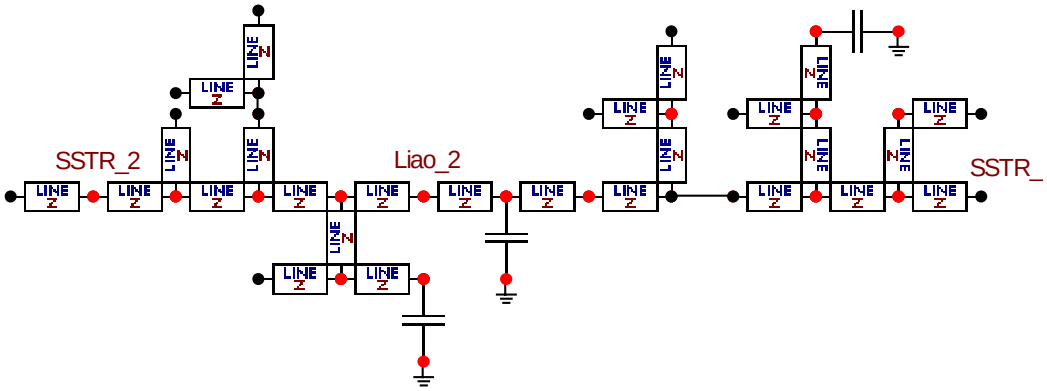

Fig.C7. Modeling of the GIS Bus 2 and Bus 4

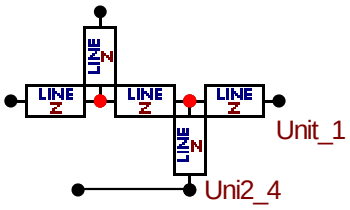

Fig.C8. Modeling of the starting bus

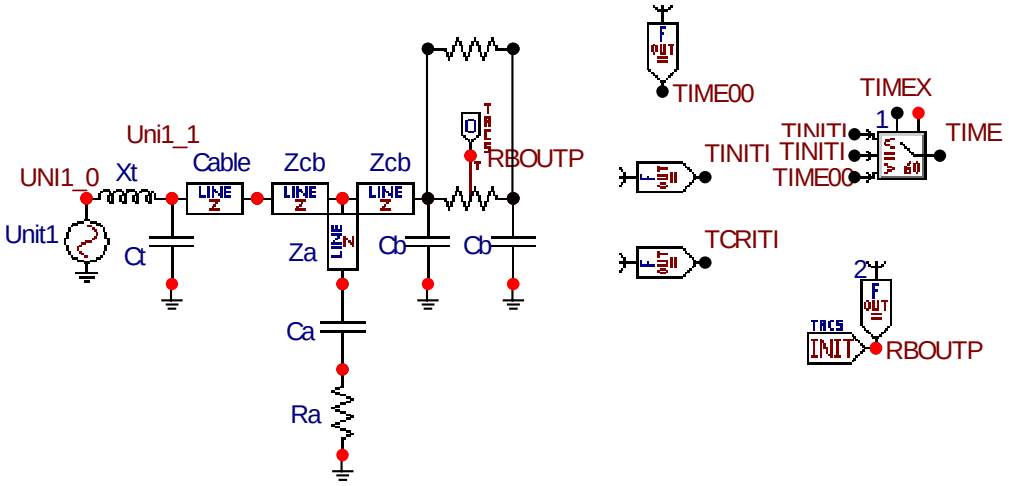

Fig.C9. Modeling of the bus bay to Tr. #1 and CB 3610

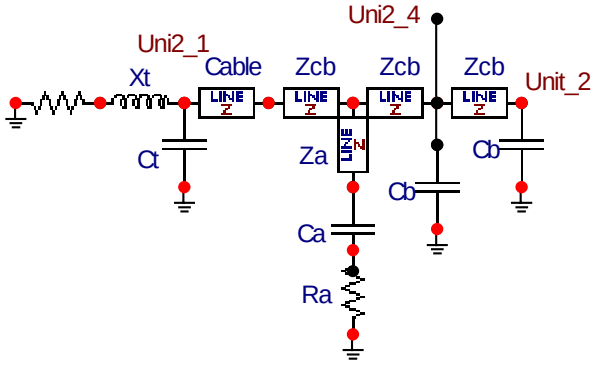

Fig.C10. Modeling of the bus bay to Tr. #2

C.2. ATP-EMTP Data File for Fig. C1~C10

```
BEGIN NEW DATA CASE
C ------------------------------------------------------
C Generated by ATPDRAW  March, Friday 2, 2001
C A Bonneville Power Administration program
C Programmed by H. K. Høidalen at SEfAS - NORWAY  1994-98
C ------------------------------------------------------
C Miscellaneous Data Card ....
C  dT  >< Tmax >< Xopt >< Copt >
  2.5E-9   .0001
     500       1       1       1       1       0       0       1       0
TACS HYBRID
/TACS
99TIME00  =TIMEX-1.0E-5
98RBOUTP  =1.0E10*EXP(-TIME11/TCRITI)+0.01
99TIME1160+TINITI +TINITI +TIME00                  1.E-5            TIMEX
```

```
99TCRITI  =1.0E-9
99TINITI  =1.0E-9
33RBOUTP
77RBOUTP       1.E10
C        1         2         3         4         5         6         7         8
C 345678901234567890123456789012345678901234567890123456789012345678901234567890
/BRANCH
C < n 1>< n 2><ref1><ref2>< R  >< L  >< C  >
C < n 1>< n 2><ref1><ref2>< R  >< A  >< B  ><Leng><><>0
  VAL_1 L1_A_1                    8.4                                          0
  L1_A_1L1_A_2              350.                                               0
-1L1_A_2L1_A_3                   258.  3.E8    8. 1 0                        0
  L1_A_3                              .0001                                    0
-1L1_A_4L1_A_3                   350.  3.E8    6. 1 0                        0
  L1_A_4                              .0001                                    0
-1L1_A_5L1_A_4                    80. 2.7E8    1. 1 0                        0
-1L1_A_5L1_A_7                    80. 2.7E8    1. 1 0                        0
  L1_A_7L1_A_8                       1.5E-5                                    0
  L1_A_8                     .1                                               0
-1L1_A_6L1_A_5                    80. 2.7E8   6.6 1 0                        0
  L1_A_6                              .0001                                    0
-1Liao_1L1_A_6                    80. 2.7E8  5.86 1 0                        0
-1Bus3_0Bus3_1                    80. 2.7E8    1. 1 0                        0
-1STR2_BBus3_1                    80. 2.7E8   4.2 1 0                        0
-1Bus3_1Liao_1                    80. 2.7E8  3.75 1 0                        0
-1Liao_1Bus3_2                    80. 2.7E8    8. 1 0                        0
-1Bus3_3Bus3_2                    80. 2.7E8    1. 1 0                        0
-1Bus3_2Bus3_4                    80. 2.7E8    6. 1 0                        0
-1B3PT_2B3PT_1                    80. 2.7E8    1. 1 0                        0
  B3PT_2                             .00015                                   0
-1Bus3_4Bus3_5                    80. 2.7E8    6. 1 0                        0
-1Bus3_5Lia2_C                    80. 2.7E8    1. 1 0                        0
-1Bus3_5CB3700                    80. 2.7E8  10.5 1 0                        0
  CB3700                              .0003                                    0
-1CB3700Bus1_0                    80. 2.7E8    5. 1 0                        0
-1Bus1_0Liao_3                    80. 2.7E8   9.1 1 0                        0
  VAL_3 L3_A_1                    8.4                                          0
  L3_A_1L3_A_2              350.                                               0
-1L3_A_2L3_A_3                   258.  3.E8    8. 1 0                        0
  L3_A_3                              .0001                                    0
-1L3_A_4L3_A_3                   350.  3.E8    6. 1 0                        0
  L3_A_4                              .0001                                    0
-1L3_A_5L3_A_4                    80. 2.7E8    1. 1 0                        0
-1L3_A_5L3_A_8                    80. 2.7E8    1. 1 0                        0
  L3_A_8L3_A_9                       1.5E-5                                    0
  L3_A_9                     .1                                               0
-1L3_A_6L3_A_5                    80. 2.7E8   6.6 1 0                        0
  L3_A_6                              .0001                                    0
-1L3_A_7L3_A_6                    80. 2.7E8  4.86 1 0                        0
-1Liao_3Bus1_1                    80. 2.7E8    6. 1 0                        0
-1Bus1_1B1PT_1                    80. 2.7E8    1. 1 0                        0
  B1PT_2                             .00015                                   0
-1Bus1_1Bus1_2                    80. 2.7E8    6. 1 0                        0
-1Bus1_2Bus1_3                    80. 2.7E8   11. 1 0                        0
-1STR1_BBus1_3                    80. 2.7E8   4.2 1 0                        0
-1DS3501Bus1_2                    80. 2.7E8    1. 1 0                        0
-1BUS_2 CB3500                    80. 2.7E8   4.8 1 0                        0
  CB3500                              .0003                                    0
-1Bus4_0SSTR_2                    80. 2.7E8    1. 1 0                        0
-1Bus4_1Lia1_B                    80. 2.7E8    2. 1 0                        0
  VAL_2 L2_A_1                    8.4                                          0
-1SSTR_2Bus4_1                    80. 2.7E8  3.75 1 0                        0
-1Bus4_1Bus4_2                    80. 2.7E8    8. 1 0                        0
```

```
  L2_A_1L2_A_2              350.                                          0
-1Bus4_2Bus4_4                     80. 2.7E8    6. 1 0                   0
-1B4PT_1B4PT_2                     80. 2.7E8    1. 1 0                   0
  B4PT_2                              .00015                             0
-1Bus4_4Liao_2                     80. 2.7E8    6. 1 0                   0
-1Bus2_1Lia3_C                     80. 2.7E8    1. 1 0                   0
-1Liao_2CB3800                     80. 2.7E8  10.5 1 0                   0
  CB3800                              .0003                              0
-1CB3800Bus2_0                     80. 2.7E8    5. 1 0                   0
-1Bus2_0Bus2_1                     80. 2.7E8   9.1 1 0                   0
-1Bus2_1Bus2_2                     80. 2.7E8    6. 1 0                   0
-1B2PT_1Bus2_2                     80. 2.7E8    1. 1 0                   0
  B2PT_2                              .00015                             0
-1Bus2_2Bus2_3                     80. 2.7E8    6. 1 0                   0
-1Bus2_3SSTR_1                     80. 2.7E8   11. 1 0                   0
        STR2_0                        .0005                              0
-1STR2_0STR2_1                     80. 2.7E8    5. 1 0                   0
  STR2_2                              .0003                              0
-1STR2_1STR2_2                     80. 2.7E8  2.34 1 0                   0
-1STR2_2SSTR_2                     80. 2.7E8  8.03 1 0                   0
-1STR2_3STR2_1                     80. 2.7E8    1. 1 0                   0
  STR2_3STR2_4                        1.5E-5                             0
  STR2_4                    .1                                           0
-1L2_A_2L2_A_3                  258.  3.E8    8. 1 0                   0
  L2_A_3                             .0001                              0
-1L2_A_4L2_A_3                  350.  3.E8    6. 1 0                   0
  L2_A_4                             .0001                              0
-1L2_A_5L2_A_4                     80. 2.7E8    1. 1 0                   0
-1L2_A_5L2_A_8                     80. 2.7E8    1. 1 0                   0
  L2_A_8L2_A_9                        1.5E-5                             0
  L2_A_9                    .1                                           0
-1L2_A_6L2_A_5                     80. 2.7E8   6.6 1 0                   0
  L2_A_6                             .0001                              0
-1Liao_2L2_A_7                     80. 2.7E8    1. 1 0                   0
-1Bus4_2Bus4_3                     80. 2.7E8    1. 1 0                   0
        STR1_0                        .0005                              0
-1STR1_0STR1_1                     80. 2.7E8    5. 1 0                   0
  STR1_2                              .0003                              0
-1STR1_1STR1_2                     80. 2.7E8  2.34 1 0                   0
-1STR1_2SSTR_1                     80. 2.7E8  8.03 1 0                   0
-1STR1_3STR1_1                     80. 2.7E8    1. 1 0                   0
  STR1_3STR1_4                        1.5E-5                             0
  STR1_4                    .1                                           0
-1BC34_3Bus3_3                     80. 2.7E8    1. 1 0                   0
-1Un6B_3Bus3_3                     80. 2.7E8    3. 1 0                   0
-1B3PT_1Bus3_4                     80. 2.7E8    1. 1 0                   0
-1B3PT_1Un5B_3                     80. 2.7E8    3. 1 0                   0
-1Lia2_CLia2_B                     80. 2.7E8    1. 1 0                   0
-1Lia2_CUn4B_3                     80. 2.7E8    3. 1 0                   0
-1Liao_3L3_A_7                     80. 2.7E8    1. 1 0                   0
-1L3_A_7Un3B_1                     80. 2.7E8    3. 1 0                   0
-1B1PT_1B1PT_2                     80. 2.7E8    1. 1 0                   0
-1B1PT_1Unit_2                     80. 2.7E8    7. 1 0                   0
-1Bus4_3BC34_4                     80. 2.7E8    1. 1 0                   0
-1Un6B_4Bus4_3                     80. 2.7E8    3. 1 0                   0
-1B4PT_1Bus4_4                     80. 2.7E8    1. 1 0                   0
-1Un5B_4B4PT_1                     80. 2.7E8    3. 1 0                   0
-1L2_A_7L2_A_6                     80. 2.7E8  4.86 1 0                   0
-1L2_A_7Un4B_4                     80. 2.7E8    3. 1 0                   0
-1Lia3_CLia3_B                     80. 2.7E8    1. 1 0                   0
-1Un3B_2Lia3_C                     80. 2.7E8    3. 1 0                   0
-1B2PT_2B2PT_1                     80. 2.7E8    1. 1 0                   0
-1Un2B_2B2PT_1                     80. 2.7E8    3. 1 0                   0
```

```
-1CB3500DS3501                    80. 2.7E8  11.6 1 0                          0
-1DS3501Un1B_1                    80. 2.7E8    3. 1 0                          0
-1BUS_2 Bus2_3                    80. 2.7E8    1. 1 0                          0
-1BUS_2 Un1B_2                    80. 2.7E8    3. 1 0                          0
-1STAR_0STAR_1                    80. 2.7E8    5. 1 0                          0
-1STAR_1U3ST_B                    80. 2.7E8    4. 1 0                          0
-1STAR_1STAR_2                    80. 2.7E8    6. 1 0                          0
-1STAR_2Unit_1                    80. 2.7E8  13.8 1 0                          0
-1Uni2_4STAR_2                    80. 2.7E8    6. 1 0                          0
-1Uni2_3Uni2_4                    80. 2.7E8   5.1 1 0                          0
$VINTAGE,1
-1Uni2_1Uni2_2              .00106788     37.7692   2.10977E8        630. 1 0 0
$VINTAGE,0
-1Uni2_4Unit_2                    80. 2.7E8   2.5 1 0                          0
  Uni2_4                             .00015                                    2
-1Uni2_2Uni2_3                    80. 2.7E8    1. 1 0                          0
-1Un2LA1Uni2_3                    80. 2.7E8   1.5 1 0                          0
  Un2LA1UN2LA2                       1.5E-5                                    0
  UN2LA2                     .1                                                0
  UNI1_0Uni1_1                   158.                                          0
  Uni2_1                               .005                                    2
  Unit_2                             .00015                                    0
-1Uni1_3Uni1_4                    80. 2.7E8    7. 1 0                          0
$VINTAGE,1
-1Uni1_1Uni1_2              .00106788     37.7692   2.10977E8        630. 1 0 0
$VINTAGE,0
  Uni1_4                             .00015                                    2
-1Uni1_2Uni1_3                    80. 2.7E8    1. 1 0                          0
-1Un1LA1Uni1_3                    80. 2.7E8   1.5 1 0                          0
  Un1LA1Un1LA2                       1.5E-5                                    0
  Un1LA2                     .1                                                0
  Uni1_1                               .005                                    2
  Unit_1                             .00015                                    2
  XX0297STR2_0                    1292.                                        0
  XX0299XX0297                   57420.                                        0
        XX0299               3819.                                           0
  XX0303STR1_0                    1292.                                        0
  XX0305XX0303                   57420.                                        0
        XX0305               3819.                                           0
  TR2R  Uni2_1                     158.                                        0
        TR2R                99200.                                           0
  Uni1_4Unit_1                  1.E6                                          0
91Uni1_4Unit_1TACS  RBOUTP                                                    2
/SWITCH
C < n 1>< n 2>< Tclose ><Top/Tde ><   Ie   ><Vf/CLOP ><  type  >
/SOURCE
C < n 1><>< Ampl.  >< Freq.  ><Phase/T0><   A1   ><   T1   >< TSTART >< TSTOP  >
14VAL_1  0   281690.       60.                                    -1.       10.
14VAL_3  0   281690.       60.                                    -1.       10.
14VAL_2  0   281690.       60.                                    -1.       10.
14UNI1_0 0   281690.       60.      180.                          -1.       10.
BLANK TACS
BLANK BRANCH
BLANK SWITCH
BLANK SOURCE
  Uni1_4Unit_1
BLANK OUTPUT
BLANK PLOT
BEGIN NEW DATA CASE
BLANK
```

APPENDIX D

INFORMATION MODEL FOR POWER EQUIPMENT DIAGNOSIS AND MAINTENANCE

D.1. The Class Diagram of the Information Model

The information model is maintained using UML class diagram, as shown in Fig.D1 in the following page. The class diagram describes the types of information objects related to power equipment diagnosis and maintenance, and the various kinds of static relationships that exist among them. There are three principal kinds of static relationships: Association, Generalization, and Aggregation. Details are discussed in [Dors99].

D.2. Attribute Description of Entities

There are over 115 entities. For each entity, the attributes are shown below the entity title. All entities are shown in Fig.D2 following Fig.D1.

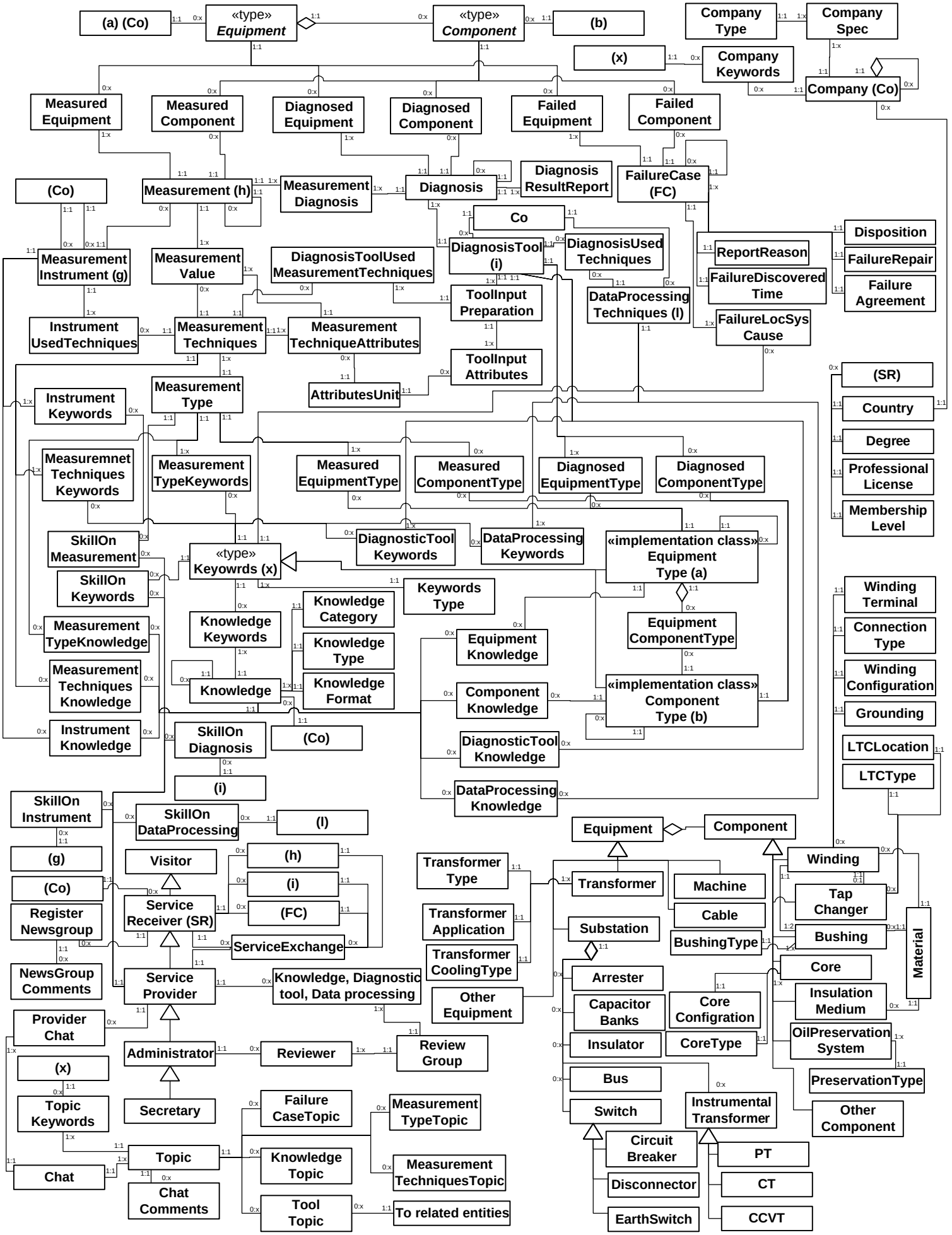

Fig.D1. The class diagram of the information model

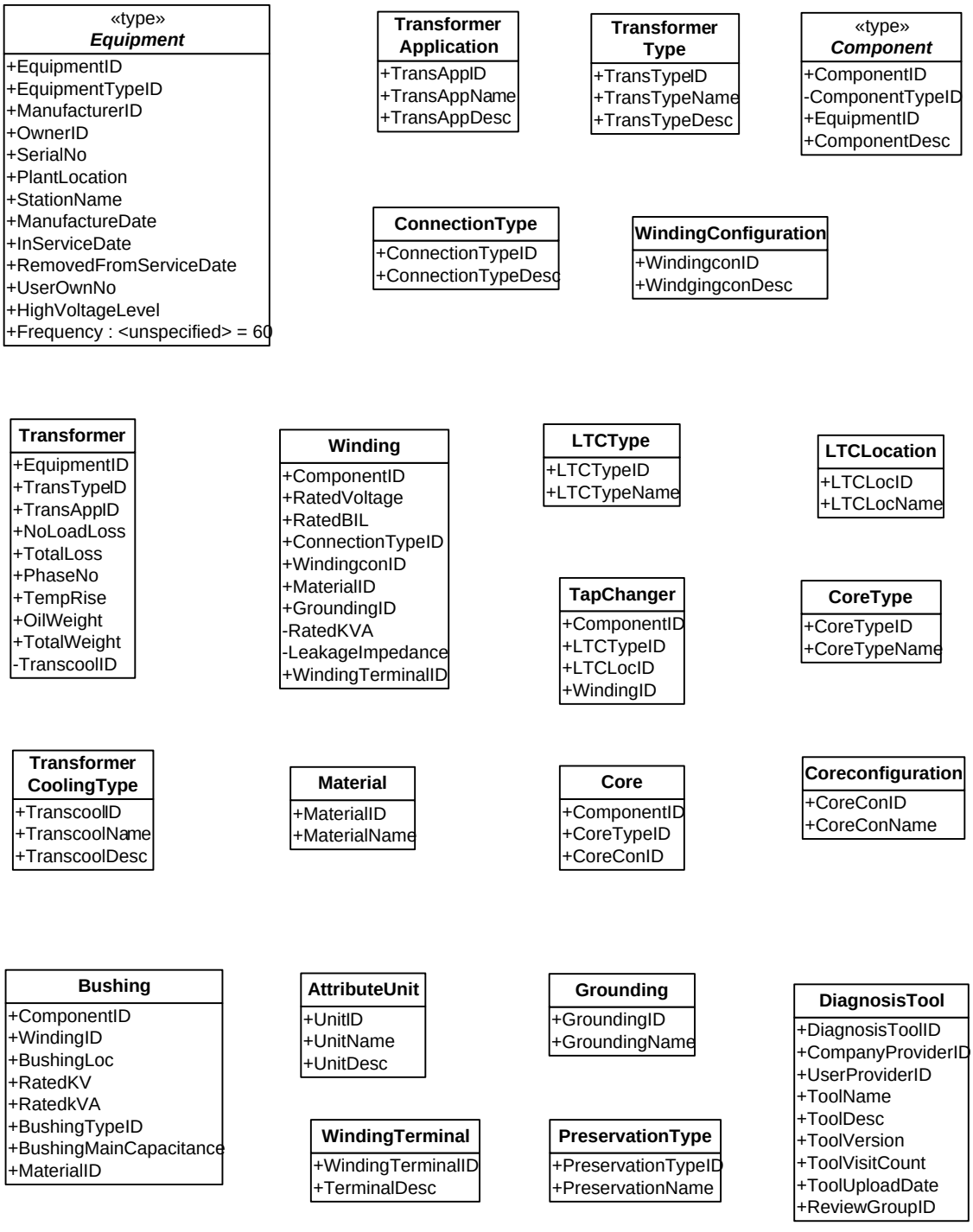

Fig.D2. Entities and their attributes

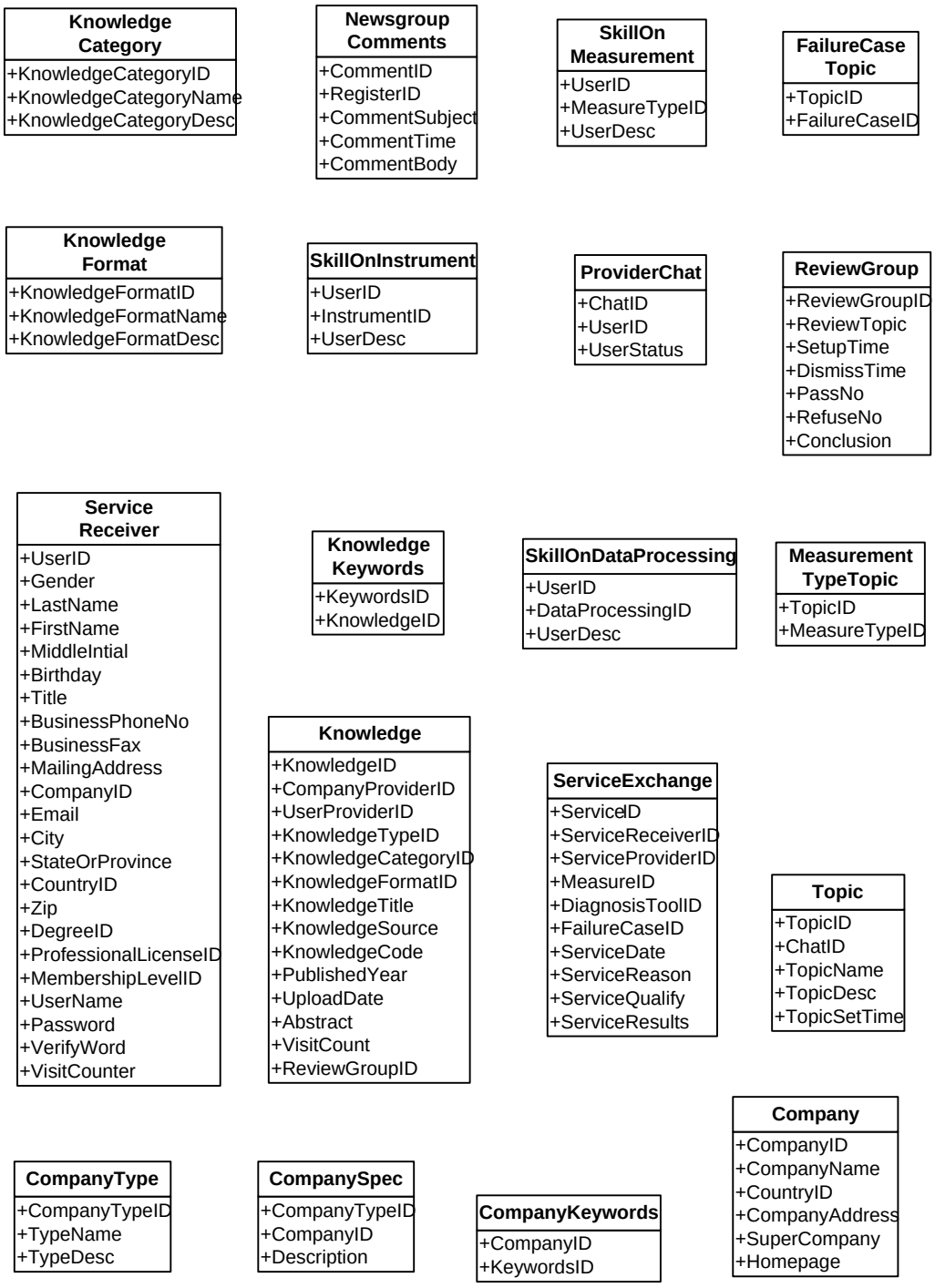

Fig.D2. Entities and their attributes (Cont.)

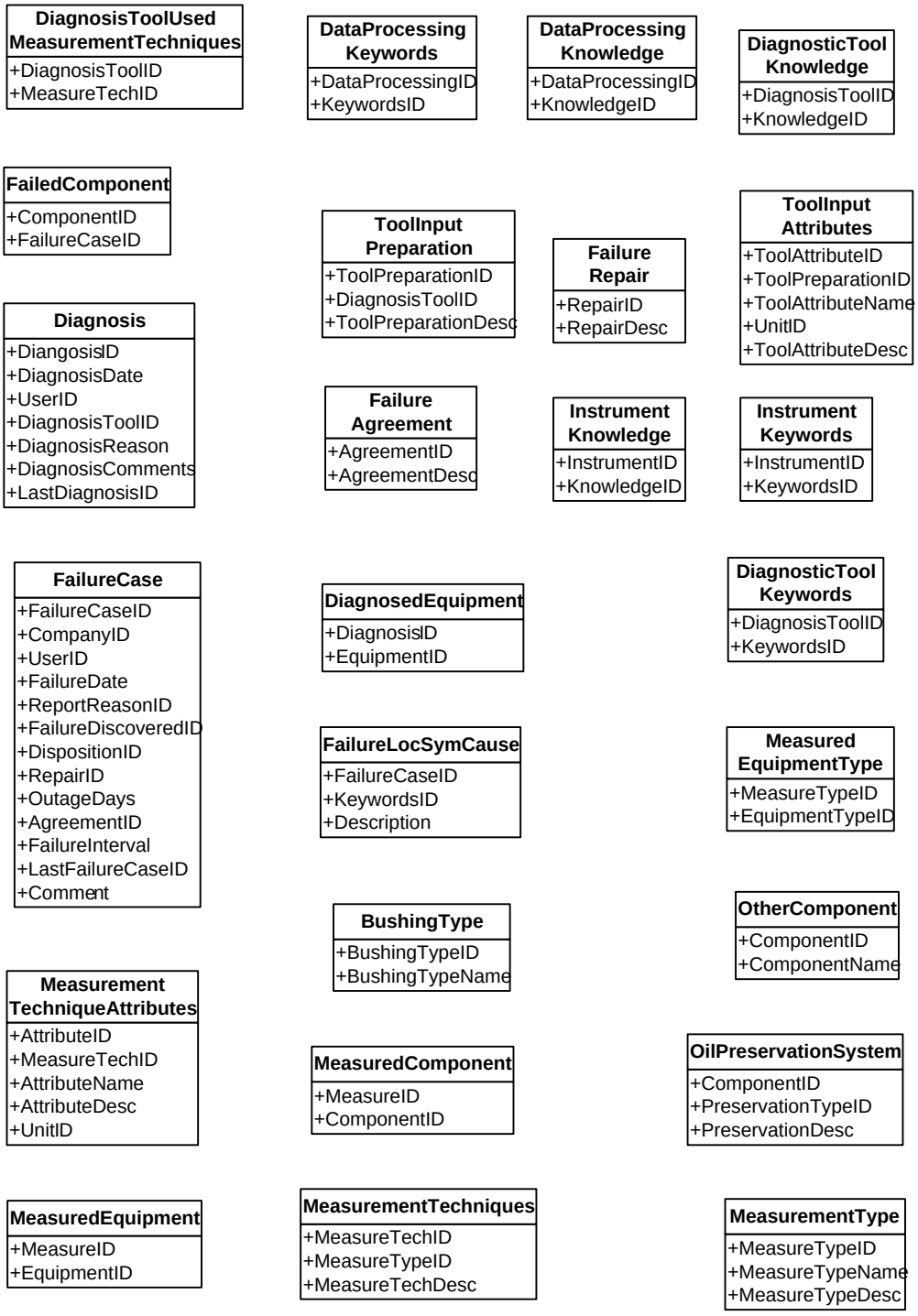

Fig.D2. Entities and their attributes (Cont.)

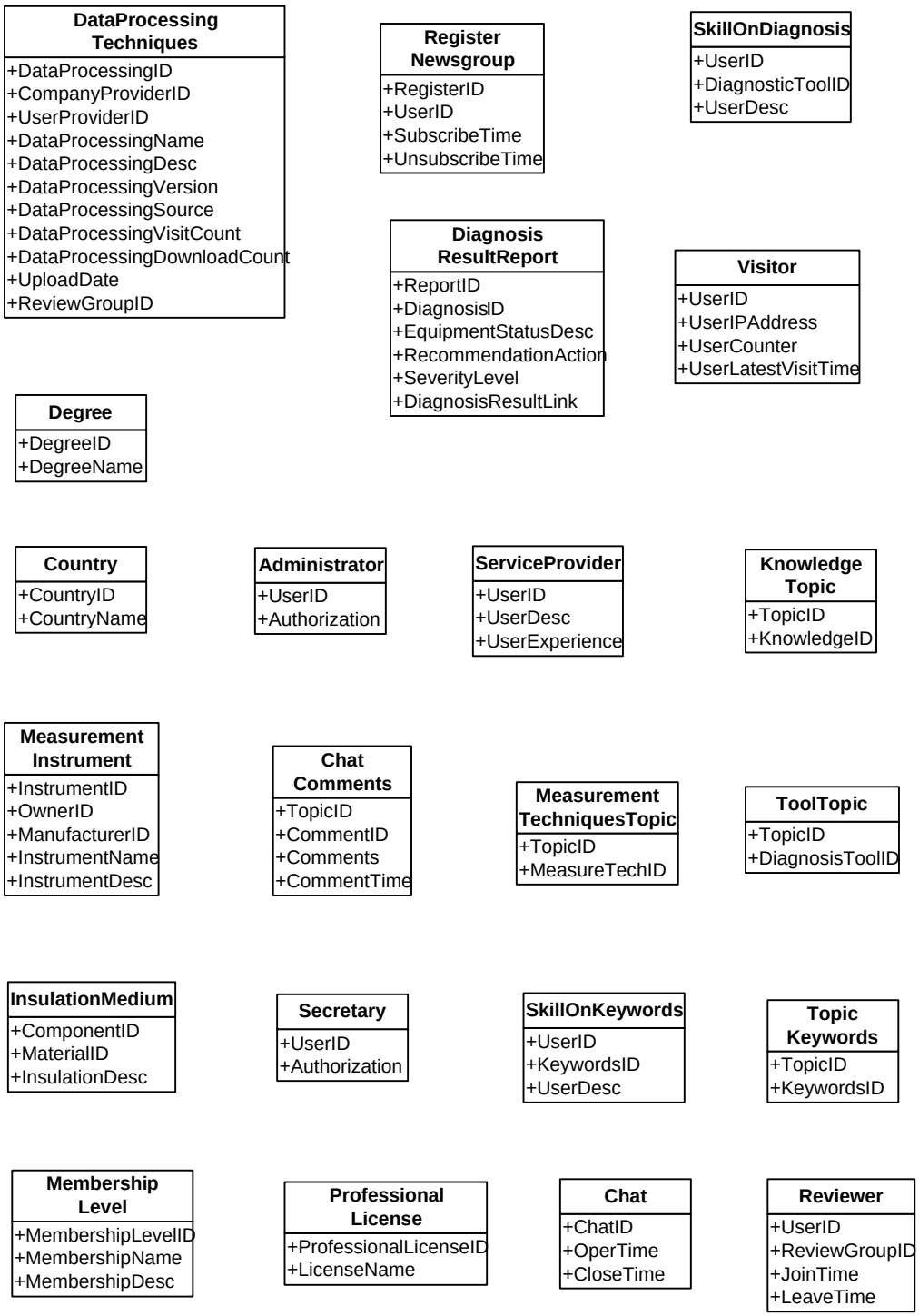

Fig.D2. Entities and their attributes (Cont.)

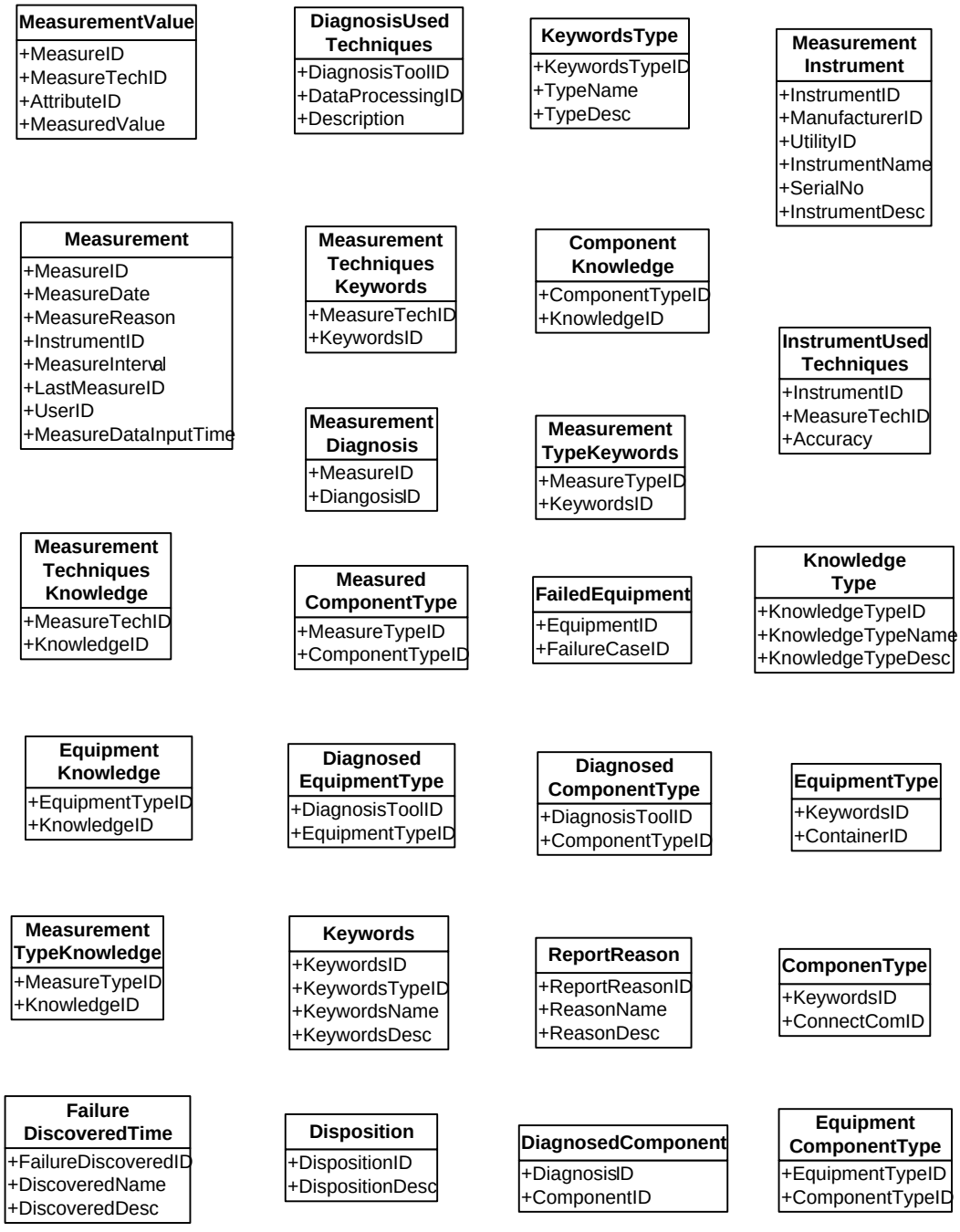

Fig.D2. Entities and their attributes (Cont.)